

ENGINEERING OF BIOMATERIALS

INŻYNIERIA BIOMATERIAŁÓW

JOURNAL OF POLISH SOCIETY FOR BIOMATERIALS AND FACULTY OF MATERIALS SCIENCE AND CERAMICS AGH-UST
CZASOPISMO POLSKIEGO STOWARZYSZENIA BIOMATERIAŁÓW I WYDZIAŁU INŻYNIERII MATERIAŁOWEJ I CERAMIKI AGH

Number 113

Numer 113

Volume XV

Rok XV

APRIL 2012

KWIECIEŃ 2012

ISSN 1429-7248

PUBLISHER:

WYDAWCA:

**Polish Society
for Biomaterials
in Krakow**

Polskie
Stowarzyszenie
Biomateriałów
w Krakowie

**EDITORIAL
COMMITTEE:**

KOMITET
REDAKCYJNY:

Editor-in-Chief

Redaktor naczelny
Jan Chłopek

Editor

Redaktor
Elżbieta Pamuła

Secretary of editorial

Sekretarz redakcji

Design

Projekt
**Katarzyna Trała
Augustyn Powroźnik**

ADDRESS OF

EDITORIAL OFFICE:

ADRES REDAKCJI:

AGH-UST

**30/A3, Mickiewicz Av.
30-059 Krakow, Poland**

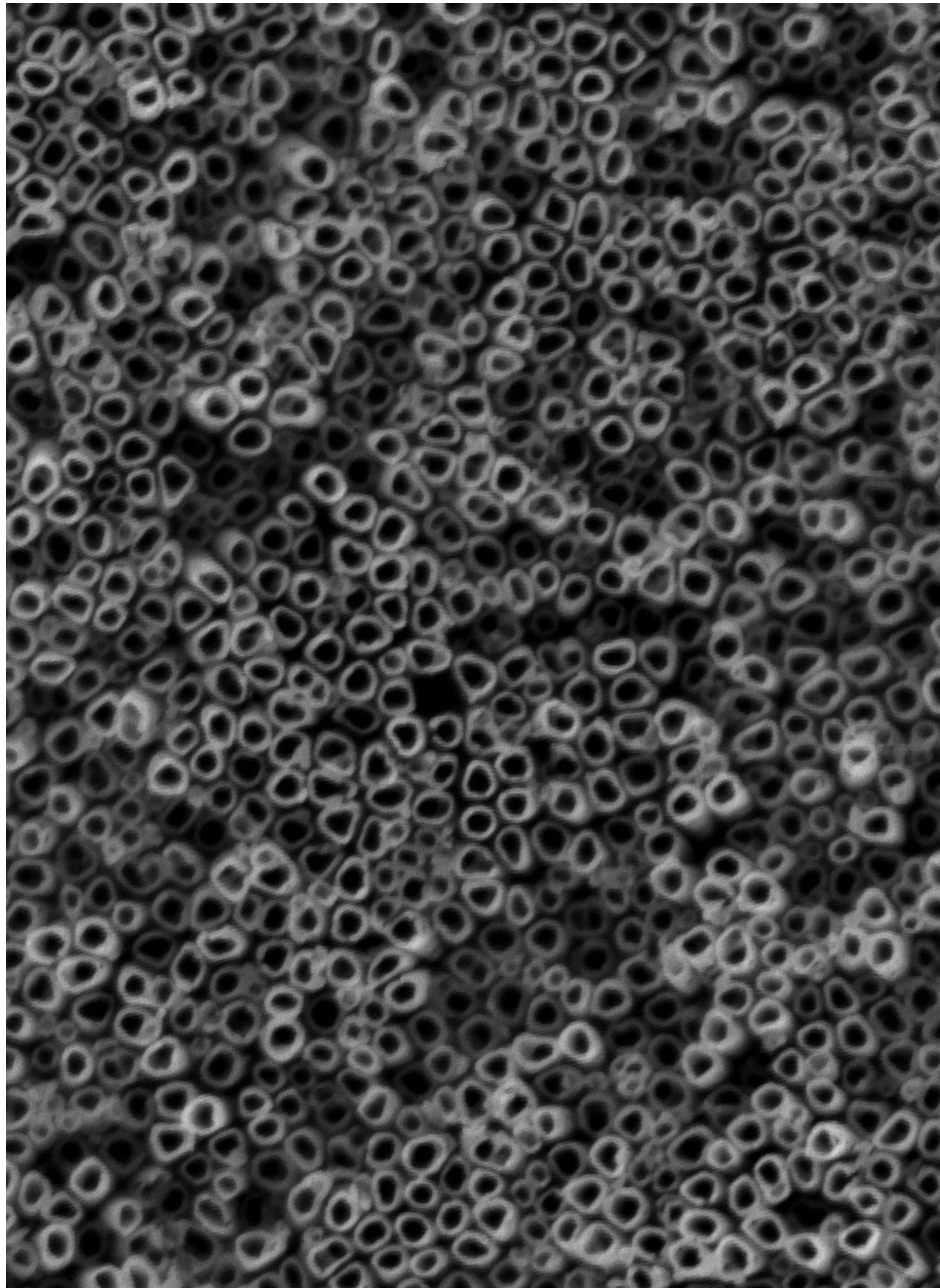
Akademia
Górniczno-Hutnicza
al. Mickiewicza 30/A-3
30-059 Kraków

Issue: 200 copies

Nakład: 200 egz.

**Scientific Publishing
House AKAPIT**

Wydawnictwo Naukowe
AKAPIT
e-mail: wn@akapit.krakow.pl



INTERNATIONAL EDITORIAL BOARD
MIĘDZYNARODOWY KOMITET REDAKCYJNY

Iulian Antoniac

UNIVERSITY POLITEHNICA OF BUCHAREST, ROMANIA

Lucie Bacakova

ACADEMY OF SCIENCE OF THE CZECH REPUBLIC, PRAGUE, CZECH REPUBLIC

Romuald Będziński

POLITECHNIKA WROCLAWSKA / WROCLAW UNIVERSITY OF TECHNOLOGY

Marta Błażewicz

AKADEMIA GÓRNICZO-HUTNICZA, KRAKÓW / AGH UNIVERSITY OF SCIENCE AND TECHNOLOGY, KRAKOW

Stanisław Błażewicz

AKADEMIA GÓRNICZO-HUTNICZA, KRAKÓW / AGH UNIVERSITY OF SCIENCE AND TECHNOLOGY, KRAKOW

Maria Borczuch-Łączka

AKADEMIA GÓRNICZO-HUTNICZA, KRAKÓW / AGH UNIVERSITY OF SCIENCE AND TECHNOLOGY, KRAKOW

Wojciech Chrzanowski

UNIVERSITY OF SYDNEY, AUSTRALIA

Tadeusz Cieślik

ŚLAŃSKI UNIWERSYTET MEDYCZNY / MEDICAL UNIVERSITY OF SILESIA

Jan Ryszard Dąbrowski

POLITECHNIKA BIAŁOSTOCKA / BIAŁYSTOK TECHNICAL UNIVERSITY

Matthias Epple

UNIVERSITY OF DUISBURG-ESSEN, GERMANY

Andrzej Górecki

WARSZAWSKI UNIWERSYTET MEDYCZNY / MEDICAL UNIVERSITY OF WARSAW

Robert Hurt

BROWN UNIVERSITY, PROVIDENCE, USA

James Kirkpatrick

JOHANNES GUTENBERG UNIVERSITY, MAINZ, GERMANY

Wojciech Maria Kuś

WARSZAWSKI UNIWERSYTET MEDYCZNY / MEDICAL UNIVERSITY OF WARSAW

Małgorzata Lewandowska-Szumiel

WARSZAWSKI UNIWERSYTET MEDYCZNY / MEDICAL UNIVERSITY OF WARSAW

Jan Marciński

POLITECHNIKA ŚLAŃKA / SILESIAN UNIVERSITY OF TECHNOLOGY

Sergey Mikhalovsky

UNIVERSITY OF BRIGHTON, UNITED KINGDOM

Stanisław Mitura

POLITECHNIKA ŁÓDZKA / TECHNICAL UNIVERSITY OF LODZ

Roman Pampuch

AKADEMIA GÓRNICZO-HUTNICZA, KRAKÓW / AGH UNIVERSITY OF SCIENCE AND TECHNOLOGY, KRAKOW

Stanisław Pielka

AKADEMIA MEDYCZNA WE WROCLAWIU / WROCLAW MEDICAL UNIVERSITY

Vehid Salih

UCL EASTMAN DENTAL INSTITUTE, UNITED KINGDOM

Jacek Składzień

UNIWERSYTET JAGIELLOŃSKI, COLLEGIUM MEDICUM, KRAKÓW / JAGIELLONIAN UNIVERSITY, COLLEGIUM MEDICUM, KRAKOW

Andrei V. Stanishevsky

UNIVERSITY OF ALABAMA AT BIRMINGHAM, USA

Anna Ślósarczyk

AKADEMIA GÓRNICZO-HUTNICZA, KRAKÓW / AGH UNIVERSITY OF SCIENCE AND TECHNOLOGY, KRAKOW

Tadeusz Trzaska

AKADEMIA WYCHOWANIA FIZYCZNEGO, POZNAŃ / UNIVERSITY SCHOOL OF PHYSICAL EDUCATION, POZNAŃ

Dimitris Tsipas

ARISTOTLE UNIVERSITY OF THESSALONIKI, GREECE

Wskazówki dla autorów

1. Prace do opublikowania w kwartalniku „Engineering of Biomaterials / Inżynieria Biomateriałów” przyjmowane będą wyłącznie z tłumaczeniem na język angielski. Obcojęzycy obowiązuje tylko język angielski.
2. Wszystkie nadsyłane artykuły są recenzowane.
3. Materiały do druku prosimy przysyłać na adres e-mail: kabe@agh.edu.pl.
4. Struktura artykułu:
 - TYTUŁ • Autorzy • Streszczenie (100-200 słów) • Słowa kluczowe • Wprowadzenie • Materiały i metody • Wyniki i dyskusja • Wnioski • Podziękowania • Piśmiennictwo
5. Materiały ilustracyjne powinny znajdować się poza tekstem w oddzielnych plikach (format .jpg, .gif, .tiff, .bmp). Rozdzielczość rysunków min. 300 dpi. Wszystkie rysunki i wykresy powinny być czarno-białe lub w odcieniach szarości i ponumerowane cyframi arabskimi. W tekście należy umieścić odnośniki do rysunków i tabel. W tabelach i na wykresach należy umieścić opisy polskie i angielskie. W dodatkowym dokumencie należy zamieścić spis tabel i rysunków (po polsku i angielsku).
6. Na końcu artykułu należy podać wykaz piśmiennictwa w kolejności cytowania w tekście i kolejno ponumerowany.
7. Redakcja zastrzega sobie prawo wprowadzenia do opracowań autorskich zmian terminologicznych, poprawek redakcyjnych, stylistycznych, w celu dostosowania artykułu do norm przyjętych w naszym czasopiśmie. Zmiany i uzupełnienia merytoryczne będą dokonywane w uzgodnieniu z autorem.
8. Opinia lub uwagi recenzenta będą przekazywane Autorowi do ustosunkowania się. Nie dostarczenie poprawionego artykułu w terminie oznacza rezygnację Autora z publikacji pracy w naszym czasopiśmie.
9. Za publikację artykułów redakcja nie płaci honorarium autorskiego.
10. Adres redakcji:

Czasopismo
„Engineering of Biomaterials / Inżynieria Biomateriałów”
Akademia Górniczo-Hutnicza im. St. Staszica
Wydział Inżynierii Materiałowej i Ceramiki
al. Mickiewicza 30/A-3, 30-059 Kraków

tel. (48) 12 617 25 03, 12 617 25 61
tel./fax: (48) 12 617 45 41
e-mail: chlopek@agh.edu.pl, kabe@agh.edu.pl

Szczegółowe informacje dotyczące przygotowania manuskryptu oraz procedury recenzowania dostępne są na stronie internetowej czasopisma:
www.biomat.krakow.pl

Warunki prenumeraty

Zamówienie na prenumeratę prosimy przysyłać na adres: apowroz@agh.edu.pl, tel/fax: (48) 12 617 45 41
Cena pojedynczego numeru wynosi 20 PLN
Konto:
Polskie Stowarzyszenie Biomateriałów
30-059 Kraków, al. Mickiewicza 30/A-3
ING Bank Śląski S.A. O/Kraków
nr rachunku 63 1050 1445 1000 0012 0085 6001

Instructions for authors

1. Papers for publication in quarterly journal „Engineering of Biomaterials / Inżynieria Biomateriałów” should be written in English.
2. All articles are reviewed.
3. Manuscripts should be submitted to editorial office by e-mail to kabe@agh.edu.pl.
4. A manuscript should be organized in the following order:
 - TITLE • Authors and affiliations • Abstract (100-200 words) • Keywords (4-6) • Introduction • Materials and methods • Results and discussions • Conclusions • Acknowledgements • References
5. All illustrations, figures, tables, graphs etc. preferably in black and white or grey scale should be presented in separate electronic files (format .jpg, .gif, .tiff, .bmp) and not incorporated into the Word document. High-resolution figures are required for publication, at least 300 dpi. All figures must be numbered in the order in which they appear in the paper and captioned below. They should be referenced in the text. The captions of all figures should be submitted on a separate sheet.
6. References should be listed at the end of the article. Number the references consecutively in the order in which they are first mentioned in the text.
7. The Editors reserve the right to improve manuscripts on grammar and style and to modify the manuscripts to fit in with the style of the journal. If extensive alterations are required, the manuscript will be returned to the authors for revision.
8. Opinion or notes of reviewers will be transferred to the author. If the corrected article will not be supplied on time, it means that the author has resigned from publication of work in our journal.
9. Editorial does not pay author honorarium for publication of article.
10. Address of editorial office:

Journal
„Engineering of Biomaterials / Inżynieria Biomateriałów”
AGH University of Science and Technology
Faculty of Materials Science and Ceramics
30/A-3, Mickiewicz Av., 30-059 Krakow, Poland

tel. (48) 12) 617 25 03, 12 617 25 61
tel./fax: (48) 12 617 45 41
e-mail: chlopek@agh.edu.pl, kabe@agh.edu.pl

Detailed information concerning manuscript preparation and review process are available at the journal's website:
www.biomat.krakow.pl

Subscription terms

Subscription rates:
Cost of one number: 20 PLN
Payment should be made to:
Polish Society for Biomaterials
30/A3, Mickiewicz Av.
30-059 Krakow, Poland
ING Bank Slaski S.A.
account no. 63 1050 1445 1000 0012 0085 6001

*XXII Conference on
BIOMATERIALS
IN MEDICINE
AND
VETERINARY
MEDICINE*

*11-14 October 2012
Hotel "Perła Południa"
Rytro, Poland*

www.biomat.agh.edu.pl



SPIS TREŚCI

CONTENTS

<p>EXPRESSION PATTERN OF HISTONE H3 SUBTYPES IN ARTICULAR CHONDROCYTES A. KULCZYCKA, J. ORCHEL, A. ORCHEL, Z. DZIERŻEWICZ, I. BEDNAREK</p>	2
<p>SELF-ASSEMBLING MICELLES OBTAINED FROM PLLA/PEG AND PDLA/PEG BLOCK COPOLYMERS IN AQUEOUS SOLUTIONS X. WU, S. LI</p>	6
<p>SYNTHESIS AND PROPERTIES OF BIORESORBABLE AND HIGHLY FLEXIBLE 1,3-TRIMETHYLENE CARBONATE/ϵ-CAPROLACTONE COPOLYMERS M. PASTUSIAK, P. DOBRZYŃSKI, A. SMOLA, M. SOBOTA</p>	9
<p>DEVELOPMENT OF INNOVATIVE BIOPOLYMERS DESIGNED FOR BONE REGENERATION APPLICATIONS AND IN VITRO STUDY OF THEIR BIOCOMPATIBILITY AND OSTEOGENIC CAPACITY ON HUMAN BONE MARROW MESENCHYMAL STEM CELLS M. A. BASILE, G. GOMEZ D'AYALA, P. LAURIENZO, M. MALINCONICO, A. OLIVA</p>	13
<p>DEGRADATION ANALYSIS OF RADIOSENSITIZER CONTROL RELEASE SYSTEM BASED ON THE NMR SPECTROSCOPY A. BUSZMAN, J. KASPERCZYK, J. JAWORSKA</p>	16
<p>HARNESSING BIOPOLYESTERS IN THE DESIGN OF FUNCTIONAL MATERIALS FOR BIOMEDICAL APPLICATIONS E. RENARD, J. BABINOT, P. LEMECHKO, J. RAMIER, G. VERGNOL, D. L. VERSACE, D. GRANDE, V. LANGLOIS</p>	19

<p>BIOCOMPATIBILITY OF L-LACTIDE-CO-GLYCOLIDE-CO-TRIMETHYLENE-CARBONATE SHAPE MEMORY TERPOLYMER WITH HUMAN CHONDROCYTES R. KŁOSEK, J. KOMACKI, A. ORCHEL, K. JELONEK, P. DOBRZYŃSKI, J. KASPERCZYK, Z. DZIERŻEWICZ</p>	23
<p>DEGRADATION PROCESS OF TMC-BASED POLYMERS BY MASS SPECTROMETRY J. JAWORSKA, J. KASPERCZYK, M. MAKSYMIAK, G. ADAMUS, P. DOBRZYŃSKI</p>	26
<p>BIOMIMETIC Ca-P COATINGS OBTAINED BY CHEMICAL/ELECTROCHEMICAL METHODS FROM HANKS' SOLUTION ON A Ti SURFACE M. PISAREK, A. ROGUSKA, L. MARCON, M. ANDRZEJCZUK</p>	29
<p>A REVISED SURGICAL CONCEPT OF ANTERIOR CRUCIATE LIGAMENT REPLACEMENT IN A RABBIT MODEL. PRELIMINARY INVESTIGATIONS K. FICEK, J. WIECZOREK, E. STODOLAK-ZYCH, Y. KOSENYUK</p>	33
<p>COMPOSITE ELECTROSPUN MEMBRANES STIMULATE MINERALIZATION IN BONE CELL CULTURE I. RAJZER, E. MENASZEK</p>	35

WERSJA PAPIEROWA CZASOPISMA „ENGINEERING OF BIOMATERIALS / INŻYNIERIA BIOMATERIALÓW” JEST JEGO WERSJĄ PIERWOTNĄ
 PRINTED VERSION OF „ENGINEERING OF BIOMATERIALS / INŻYNIERIA BIOMATERIALÓW” IS A PRIMARY VERSION OF THE JOURNAL

WYDANIE DOFINANSOWANE PRZEZ MINISTRA NAUKI I SZKOLNICTWA WYŻSZEGO
 STRESZCZANE W APPLIED MECHANICS REVIEWS

EDITION FINANCED BY THE MINISTER OF SCIENCE AND HIGHER EDUCATION
 ABSTRACTED IN APPLIED MECHANICS REVIEWS

EXPRESSION PATTERN OF HISTONE H3 SUBTYPES IN ARTICULAR CHONDROCYTES

ANNA KULCZYCKA^{1*}, JOANNA ORCHEL², ARKADIUSZ ORCHEL³, ZOFIA DZIERŻEWICZ³, IŁONA BEDNAREK¹

¹ DEPARTMENT OF BIOTECHNOLOGY AND GENETIC ENGINEERING, MEDICAL UNIVERSITY OF SILESIA, NARCYZÓW 1, 41-206 SOSNOWIEC, POLAND

² DEPARTMENT OF MOLECULAR BIOLOGY, MEDICAL UNIVERSITY OF SILESIA, NARCYZÓW 1, 41-206 SOSNOWIEC, POLAND

³ DEPARTMENT OF BIOPHARMACY, MEDICAL UNIVERSITY OF SILESIA, NARCYZÓW 1, 41-206 SOSNOWIEC, POLAND

* E-MAIL: A_KULCZYCKA@WP.PL

Abstract

Three-dimensional cell culture used for tissue engineering has its own rules and directions. There is a deficiency of proliferative markers suitable for tissue engineering research when cells are cross-linked in network of fibers or suspended in hydrogel. It limits cell harvesting or impairs the flow to cell area conventional chemicals used as proliferative markers. According to current published data, the expression of replication-dependent histone H3 genes could be novel proliferative marker of cells. The intensive synthesis of H3 histones is tightly correlated with DNA synthesis and H3 mRNA is rapidly degraded when the S phase is completed or inhibited by cell cycle inhibitors. Based on this relation, non-dividing cells contain no H3 mRNA. The aim of the study was to determine expression pattern of replication-dependent H3 subtypes and tissue-specific H3/t subtype in normal human connective tissue cells. Analyzed cellular model was chondrocytes cell line due to the phenomenon that articular cartilage doesn't have natural ability to heal its injuries, consequently development of cartilage engineering is necessary. Evaluation of expression pattern was performed using Reverse Transcription PCR and reaction products were visualized on the gel electrophoresis. This study demonstrated that RT-PCR technique can be successfully used to study the expression of different histone H3 subtypes. Presented electrophoregram showed differential expression of the analyzed subtypes (no expression of H3/g and H3/t subtypes). Incubation with sodium butyrate and quantitative Real Time PCR enabled quantification of mRNA level of selected H3/d subtype. This part of study showed a significant reduction in the mRNA level of H3/d when the sodium butyrate was added. Obtained results indicated the possibility of using the expression of individual histone H3 subtype as a new proliferative marker.

Keywords: histone H3 subtypes, proliferative marker, chondrocytes, RT-PCR, sodium butyrate.

[*Engineering of Biomaterials* 113 (2012) 2-5]

Introduction

Tissue engineering allows researchers to form three-dimensional living constructs where cells proliferate, gradually settle the biomaterial and restore the desired tissue. It exploits three main components like cells, scaffolds (made of natural or synthetic polymers) and growth factors [1]. Cartilage engineering is useful in treatment of cartilage defects by ACI (autologous chondrocyte implantation), reconstruction of growth plate, facial reconstruction surgery, reconstruction of long segmental tracheal defects or treatment of urinary incontinence and vesicoureteral reflux [2]. Conventional proliferative tests, like flow cytometry, sulforhodamine B test, MTT test, alamarBlue test, immunohistochemical staining, BrdU labelling, aren't sufficient for these types of culture. In spatial cultures, when cells are suspended in hydrogel or cross-linked in a network of woven or non-woven fibers, there are some limitations in cell harvesting or flow of conventional proliferative markers to cell area. Immunostaining of proliferation-associated antigens e.g. Ki-67 or PCNA (proliferating cell nuclear antigen) also has some limitations. It was found that PCNA accumulates in cell nuclei, not only in the S phase of the cell cycle, but also during DNA repair. In turn, Ki-67 is characterized by a long half-life and the ability to accumulate throughout the cell cycle. Generally it can be concluded that there is a deficiency of methods for measuring proliferative activity for tissue engineering studies [3-5].

Because of the unique histone H3 gene expression and expression products turnover and due to deficiency of methods for measuring proliferative activity and cell viability suitable for tissue engineering studies, the expression of histone H3 subtypes may be a new marker for this field of biomedical science. H3 subtypes were chosen for two main reasons. Firstly, the intensive synthesis of DNA during S phase is tightly correlated with intensive synthesis of replication-dependent subtypes of H3 [6]. Secondly, phosphorylation of H3 (10Ser) is required in chromosome segregation and it'll be probably a very good marker of cell division [7].

The human genome contains 11 replication-dependent histone H3 genes. Ten of these codes for H3.1 protein (H3/a, H3/b, H3/c, H3/d, H3/e, H3/f, H3/g, H3/h, H3/i, H3/j) and one code for H3.2 protein (H3/n). Histone H3.1, compared to H3.2, has a single amino acid variation (Ser96 instead of Cys96). The genes encoding histone 3.1 and 3.2 are localized in three clusters on chromosome 6 (6p21.3-22) and chromosome 1 (1q21) [8]. Other genes which encode histone H3 subtypes are replacement histone H3 genes – H3.3a, H3.3b and tissue-specific histone H3 gene – H3/t. Histone H3/t probably occurs only in testis and is probably the rat TH3 homologue. The structure of that gene is similar to replication-dependent histone genes but its expression level has not been elucidated more precisely [9]. Genes which code replication-dependent subtypes are intronless and contain a stem-loop structure called 'hairpin' that forms 3'-end of mRNA. This structure is involved into processing, transport and stability of nuclear histone mRNA during replication. Histone mRNA of these subtypes is rapidly degraded both when the S phase is completed and when the DNA synthesis is inhibited by e.g. hydroxyurea. In other words, non-dividing cells contain no H3 mRNA [10,11].

The aim of the study was to determine the expression pattern of replication-dependent H3 subtypes and H3/t subtype in human connective tissue cells. Due to correlation between expression of these subtypes and DNA replication they may be new markers of proliferative activity in tissue cultures.

Materials and methods

Cell culture

Chondrocytes were purchased from Lonza. Cells were obtained from articular cartilage and maintained at 37°C and 5% CO₂ in CGM™ Chondrocyte Growth Medium. This growth medium contained supplements and growth factors like fetal bovine serum, R3-IGF-1, bFGF, transferrin, insulin and GA-1000 (aqueous solution of gentamicin sulfate and amphotericin-B) (Lonza). To study the expression of genes, chondrocytes were placed at the initial density of 2-5*10³ cells/cm² in Nunclon™ culture dishes (Nunc). The RNA isolation was performed when cells reached the state of 60% confluency.

For inhibition of DNA synthesis, 1mM, 3mM and 10mM sodium butyrate (Sigma-Aldrich) were administered to exponentially growing cells 48 hours before RNA isolation. Sodium butyrate selectively affects the activation of genes encoding proteins that block cell cycle such as, eg. p21WAF1 protein, which blocks kinase CDK2 and inhibits cell transition to the next stage of the cell cycle. The administration of this compound enabled a comparison of expression levels of selected H3 subtype in treated and untreated cells and visualized the potential changes in proliferative activity of cells.

RNA isolation

RNA preparation was carried out using NucleoSpin® kit (Macherey-Nagel). The RNA extracts were digested with DNase I to eliminate DNA contamination during the isolation procedure. RNA quantification was performed by ultrasensitive fluorescent RNA stain using Quant-IT™ RiboGreen® RNA Reagent (Invitrogen).

Reverse transcription PCR analysis and quantitative Real time PCR analysis

Evaluation of expression pattern was performed using RT-PCR (Reverse Transcription PCR). Gene-specific primers were designed using Primer Express™ 1.0 software (Abi Prism). To ensure efficient and accurate amplification of template, conditions for these reactions were optimized. The most important step in pre-standardization was the optimization of annealing temperature. The greatest specificity and efficiency of amplification for each pair of primers was at 60°C and this temperature was used in both types of reactions. The reaction mix at the final volume of 20 µl consisted of: 50 ng of RNA template, 500 nM of each primer, 2.5 units MasterAmp *Tth* DNA Polymerase, 2.5 mM MgCl₂, 0.5 mM MnSO₄, 400 µM dNTP mix, 1x MasterAmp *Tth* PCR Buffer, 1x MasterAmp PCR Enhancer (Epicentre) and sterile water. The RT-PCR reactions were performed by C-1000 Thermal Cycler (Bio-Rad). Cycling conditions were as follows: one step at 60°C for 30 min, one step at 94°C for 5 min, 35 cycles at 94°C for 30 s, 60°C for 30 s and 72°C for 1 min. RT-PCR products were detected using 2% agarose gel electrophoresis and ethidium bromide staining. Qualitative analysis of RT-PCR was carried out using LabWorks 4.0 software.

QRT-PCR (quantitative Real Time PCR) enabled detection and quantification of mRNA level of selected H3 subtype for each reaction cycle. The reaction mixture at final volume of 20 µl consisted of: 50 ng of RNA template, 200 nM of each primer, 1x Power SYBR®Green RT-PCR Mix, 1x RT Enzyme mix (Applied Biosystems) and sterile water. Reference gene was GAPDH (glyceraldehydes-3-phosphate dehydrogenase). QRT-PCR reaction was performed by DNA Engine Opticon system (Bio-Rad). Thermal conditions were as follows: one step at 48°C for 30 min, one step at 95°C for 10 min, 40 cycles at 95°C for 30 s, 60°C for 30 s and 72°C for 1 min. At the end of the QRT-PCR reaction, the melting curves were plotted.

Statistical analysis

The relative expression of selected *H3* gene in untreated and treated cells, normalized by *GAPDH* expression, was evaluated by REST© 2009 software (Qiagen).

Results

Each of 12 sequences (H3/a-H3/n, H3/t) for primer designing was obtained from <http://www.ncbi.nlm.nih.gov/sites/entrez>. The designed primers fulfilled the basic criteria for length, melting temperature, GC content, GC clamp, primer secondary structures or repeats. The length of primers was in the range from 18 bp to 28 bp, the GC content from 43% to 74%, and the melting temperature difference for each pair of primers was 2.6-2.7°C. The expected sizes of amplicons were 124-366 bp (TABLE 1).

TABLE 1. The accession numbers of sequences for primer designing and expected lengths of amplicons [bp].

H3 subtype	Accession No	Amplicon's length [bp]
H3/a	NM_003529.2	220
H3/b	NM_003537.3	224
H3/c	NM_003531.2	324
H3/d	NM_003530.3	190
H3/e	NM_003532.2	366
H3/f	NM_021018.2	226
H3/g	NM_003534.2	196
H3/h	NM_003536.2	268
H3/i	NM_003533.2	174
H3/j	NM_003535.2	303
H3/n	NM_001005464.2	124
H3/t	NM_003493.2	309

RNA was isolated from chondrocyte cell culture and measured using ultrasensitive fluorescent RNA stain. RNA concentrations isolates were between 139 and 195 µg/ml. After the pre-standardization, the proper RT-PCR reactions were carried out and products were visualized in 2% agarose gel electrophoresis. No expression of replication-dependent H3/g subtype and tissue-specific H3/t subtype was detected. All other subtypes were visualized in agarose gel with different efficiencies. The most strongly expressed subtypes were H3/d, H3/e and H3/h. The weakest expressed subtypes were H3/b and H3/n (FIG. 1A, B, TABLE 2).

In the assessment of cell cycle inhibition by sodium butyrate, H3/d subtype was used. It was chosen because of its detected expression in all types of connective tissue cell lines and its optimal length - 190 bp which reduces the risk of degradation by RNase. Results of this part of experiment were presented as levels of relative expression of H3/d. The higher decrease in expression was noticeable in the case of 3 mM sodium butyrate (FIG. 2). Melting curve analysis proved the specificity of the performed amplification reaction (FIG. 3). The results of the QRT-PCR and statistical analysis (REST©2009 software) indicated that there was a significant reduction of H3/d mRNA level when the sodium butyrate was added. The difference in transcriptional activity of the H3/d between treated chondrocytes (and untreated chondrocytes (control) was statistically significant ($p < 0,05$) (TABLE 3).

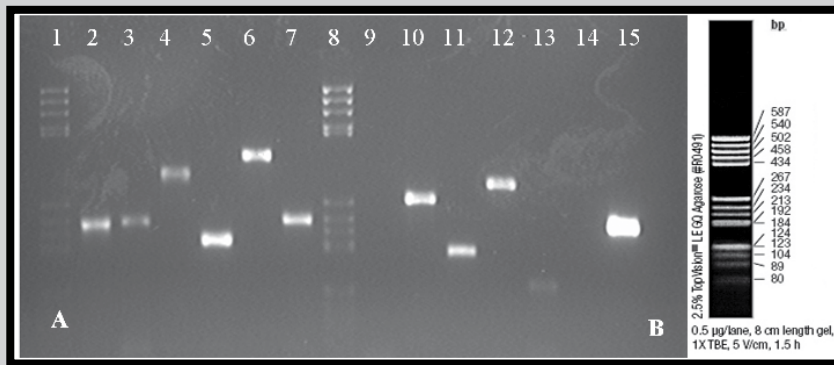


FIG. 1. A) The expression pattern of histone H3 subtypes in chondrocytes: lane 1, 8 – molecular weight marker - pBR322/BsuRI, lane 2-7, 9-14 – histone H3 subtypes, lane 15 – GAPDH. 2% agarose gel stained with ethidium bromide; **B)** Molecular weight marker pBR322/BsuRI(HaeIII) (Fermentas).

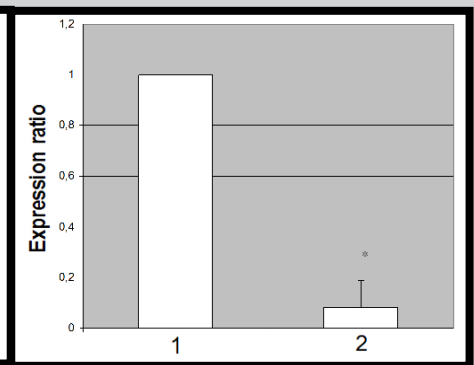


FIG. 2. The level of expression of H3/d in: 1 – untreated cells (control), 2 – cells treated by 3mM sodium butyrate.

TABLE 2. RT-PCR products visualized in agarose gel electrophoresis.

Lane	Product
1	Molecular weight marker pBR322/BsuRI
2	H3/a
3	H3/b
4	H3/c
5	H3/d
6	H3/e
7	H3/f
8	Molecular weight marker pBR322/BsuRI
9	H3/g
10	H3/h
11	H3/i
12	H3/j
13	H3/n
14	H3/t
15	GAPDH

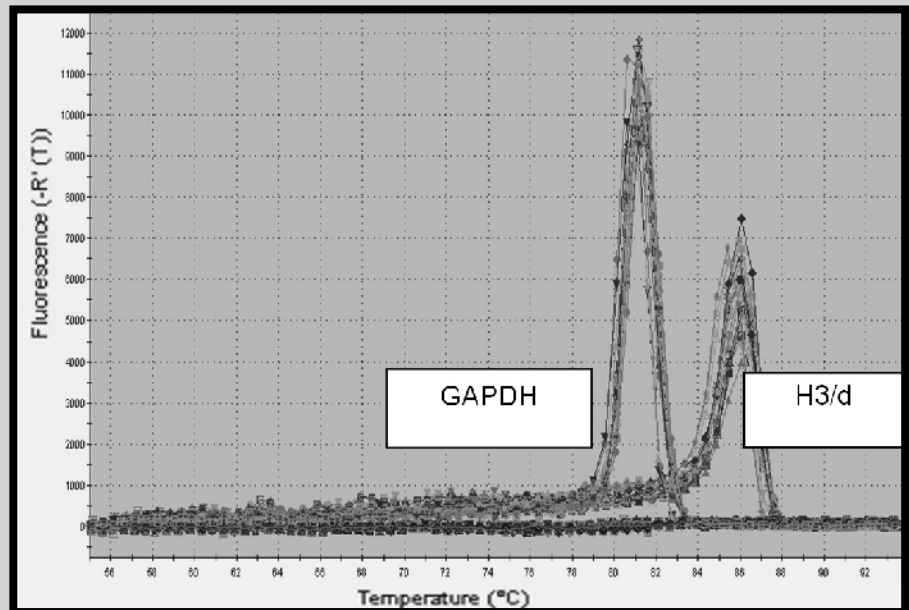


FIG 3. Melting curve analysis. First peak is for GAPDH product and second is for H3/d product.

Discussion

Tissue engineering is rapidly growing field of biomedical science. The aim of this science is to enable an effective treatment of degenerative diseases, burns and traumatic lesion using *eg.* autogenic cells which eliminate the risk of graft rejection in the recipient body. To create these implants, cells, scaffolds and growth factors are used. The presence of scaffolds allows cells to restore interactions between them and ECM (extracellular matrix) and normal cell proliferation [12]. Valid and rapid cell proliferation is needed for gradual settlement of scaffold by cells. The conventional proliferative assays, like counting mitotic figures, counting in hemocytometer or BrdU labeling, aren't sufficient for these types of cultures. It's necessary to create a rapid and effective proliferative test which enables an assessment of accurate proliferative of cells in these constructs.

This new alternative proliferative marker may be expression of replication-dependent subtypes of histone H3. In previous studies, histone mRNA was initially used in the hybridization *in situ* technique (ISH). Results of experiments using this method allow to evaluate the proliferative status at any given time, even in fixed archival samples.

TABLE 3. The values of relative expression levels and standard deviations calculated using REST©2009 software.

Sample	Relative expression level	Standard deviations
Untreated cells	1,000	-
3 mM sodium butyrate	0,081	0,039-0,186

Non-dividing cells have no detectable mRNA levels of histone H3 subtypes due to their rapid degradation after the cell division. The reason is that these subtypes don't have polyA-tail [13, 14]. Unfortunately, in the case of three-dimensional scaffolds organic reagents affect the degradation of the scaffold during the preparation of material for analysis so ISH is not recommended.

In recent studies researchers have used quantitative Real time-PCR technique and RNA protection assay to analyze expression of histone H4/i and subtypes of histone H3. Evaluation of the expression of H4/i, using QRT-PCR, was performed by Ignatus *et al* [15]. Osteoblasts used in the experiment were seeded on collagen type I scaffolds. The results indicated that the increase in mechanical load caused an increase in expression of histone H4/i in these cells. This confirmed the assumption that mechanical forces increase the proliferation of osteoblasts compared to untreated control. Koessler *et al* [16] determined the expression of 11 replication-dependent H3 subtypes in three fetal tissues (bladder, lung and liver), a diploid fibroblast line IMR-90 and seven tumor cell lines (HEK-293, Hela-S3, SAOS-2, HL-60, Hep-G2 and Capan-1) by RNase protection assay. The expression pattern of H3 subtypes in all fetal human tissues and IMR-90 line was similar. The most strongly expressed genes were *H3/m* and *H3/n*. On the other hand, the weakest expressed genes were *H3/a*, *H3/d*, *H3/f*, *H3/h* and *H3/j*. In the tumor cell lines – in the case of *H3/m*, *H3/n* and *H3/k* genes – the expression level was low or undetectable. Only in the case of Tera-2 tumor line expression of all histone H3 subtypes occurred, which is likely due to the cell line being pluripotential.

The aim of our study was to determine expression pattern of replication-dependent H3 subtypes in human connective tissue cells. According to current published data the analysis of expression of all 11 replication-dependent H3 subtypes in valid adult human cell line hasn't been performed yet. In this research, the expression pattern of histone H3 subtypes in human chondrocytes – showed no expression of histone H3/g and H3/t subtypes. No expression of histone H3/t subtype confirms probably the specificity of its occurrence in the male testis. However, no detectable level of H3/g expression may indicate either a low promoter activity, its structural changes and what's interesting a high degree of differentiation of these cells. Structural changes within promoter domains affect the regulation of expression. What is more, also alternations in the distance between two domains – CCAAT box and TATA box or CCAAT box and CCAAT box – resulted in significant loss of promoter activity [17]. Incubation with sodium butyrate depicted a decrease in the expression of H3/d gene in treated compared to untreated cells. It confirmed the statement that histone mRNA is rapidly degraded when the DNA synthesis is blocked.

The obtained results of the experiment indicate the need for further studies, using cells growing on three-dimensional scaffolds, individual chosen subtype of H3 and QRT-PCR technique, to confirm the possibility of using changes in mRNA levels of histone H3 subtype as a reliable proliferative marker for tissue engineering research.

Conclusions

(1) The results of the study demonstrated that RT-PCR can be successfully used to analyze the expression of different histone H3 subtypes. It is possible to design sets of primers allowing the specific and efficient amplification of their transcripts. (2) No expression of histone H3/g and H3/t subtypes was detected in analyzed connective human cell line. (3) Incubation with sodium butyrate – cell cycle inhibitor – led to a significant reduction in the expression level of *H3/d* gene. This conclusion indicates the possibility of using the expression of individual histone H3 subtype as a proliferative marker.

Acknowledgements

This work was supported by the European Community from the European Social Fund within the RFSD 2 project and funded by the grant MEMSTENT (brand No:UDA-POIG.01.03.01-00-123/08-04) and KNW-1-030/D/1/0.

References

- [1] Ikada Y.: Challenges in tissue engineering. *J R Soc Interface* 2006; 3(10): 589-601.
- [2] Lin Z., Willers C., Xu J., Zheng M.H.: The chondrocyte: biology and clinical application. *Tissue Eng* 2006; 7(12): 1971-1984.
- [3] Bosch F.X., Udvarhelyi N., Venter E., Herold-Mende C., Schuhmann A., Maier H., Weidauer H., Born A.I. Expression of the histone H3 gene in benign, semi-malignant and malignant lesions of the head and neck: a reliable proliferation marker. *Eur J Cancer* 1993; 29A(10): 1454-1461.
- [4] Rautiainen E., Haapasalo H., Sallinen P., Rantala I., Helen P., Helin H.: Histone mRNA in-situ hybridization in astrocytomas: a comparison with PCNA, MIB-1 and mitoses in paraffin-embedded material. *Histopathology* 1998; 32(1): 43-50.
- [5] Muskhelishvili L., Latendresse J.R., Kodell R.L., Henderson E.B.: Evaluation of cell proliferation in rat tissues with BrdU, PCNA, Ki-67(MIB-5) immunohistochemistry and in situ hybridization for histone mRNA. *J Histochem Cytochem* 2003; 51(12):1681-1688.
- [6] Wong D.T.W., Chou M.Y., Chang L.C., Gallagher G.T.: Use of intracellular H3 messenger RNA as a marker to determine the proliferation pattern of normal and 7,12-dimethylbenz[*a*]anthracene-transformed hamster oral epithelium. *Cancer Res* 1990; 50(16): 5107-5111.
- [7] Tian X., Xu J., Zhou H., Liu R., Chen J., Huang X.: Thr 3 phosphorylated histone H3 concentrates at centromeric chromatin at metaphase. *Biochem Biophys Res Commun*. 2010;401(4):618-23.
- [8] Doenecke D., Albig W., Bode C., Drabent B., Franke K., Gavenis K., Witt O.: Histones: gene diversity and tissue-specific gene expression. *Histochem Cell Biol* 1997; 107: 1-10.
- [9] Govin J., Caron C., Rousseaux S., Khochbin S.: Testis-specific histone H3 expression in somatic cells. *Trends Biochem Sci*. 2005; 30(7):357-359.
- [10] Dominski Z., Marzluff W.F.: Formation of the 3' end of histone mRNA. *Gene* 1999;239: 1-14.
- [11] Brock W.A., Trostle-Weige P.K., Williams M., Meistrich M.L.: Histone and DNA synthesis in differentiating and rapidly proliferating cells in vivo and in vitro. *Cell Differ* 1983; 12(1): 47-55
- [12] Koh C.J., Atala A.: Tissue engineering, stem cells, and cloning: opportunities for regenerative medicine. *J Am Soc Nephrol* 2004; 15(5): 1113-1125.
- [13] Slowinski J., Mazurek U., Bierzynska-Macyszyn G.: Histone mRNA In situ hybridization In assessing proliferative activity of normal and malignant cells. *Folia Histochemica et Cytobiologica* 2002 ; 40(4): 335-339.
- [14] Chou M.Y., Chang A.L.C., McBride J., Donoff B., Gallagher G.T., Wong D.T.: A rapid method to determine proliferation patterns of normal and malignant tissues by H3 mRNA in situ hybridization. *Am J Pathol* 1990; 136: 729-733.
- [15] Ignatius A., Blessing H., Liedert A., Schmidt C., Neidlinger-Wilke C., Kaspar D., Friemert B., Claes L.: Tissue engineering of bone: effects of mechanical strain on osteoblastic cells in type I collagen matrices. *Biomaterials* 2005; 26(3): 311-318.
- [16] Koessler H., Doenecke D., Albig W.: Aberrant expression pattern of replication-dependent histone H3 subtype genes in human tumor cell lines. *DNA and Cell Biology* 2003; 22(4): 233-240.
- [17] Koessler H., Kahle J., Bode C., Doenecke D., Albig W.: Human replication-dependent histone H3 genes are activated by a tandemly arranged pair of two CCAAT boxes. *Biochem J* 2004; 384(2): 317-326.

SELF-ASSEMBLING MICELLES OBTAINED FROM PLLA/PEG AND PDLA/PEG BLOCK COPOLYMERS IN AQUEOUS SOLUTIONS

XIAOHAN WU, SUMING LI*

MAX MOUSSERON INSTITUTE ON BIOMOLECULES, UMR CNRS 5247, UNIVERSITY MONTPELLIER I, 34060 MONTPELLIER, FRANCE

* E-MAIL: LISUMING@UNIV-MONTP1.FR

Abstract

A series of poly(lactide-poly(ethylene glycol) (PLA-PEG) block copolymers were synthesized by ring-opening polymerization of L- or D-lactide in the presence of mono- or dihydroxyl PEG, using nontoxic zinc lactate as catalyst. Micelles were then prepared by direct dissolution of the obtained copolymers in aqueous medium without heating or using any organic solvents. Aqueous gel permeation chromatography and dynamic light scattering measurements were carried out to characterize the resulting micelles. Generally, mixed micelles containing both PLLA/PEG and PDLA/PEG copolymers appear larger and more compact compared to single ones. However, the size of mixed micelles is smaller than that of single ones which exhibit an anisotropic structure since stereocomplexation disfavors the formation of anisotropic micelles. The copolymer parameters such as structures, molar mass and PEG fraction strongly influence the formation of anisotropic micelles, and thus lead to various micellar sizes.

Keywords: poly(lactide), poly(ethylene glycol), stereocomplexation, self-assembly, anisotropy

[*Engineering of Biomaterials* 113 (2012) 6-8]

Introduction

In the past decades, nanoparticles, micelles and vesicles prepared by self-assembly of amphiphilic copolymers have been widely investigated for applications in the field of sustained drug delivery [1]. Compared to conventional drug administration routes, these drug delivery systems (DDS) present numerous advantages such as constant blood drug concentration, reduced drug dosage, decreased drug administration frequency, reduced side effects, etc. Among all the polymers used for DDS, poly(lactide/poly(ethylene glycol) (PLA/PEG) copolymers appear the most promising due to their outstanding properties [2]. In fact, PLA exhibits good biocompatibility and degradability, while PEG is well soluble in water and in most organic solvents, non-toxic and can be eliminated through kidney filtration when the molar mass is below 30000.

Stereocomplexation between PLLA and PDLA was found to improve the properties of PLA/PEG micelles [3,4]. Kang et al. reported that the "stereocomplex-type" micelles derived from PLLA/PEG and PDLA/PEG copolymers exhibit higher aggregation number, smaller volume, and more compact structure compared to single micelles [3]. However, our previous work showed that the average size of mixed micelles is smaller than single micelles for some copolymers [4]. On the other hand, aqueous gel permeation chromatography (GPC) allowed to identify both peaks of micelles and free copolymers, and to determine the aggregation number of micelles [5].

Therefore, it is of great interest to comparatively investigate the properties of single and mixed micelles.

In this work, a series of PLA/PEG block copolymers were synthesized and characterized. Self-assembling micelles by direct dissolution in water were investigated by aqueous GPC, dynamic light scattering and transmission electron microscopy (TEM), taking into account the effects of stereocomplexation between PLLA and PDLA blocks for different copolymers.

Materials and methods

L-lactide and D-lactide were obtained from Purac and purified by crystallization from ethyl acetate. Monomethoxy poly(ethylene glycol) (mPEG) with molar masses of 2000 and 5000 and dihydroxyl PEG with molar masses of 2000, 4000 and 8000 were supplied by Fluka. Zinc lactate was purchased from Sigma. All organic solvents were of analytic grade and used without further purification.

PLA/PEG block copolymers were synthesized by ring-opening polymerization as described previously. Briefly, predetermined amounts of PEG and L- or D-lactide were introduced in a polymerization ampoule, the initial molar ratio of ethylene oxide to lactyl repeat units (EO/LA) ranging from 2 to 6. Zinc lactate (0.1 wt%) was then added. After degassing, the ampoule was sealed under vacuum, and polymerization was allowed to proceed at 130°C for 3 days. After that, the product was recovered by dissolution in dichloromethane and precipitation in diethyl ether. The product was finally dried under vacuum up to constant weight.

Predetermined amounts of PLLA/PEG, PDLA/PEG or their equal molar mixtures were dissolved in distilled water under stirring at room temperature for 2 hours, yielding homogeneous micellar solutions with different concentrations.

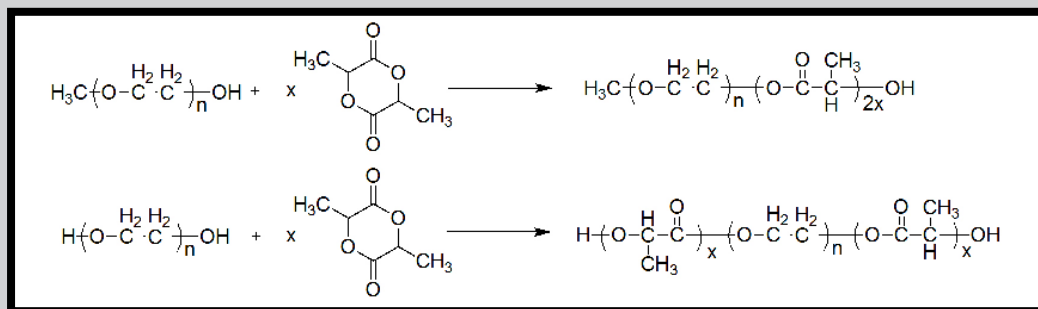
Proton nuclear magnetic resonance (¹H NMR) spectra were recorded at room temperature with a Bruker spectrometer operating at 250 MHz by using CDCl₃ as solvent. The relaxation delay used for ¹H-NMR spectra was 800 msec, and chemical shifts (δ) were given in ppm using tetramethylsilane as an internal reference.

Gel permeation chromatography (GPC) measurements in organic solvent were performed on a Waters 410 apparatus equipped with a RI detector. THF was used as the mobile phase at a flow rate of 1.0 ml/min. All the solutions were prepared at a concentration of 10 g/L and filtered through 0.22 μ m Millipore filters. 20 μ l of solution were injected for each analysis. Calibration was accomplished with polystyrene standards (Polysciences, Warrington, PA).

GPC measurements in aqueous medium were carried out with a series of 3 columns, PL aquagel-OH 30, 40 and 50, Polymer Laboratories Corporation, connected with an RI detector. Water/methanol (80:20, v/v) was used as the eluent at a flow rate of 1.0 ml/min at room temperature. PEG was used as standards for the calibration. All the solutions were prepared at a concentration of 5 g/L and filtered through 0.45 μ m Millipore membrane filters before injection.

Dynamic light scattering (DLS) was carried out on a Sympatec Nanophox equipment with vertically polarized incident light of wavelength $\lambda = 632.8$ nm supplied by a HeNe-Laser operating at 10 mW max. Measurements were made at 25°C and at an angle of 90°. All the solutions were filtered through 0.80 μ m Millipore membrane filters. The autocorrelation functions from DLS were analyzed by using the photon cross correlation spectroscopy (PCCS) method to obtain the diameter distributions.

TEM was performed on a Hitachi H-600 electron microscope, operating at an accelerating voltage of 75 kV. One drop of micelle solution was placed on a copper grid covered with nitrocellulose membrane and air dried before measurement.



SCHEME 1. Ring opening polymerization of L- or D-lactide in the presence of mono- and dihydroxyl PEG.

Results and Discussions

Both diblock and triblock PLA/PEG copolymers were synthesized by ring-opening polymerization of L- or D-lactide in the presence of mono- or dihydroxyl PEG (SCHEME 1). The reaction was performed at 130°C for 3 days. Zinc lactate was used as catalyst instead of stannous octoate or other catalysts which are more or less cytotoxic. The yield of the reactions ranged from 80 to 90%.

TABLE 1. Molecular characteristics of PLA/PEG copolymers.

Acronym	Copolymer	M _n PEG	EO/LA ^a	DP _{PEG} ^b	DP _{PLA} ^c	M _n ^d	M _n ^e	D ^f
L1	EO ₄₅ L ₁₂	2000	3.85(3.0) ^g	45	12	2864	4860	1.18
D1	EO ₄₅ D ₁₂	2000	3.80(3.0)	45	12	2864	4810	1.17
L2	EO ₁₁₃ L ₃₂	5000	3.55(3.0)	113	32	7304	9110	1.11
D2	EO ₁₁₃ D ₃₁	5000	3.63(3.0)	113	31	7232	9590	1.12
L3	L ₁₀ EO ₄₅ L ₁₀	2000	2.23(2.0)	45	20	3440	5510	1.13
D3	D ₁₁ EO ₄₅ D ₁₁	2000	2.12(2.0)	45	21	3512	5630	1.15
L4	L ₁₂ EO ₉₁ L ₁₂	4000	3.75(3.0)	91	24	5728	8460	1.10
D4	D ₁₁ EO ₉₁ D ₁₁	4000	4.10(3.0)	91	22	5584	8380	1.08

^a Calculated from the integration of NMR bands belonging to PEG block at 3.6 ppm and to PLA block at 5.2 ppm.

^b DP_{PEG} = M_{nPEG} / 44.

^c DP_{PLA} = DP_{PEG} / (EO/LA).

^d M_n = M_{nPEG} + DP_{PLA} • 72.

^e Determined by GPC.

^f Polydispersity index, determined by GPC.

^g Date in parentheses represent the EO/LA ratio in feed.

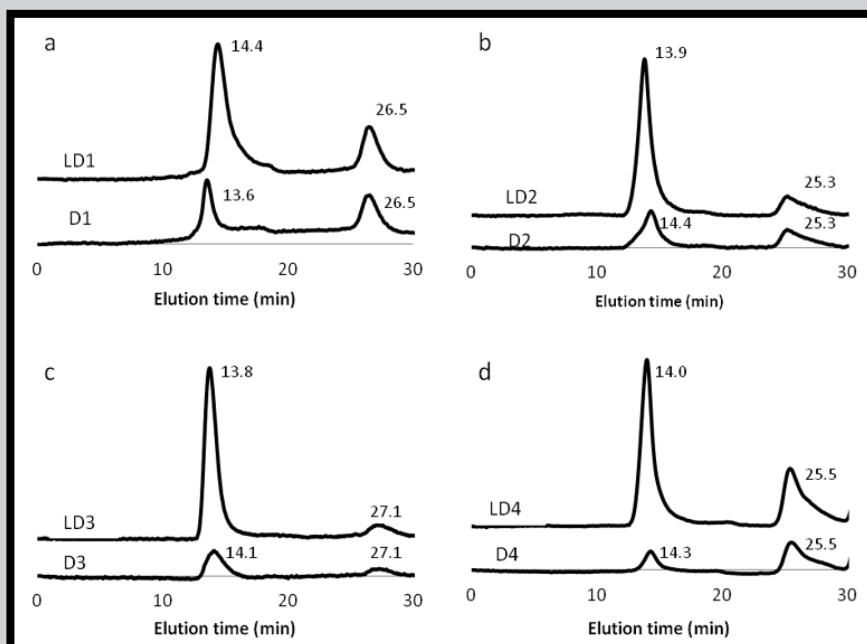


FIG. 1. Aqueous GPC chromatograms of single and mixed micelles at 5 g/l: a) D1 and LD1, b) D2 and LD2, c) D3 and LD3, d) D4 and LD4.

TABLE 1 presents the molecular characteristics of the resulting copolymers, including number average molar mass (M_n), molar mass distribution (D=M_w/M_n), and copolymer composition as determined by using ¹H NMR and GPC. ¹H NMR measurements allowed to determine the composition of various PLA/PEG copolymers from the integrations of NMR resonances belonging to the methylene protons of ethylene oxide units of PEG at 3.6 ppm and to the methine proton of lactyl units of PLA at 5.2 ppm. For the sake of clarity,

the triblock copolymers are named as L_xEO_yL_x or D_xEO_yD_x, and the diblock copolymers as EO_yL_x or EO_yD_x. In these acronyms, L, D, and EO represent PLLA, PDLA, and PEG blocks, respectively, x and y representing the number-average degree of polymerization of corresponding blocks. As reported in our previous work, the EO/LA ratio of the copolymers was found to be higher than the feed ratio because the conversion of lactide was not complete, and unreacted lactide was eliminated by the purification procedure [6]. The polydispersity index is inferior to 1.2 for all copolymers, in agreement with narrow molar mass distributions.

Aqueous GPC was employed to evaluate the average size of micelles (FIG. 1). Two peaks are observed on the GPC curves of both D1 and LD1 micelles: the peak at long elution time is assigned to free copolymer chains, while the one at short elution time belongs to the micelles. The peak at long elution time appears at 26.5 min for both solutions because the two copolymers have the same molar mass (TABLE 1). In contrast, the two samples present different elution times for micelles: the peak of D1 is detected at 13.6 min, and that of LD1 at 14.4 min. This indicates that the size of D1 micelles is larger than that of LD1 ones although the absolute molar masses cannot be determined as the peaks are beyond the calibration range. In contrast, the situation seems different in the case of D2 and LD2 micelles as shown in FIG. 1b. In fact, the peak of D2 micelles is detected at 14.4 min, and that of LD2 micelles at 13.9 min, while the peaks of free copolymers appearing at the same elution time, i.e. 25.3 min. Similar results were also found in D3/LD3 and D4/LD4 samples, which indicates that the size of mixed micelles is larger than that of single ones.

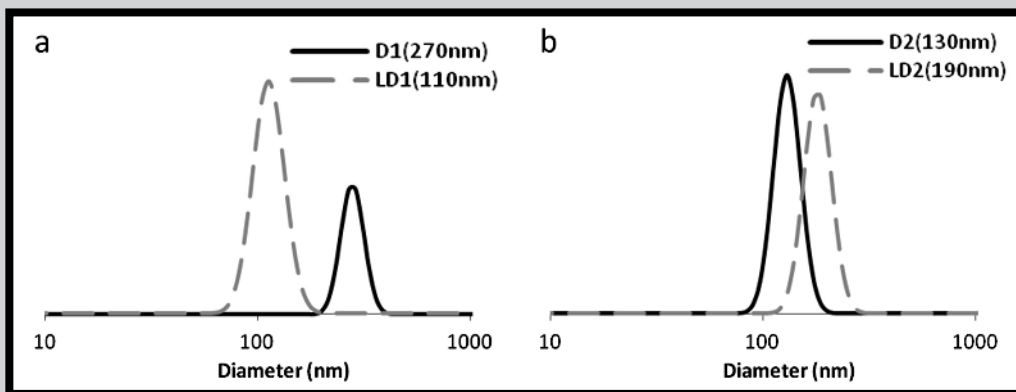


FIG. 2. DLS graphs of single and mixed micelles at 5 g/l: a) D1 and LD1, b) D2 and LD2.

The micellar size was determined by DLS measurements in comparison with aqueous GPC results. FIG. 2 shows that the size decreases from 270 nm for D1 to 110 nm for LD1 micelles, but increases from 130 nm for D2 to 190 nm for LD2 micelles. Therefore, the same size variation tendency was found in both aqueous GPC and DLS measurements. The size of mixed micelles is larger than single ones for most copolymers, except in the case of D1/LD1 micelles.

TEM measurements were then carried out to examine the morphology of the micelles. According to previously reported literature data, all the copolymers in this work are supposed to form spherical micelles in aqueous solution due to high PEO fraction [7]. Interestingly, large anisotropic micelles were found for D1 sample, while all other samples exhibit spherical structures (FIG. 3). The formation of anisotropic micelles well explained the different size variations of micelles for all the copolymers. In fact, stereocomplexation leads to larger size and more compact structure in the case of spherical micelles, as Kang et al. reported previously [3]. On the other hand, stereocomplexation disfavors the formation of anisotropic micelles [8]. Therefore, for the copolymers able to form anisotropic micelles, mixed micelles appear smaller compared to single ones. The formation of anisotropic micelles depends on the copolymer parameters such as PEG fraction, molar mass, stereocomplexation, etc., as reported in our previous work [8].

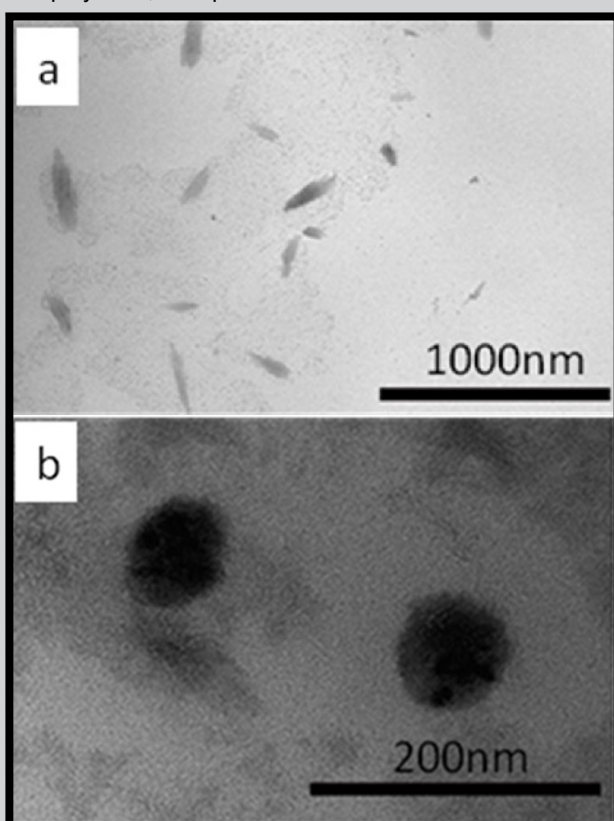


FIG. 3. TEM micrographs of single and mixed micelles at 5 g/l: a) D1 micelles, b) LD1 micelles.

Conclusions

The variation of micellar size as a consequence of stereocomplexation was investigated for a series of copolymers with different structures, molar masses and PEG fractions. Both aqueous GPC and DLS measurements show that the size of mixed micelles is larger than single ones for most copolymers. In the case of D1 and LD1 micelles, however, opposite behavior was observed, LD1 mixed micelles appearing larger than D1 single ones. This difference is well explained by the formation of anisotropic micelles in the case of D1 copolymer as shown in TEM images. Therefore, stereocomplexation leads to a larger size and more compact structure of spherical micelles, as reported previously [3]. However, the size of mixed micelles is smaller than that of single ones which exhibit an anisotropic structure since stereocomplexation disfavors the formation of anisotropic micelles as reported in our previous work [8]. The copolymer parameters such as structures, molar mass and PEG fraction strongly influence the formation of anisotropic micelles, and thus lead to various micellar sizes.

References

- [1] G.S. Kwon, K. Kataoka: Block copolymer micelles as long-circulating drug vehicles. *Adv. Drug Deliv. Rev.* 16 (1995) 295-309.
- [2] S.M. Li: Bioresorbable hydrogels prepared through stereocomplexation between poly(L-lactide) and poly(D-lactide) blocks attached to poly(ethylene glycol). *Macromol. Biosci.* 3 (2003) 657-661.
- [3] N. Kang, M.E. Perron, R.E. Prud'homme, Y.B. Zhang, G. Gaucher, J.C. Leroux: Stereocomplex block copolymer micelles: core-shell nanostructures with enhanced stability. *Nano Lett.* 5 (2005) 315-319.
- [4] L. Yang, Z.X. Zhao, J. Wei, A. El Ghzaoui, S.M. Li: Micelles formed by self-assembling of polylactide/poly(ethylene glycol) block copolymers in aqueous solutions. *J. Colloid Interface Sci.* 314 (2007) 470.

- [5] L. Yang, X. Qi, P. Liu, A. El Ghzaoui, S.M. Li: Aggregation behavior of self-assembling polylactide/poly(ethylene glycol) micelles for sustained drug delivery. *Int. J. Pharm.* 394 (2010) 43-49.
- [6] S.M. Li, M. Vert: Synthesis, characterization and stereocomplex-induced gelation of block copolymers prepared by ring opening polymerization of L(D)-lactide in the presence of poly(ethylene glycol). *Macromolecules* 36 (2003) 8008-8014.
- [7] F. Ahmed, D.E. Discher: Self-porating polymersomes of PEG-PLA and PEG-PCL: hydrolysis-triggered controlled release vesicles. *Journal of Controlled Release* 96 (2004) 37-53.
- [8] X. WU, A.E. Ghzaoui, S. Li: Anisotropic self-assembling micelles prepared by the direct dissolution of PLA/PEG block copolymers with a high PEG fraction. *Langmuir* 27 (2011) 8000-8008.

SYNTHESIS AND PROPERTIES OF BIORESORBABLE AND HIGHLY FLEXIBLE 1,3-TRIMETHYLENE CARBONATE/ ϵ -CAPROLACTONE COPOLYMERS

MAŁGORZATA PASTUSIAK, PIOTR DOBRZYŃSKI*, ANNA SMOLA, MICHAŁ SOBOTA

POLISH ACADEMY OF SCIENCES,
CENTRE OF POLYMER AND CARBON MATERIALS,
34 SKŁODOWSKA-CURIE STREET, 41-819 ZABRZE, POLAND
* E-MAIL: PDOBRZYNSKI@CMPW-PAN.EDU.PL

Abstract

Ethyl ethoxy zinc (II) has been prepared and emerged as very effective initiators for ring-opening polymerization of 1,3-trimethylene carbonate (TMC) and its copolymerization with ϵ -caprolactone (CL) to produce high molar mass polymers. The copolymerization of TMC and CL was performed in bulk at 120°C. The obtained copolymers were characterized by multiblock microstructure. The highest reactivity rate was demonstrated by trimethylene carbonate in comparison with ϵ -caprolactone monomer. The thermal and mechanical properties of the copolymers were strongly dependent on the monomer composition. Preliminary tests of monomers copolymerization using reactive extrusion yielded positive result.

Keywords: copolymerization, caprolactone, trimethylene carbonate, bioresorbable polymers

[Engineering of Biomaterials 113 (2012) 9-12]

Introduction

The recent rapid progress of many medical disciplines creates the need numerous new bioresorbable materials with physical and biological properties tailored strictly to a particular purpose. In many cases, for manufacturing bioresorbable implants such as nerve guides, stents, or scaffolds for culturing fibroblasts, very flexible, biocompatible and biodegradable materials with good tensile strength are required. For such applications, aliphatic polyester copolymers or poly (ester-co-carbonates) containing flexible carbonate and caproyl units in chain composition seem to be very useful. Introduction of carbonate linkages into a rigid polymer chain not only improves the elasticity of final copolymers, but also influences the hydrolytic degradation profiles and decreases total acidity of the degradation products. Copolymers of ϵ -caprolactone (CL) and trimethylene carbonate (TMC) due to its high permeability to drugs, and very good mechanical properties and flexibility seem to be very interesting, especially for many applications as carriers in controlled drug release systems or as a material for forming different kinds of scaffolds and membranes used in tissue engineering.

Copolymers of CL and TMC were mostly prepared according to ring opening polymerization (ROP) using different metal complexes as insertion-coordination initiators, as well as; stannous octoate [1,2], lanthanide or yttrium tripropoxide [3], lanthanide phenoxide complexes [4] or acetylacetonate zirconium (IV) [5]. The A-B-A triblock copolymers of TMC/CL were prepared with 2,2-dibutyl-2-stanna-1,3-dioxepane (DSDOP) [6].

In this publication we are presenting studies on the ROP of cyclic TMC with CL in the presence of simple, practically nontoxic ethoxy ethyl zinc (II) complex as an initiator. This compound has proven to be very active and effective initiator of the copolymerization and allowed to obtain copolymers with yield of nearly 100% within several minutes. The high reaction rate, high efficiency and not specially demanding conditions for its conducting, led us to attempt the synthesis of TMC/CL copolymers directly with extruder, thus combining the synthesis of these copolymers with processing.

Materials and Methods

Monomers and initiators

The used cyclic 1,3-trimethylene carbonate (TMC) was obtained from Boehringer (Ingelheim, Germany) and purified by recrystallization from dried ethyl acetate. The second monomer; ϵ -caprolactone (ϵ -CL) (Fluka) was distilled in vacuum over freshly powdered calcium hydride before use. Ethyl ethoxy zinc (II) was synthesized in our laboratory. This compound was obtained after reaction of diethylzinc (1,1 M solution in toluene -Aldrich) with absolute ethyl alcohol 99.8% pure p.a. (POCH Gliwice) conducted in anhydrous tetrahydrofuran (THF) 99.9 % (Aldrich) solution at 60°C.

Synthesis of poly(trimethylenecarbonate) and trimethylene/ ϵ -caprolactone copolymers

TMC model polymerization reaction was carried out within one hour in THF solution and with the presence of ethyl ethoxy zinc (II) as the initiator and initiator to monomer molar ratio (I/M) as 1: 10, at 90°C. The resulting oligomer TMC solution was hydrolyzed, to separate the zinc compounds by mixing with a small amount of hydrochloric acid solution in THF. The volume of evolved gas which was obtained during this reaction was measured using a burette filled with anhydrous ethanol, connected directly to the reaction vessel.

The process of trimethylene carbonate with ϵ -caprolactone copolymerization was conducted in bulk. The produced copolymers were purified from residual monomer by dissolving in chloroform and then precipitation in cold methanol. The final product was dried at 45°C in vacuum.

Preliminary tests of 1,3-trimethylene carbonate with ϵ -caprolactone copolymerization and processing by reactive extrusion were conducted with the use of Haake MiniLab IIs micro-extruder. The monomers with a proper amount of initiator (M/I rate as 1000/1) were placed in a dry, cooled glass ampoule (approximately at 7-10°C) in argon atmosphere. Then, the premixed whole content of this ampoule was introduced by specially designed dispenser to the extruder, previously heated to temperature of 120°C and mixing with bypass cycle was started. The conical screws' rotation of the device was set up at the maximum - 300 rpm. During stirring of the mixture, temperature and torque was continuously monitored. After 4 minutes, we observed rapid growth of torque to a virtually constant value, which indicated a strong increase of mixture viscosity due to its high conversion. At this moment, we switched the mode cycle of device and extruded samples in the form of a wire with diameter of 5 mm.

Measurements

The conversion of the reaction was determined with ^1H NMR spectroscopy. The ^1H NMR spectra were recorded at 600 MHz with Avance II Bruker TM at 25°C. Dried chloroform- d_6 was used as solvent and tetramethylsilane was applied as the internal standard.

The number-average and weight-average molar masses (M_n and M_w , respectively) as well as dispersity indexes (M_w/M_n) of the copolymers were determined by gel permeation chromatography with a Viscotek RImax chromatograph. Chloroform was used as the eluent; the temperature and the flow rate were 35°C and 1 mL/min, respectively. Two PL Mixed E columns with a Viscotek model 3580 refractive index detector and injection volume equal to 100 μ L were used. The molar masses of copolymers were calibrated with polystyrene standards but the correct M_n value for PTMC was determined by appropriate conversion, according to the method described by Kricheldorf et al. [7].

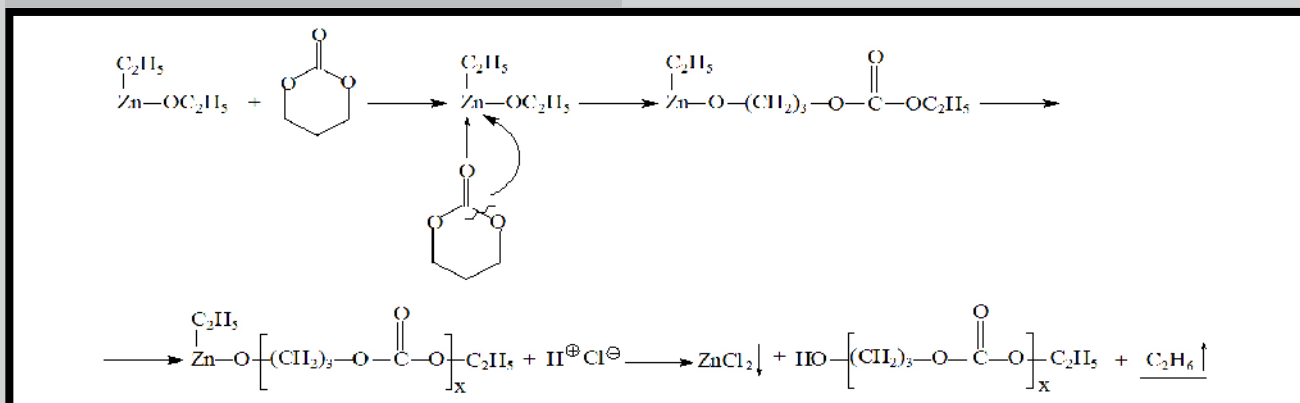
Thermal properties, such as glass transition temperatures and enthalpies of crystallization or melting, were studied by differential scanning calorimeter using a DSC Du Pont 1090B apparatus calibrated with gallium and indium.

Results and Discussions

Proposed mechanism of TMC polymerization initiated with ethyl etoxy zinc (II)

To know the TMC polymerization mechanism, the model reaction with using ethyl etoxy zinc (II) as an initiator and with I/M ratio as 1:10 was carried out. Then, we hydrolyzed the products by reaction with solution of hydrochloric acid, in order to separate the metal in the form of zinc chloride (II) from the organic part. During this reaction strong emission of ethane was observed (SCHEME 1).

SCHEME. 1. Proposed mechanism of TMC initiated with ethyl etoxy zinc (II).



The measured amount of evolved gas and maintained reaction stoichiometry indicates that polymer chain growth occurred only on the ethoxy groups of the initiator, as shown in diagram (FIG. 1). The obtained average molar mass of the final product proved the proposed mechanism too. The number average molar mass of the final TMC oligomer, calculated both on the basis of the number of formed oligomers end groups (^1H NMR measurements) and with GPC measurements (after appropriate conversion due to the applied calibration styrene standards [7]) was close to the theoretical, calculated value, taking into account the possibility of chain propagation on only one ligand of started initiating complex. Analysis of the NMR spectra revealed that the coordination of TMC monomer to the central metal atom, and then ring opening of this cyclic monomer and its insertion between the central zinc and the ethoxy group (metal – oxygen bond) was the first initiation stage of observed polymerization. The growth of polycarbonate chain on the ligand formed this way was the next main stage of this reaction according to the well-known coordination – insertion mechanism.

If during the initiation of the tested reaction, the insertion reaction was followed also by the opening of the ethyl ligand's metal-carbon bond, we would observe propagation of two polymer chains on one initiation complex, which means that after the hydrolysis of the resulting polycarbonate the average molar mass of final products would be about twice lower than this calculated theoretically with our previous assumption. If the investigated reaction proceeded according to this hypothetical mechanism with insertion on both ligands we would not observe the gas evolution during hydrolysis of polymerization product because of lack of metal-carbon bindings in this case too.

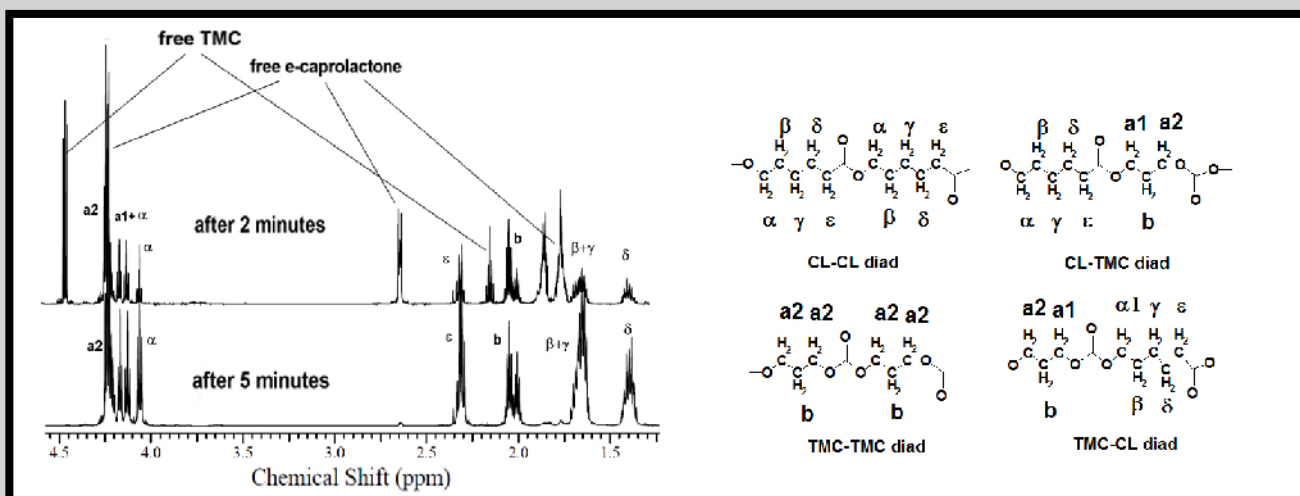


FIG. 1. ^1H NMR spectra (in CDCl_3) of equimolar ϵ -caprolactone/TMC copolymer obtained with $\text{Zn}(\text{OC}_2\text{H}_5)_2(\text{C}_2\text{H}_5)$ at different conversion after 2 minutes or 5 minutes of reaction.

TABLE 1. Results of TMC with CL copolymerization.

No.	TMC ⁰ [mol %]	TMC ^N [mol %]	Time [min]	C [%]	M _n [kDa]	D	L _{CL}	L _T
1	15	17	18	98	78.2	1.7	6.6	1.6
2	30	31	15	~100	92.1	2.1	3.7	1.6
3	40	40	10	~100	110.2	2.0	2.8	1.9
4	70	70	10	~100	140.2	2.0	3.1	7.2
5	85	86	8	99	150.2	2.1	2.0	11.5
6	100	100	5	~100	128.0	2.1	-	-

Where: TMC⁰ - initial feed molar fraction of TMC, TMC^N - feed molar fraction of TMC in the product, C - total conversion of copolymerization, M_n - number average molar mass, calibration with polystyrene standards, D - molar mass dispersion, L_{CL}, L_{TMC} - average length of caproyl and carbonate microblock calculated with NMR. Copolymerization in bulk, at 120°C with M/I ratio as 800/1.

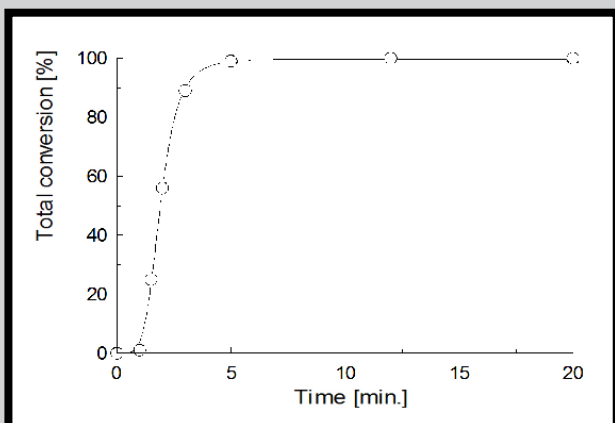


FIG. 2. Total conversion of monomers in copolymerization with M/I ratio as 800:1 of equimolar mixture of TMC with CL, initiated with $\text{Zn}(\text{OC}_2\text{H}_5)_2(\text{C}_2\text{H}_5)$ and carried out in bulk at 120°C.

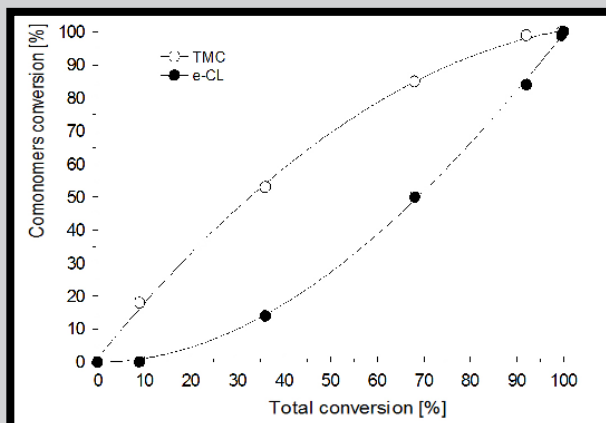


FIG. 3. Dependence of the CL and TMC conversion on the total conversion of the copolymerization. The starting CL/TMC molar ratio was of 1:1, initiated with $\text{Zn}(\text{OC}_2\text{H}_5)_2(\text{C}_2\text{H}_5)$, with M/I ratio as 800:1 and carried out in bulk at 120°C.

Synthesis and characterization of copolymers

A series of TMC/CL copolymers with different composition, using ethyl etoxy zinc (II) as an initiator was obtained. The results are presented in TABLE 1 and FIG. 1.

The conducted copolymerization yielded rather surprising results. At a relatively short period, after several minutes (FIG. 2), regardless of the composition of the reaction mixture, we obtained almost total conversion of both comonomers. The resulting copolymers were characterized with high molar masses, close to the expected values. The copolymer chain propagation proceeded only on one ethanolic ligand, similar to the previously investigated TMC homopolymerization. During the investigated copolymerization, TMC comonomer presented higher reactivity than CL (FIG. 3), in contrast to the case of TMC/CL copolymerization conducted with the use of $\text{Zr}(\text{acac})_4$ [5] or $\text{Sn}(\text{oct})_2$ [4]. The obtained copolymers presented multiblock chain structure, significantly different from those obtained using aforementioned initiators. The reason for this phenomenon was mainly a low rate of intermolecular transesterification, significantly lower than during the copolymerization initiated by zirconium or tin compounds.

Copolymerization of TMC with CL using reactive extrusion

During our investigations, we tried to carry out continuous production of TMC/CL bioresorbable products by reactive extrusion, according to the method presented above. For this purpose, copolymerization of TMC (about 85 mol.%) with CL and processing of obtaining TMC/CL copolymers in properly equipped laboratory extruder was conducted (FIG. 4). We obtained samples of high molar mass copolymers with good yield and composition practically this same as started reaction mixture, in form of extruded homogenous rods. The obtained results are presented in TABLE 2.

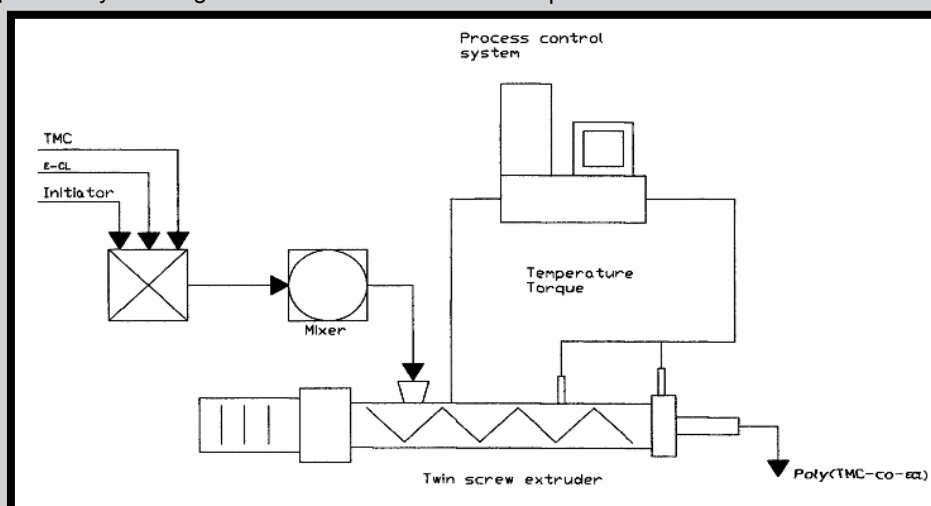


FIG. 4. Scheme of the TMC/CL copolymerization with extruder use.

TABLE 2. Results of TMC/CL copolymers obtained with extruder.

No.	TMC:CL copolymer [mol %]	Time [min]	C [%]	M_n [kDa]	D
1	87 : 13	5	98	201.1	2.2
2	88 : 12	4	92	195.5	2.2

Where: C – total conversion of monomers, Time – time of reaction and extrusion cycle, M_n – average number molar mass of obtained copolymer, D – molar mass dispersity

TABLE 3. Thermal and mechanical properties of TMC/CL copolymers.

No.	TMC:CL copolymer [mol %]	T_g [°C]	ΔH_m [J/g]	T_m [°C]	E [MPa]	σ_{max} [MPa]	ϵ_{max} [%]	σ_{break} [MPa]
1	19:81	-46.6	36.5	56.3	112.7	12.6	1500	12.6
2	50:50	-37.5	-	-	12.9	1.5	1500	1.46
3	82:18	-14.7	-	-	3.2	0.8	105	0.43

Where: T_g – glass transition temperature, ΔH_m – heat of melting, T_m – melting temperature, E- Young's modulus; $\sigma_{max, break}$ – maximal stress, stress at break; ϵ_{max} – maximal elongation,

Thermal and mechanical characteristics of copolymers

In TABLE 3 we summarized the thermal and mechanical investigation results obtained for TMC/CL copolymer with selected composition. The results proved that the thermal and mechanical properties of synthesized copolymers were strongly dependent on the monomer composition. The semi-crystalline copolymer with the highest caproyl content presents the best parameters. With decreasing of CL microblocks average length, deterioration of the mechanical strength of copolymers was observed.

Conclusions

Ethyl etoxy zinc (II) proved to be very active initiator for the homopolymerization of TMC and its copolymerization with ϵ -caprolactone. TMC/CL copolymers obtained this way, with caproyl units content of more than 70%, showed semi-crystallinity. Other synthesized copolymers were amorphous because of the impossibility to create separate ordered crystalline phase when the average length of caproyl microblocks was less than 5-6 units. This phenomenon resulted in Young module decrease of copolymers which proceeds with increase of TMC content in the started copolymerization mixture. Received copolymers, especially those containing caproyl units in amount more than 50% mol., are the most promising materials for the manufacturing of porous nerve guides or drug loading coating materials because of their good mechanical properties and demonstrated high flexibility. What seems to be important, these TMC/CL copolymers using the proposed simple and non-toxic zinc initiator, due to their high rate of reaction, are possible to synthesize and simultaneously to process using conventional extruder for plastics.

Acknowledgements

This research was investigated in the frame of project MEMSTEND UDA- POIG.01.03.01-00-123/08-00, co-financed by European Union.

References

- [1] Lemmouchi Y., Schacht E., Kageruka P., De Deken R., Diarra B., Diall O., Geerts S.: Biodegradable polyesters for controlled release of trypanocidal drugs: In vitro and in vivo studies. *Biomaterials* 19 (1998) 1827-1837.
- [2] Pêgo A.P., Zhong Z., Dijkstra P.J., Grijpma D.W., Feijen J.: Influence of catalyst and polymerization conditions on the properties of 1,3-trimethylene carbonate and ϵ -caprolactone copolymers. *Macromol. Chem. Phys.* 204 (2003) 747-754.
- [3] Schappacher M., Fabre T., Mingotaud A.F., Soum A.: Study of a (trimethylenecarbonate-co- ϵ -caprolactone) polymer - Part 1: preparation of a new nerve guide through controlled random copolymerization using rare earth catalysts *Biomaterials* 22 (2001) 2849-2855.
- [4] Sheng H., Zhou L., Zhang Y., et al.: Anionic lanthanide phenoxide complexes as novel single-component initiators for the polymerization of ϵ -caprolactone and trimethylene carbonate. *J. Polym. Sci.: Part A: Polym. Chem.* 45 (2007) 1210-1218.
- [5] Dobrzynski P.: Mechanism of ϵ -caprolactone polymerization and ϵ -caprolactone/trimethylene carbonate copolymerization carried out with $Zr(Acac)_4$. *Polymer* 48 (2007) 2263-2279.
- [6] Kricheldorf H.R., Stricker A.: Poly(lactones), 47 A-B-A triblock copolyesters and random copolyesters of trimethylene carbonate and various lactones via macrocyclic polymerization. *Macromol. Chem. Phys.* 200 (1999) 1726-1733.
- [7] Kricheldorf H. R., Stricker A., Gomurashvili Z.: Polymers of carbonic acid, 30. Ring-expansion polymerization of trimethylene carbonate (TMC, 1,3-dioxanone-2) with dibutyltin succinate or adipate. *Macromol. Chem. Phys.* 202 (2001) 413-420.

DEVELOPMENT OF INNOVATIVE BIOPOLYMERS DESIGNED FOR BONE REGENERATION APPLICATIONS AND IN VITRO STUDY OF THEIR BIOCOMPATIBILITY AND OSTEOGENIC CAPACITY ON HUMAN BONE MARROW MESENCHYMAL STEM CELLS

MARIA ASSUNTA BASILE^{1*}, GIOVANNA GOMEZ D'AYALA², PAOLA LAURIENZO², MARIO MALINCONICO², ADRIANA OLIVA¹

¹ DEPARTMENT OF BIOCHEMISTRY AND BIOPHYSICS, SECOND UNIVERSITY OF NAPLES, VIA DE CRECCHIO 7, 80138 NAPLES, ITALY

² INSTITUTE OF CHEMISTRY AND TECHNOLOGY OF POLYMERS, VIA CAMPI FLEGREI 34, 80078 POZZUOLI, ITALY

* E-MAIL: MARIAASSUNTA.BASILE@UNINA2.IT

Abstract

In the frame of a project aiming to the improvement of the properties of biodegradable polyester-based devices, designed for bone regeneration, we have prepared and characterized novel composites based on poly(ϵ -caprolactone) (PCL). In particular, we report in this paper the functional changes made through radical grafting on PCL to obtain the less hydrophobic derivatives, PCL-MA-GMA [maleic anhydride (MA)-glycidylmethacrylate (GMA)] and PCL-DMAEA [N-(dimethyl-amino)ethylacrylate]. In addition, we studied in vitro the biocompatibility and the osteogenic capacity of these novel polyesters on human bone marrow (BM) mesenchymal stem cells (MSC).

Keywords: functionalization of poly(ϵ -caprolactone), bone marrow mesenchymal stem cells.

[*Engineering of Biomaterials* 113 (2012) 13-15]

Introduction

Bone is a complex and highly specialized connective tissue and is also a very dynamic tissue, having a unique capability of self-remodeling throughout the life. However, many circumstances call for bone grafting owing to bone defects either from traumatic or pathological destruction.

Although autografting and allografting are clinically considered as good therapies, they have several limitations. Consequently, there is a great need for the use of synthetic bone grafts. Nowadays, numerous synthetic bone graft materials are available which are capable of alleviating some of the practical complications associated with the autogenous or allogeneic bone. Among the different materials proposed for bone substitution application (ceramics, metals and polymers), biodegradable polyesters have acquired a particular niche of interest, since they contain unstable bonds that are hydrolytically cleaved and release degradation products that are normal intermediates of metabolic pathways.

In the frame of a project aiming to the improvement of the properties of biodegradable polyester-based devices, we have prepared and characterized novel composites based on polycaprolactone (PCL). PCL is highly biocompatible and degrades slowly thus providing, in the long time of the degradation, adequate support until bone regeneration is completed. Two major limitations of the PCL are the strong hydrophobic character and the poor mechanical properties when compared with those of the bone. With respect to the first aspect, the functionalization is a particularly relevant approach in order to lower hydrophobicity. In this paper we report the functional changes made through radical grafting on PCL to obtain the less hydrophobic derivatives PCL-DMAEA and PCL-MAGMA.

In a second part of our experimentation, we studied in vitro the biocompatibility and the capability of these novel polyesters to induce osteogenic phenotype of human bone marrow (BM) mesenchymal stem cells (MSC). The rationale for this cellular model choice resides in the fact that these cells are multipotent and can differentiate into a variety of cell phenotypes including osteoblasts, adipocytes, chondrocytes. The response of MSC was assessed in terms of cell adhesion, proliferation, and differentiation.

Materials and Methods

Polycaprolactone (PCL, CAPA 6503, molar mass 50-80 kDa) was purchased from Solvay (Belgium). Maleic anhydride (MA) and benzoyl peroxide (BPO) were obtained from Fluka and used as received. Glycidyl methacrylate (GMA) and N-(dimethylamino)ethylacrylate (DMAEA) were supplied by Aldrich Chemicals. All other chemicals were obtained from Sigma (USA) and were of the highest grade available commercially. Tissue culture biochemicals were from Gibco-Invitrogen (USA) and plasticware was obtained from BD Falcon (USA).

Synthesis of copolymers of PCL

PCL modified by insertion of anhydride groups was obtained by radical grafting, performed in a Brabender mixer, of maleic anhydride (MA) and glycidyl-methacrylate (GMA) molecules (PCL-g-MAGMA). Details of the synthesis and characterization have been published previously [1,2]. Briefly, a powder mixture of 45 g of PCL, 2.5 g (0.025 mol) of MA, and 0.5 g (2.1 mmol) of benzoyl peroxide (BPO) was first fed into the mixer at 100°C, and then 2.5 g (0.018 mol) of GMA was added drop wise. The reaction was carried out at 100°C for 20 min at a rate of 32 rpm. The product was dissolved in 500 ml of chloroform (CHCl₃) and re-precipitated in a large excess of n-hexane. The purification procedure was repeated twice. The % grafted anhydride of the final sample, as determined by infrared spectroscopy on chloroform solution [13a-c], was 9.5 (\pm 0.9)% (IR diagnostic bands (KBr): 1777 and 1850 cm⁻¹ (s, O=C-O-C=O)).

PCL modified by insertion of N-(dimethylamino)ethylacrylate (DMAEA) of tertiary amines groups (PCL-g-DMAEA) was obtained as follows: 45 g of PCL, 5 g of DMAEA, 0.5 g of BPO were fed into a static mixer (Rheocord Haake 9000, USA) at 100°C. The reaction was carried out at this temperature for 20 min at a rate of 32 rpm. PCL-g-DMAEA was first dissolved in 500 ml of chloroform (CHCl₃) and then re-precipitated in a large excess of n-hexane, in order to remove all the ungrafted components (residual monomer and oligomers). The obtained product was dried under nitrogen stream at room temperature overnight until constant weight (average yield: 80%).

Films preparation

The various films were prepared by solution casting. Typically, 1.50 g of each material was dissolved in 10 ml of anhydrous CHCl_3 under stirring in a bath at 60°C for 24 h. After this time the cool solution was poured in a petri dish. The solvent was let to evaporate slowly at atmospheric pressure and room temperature for 24 h. Before use each film was placed in a hydraulic press at 50°C for 3 min under a 5 ton load.

The material films were cut to get discs with diameter of 22 mm that were attached with biologic silicone in 12-well plates and sterilized with 2 ml phosphate buffer containing 1% of fungizone and a graded series of penicillin-streptomycin solution from 10% v/v to final concentration of 1%. Finally the complete cell culture medium was added and plates were incubated for 24 hours to control the sterilization efficiency.

Preparation and characterization of MSC

The preparation of MSC was performed employing heparinized human BM from six healthy volunteers; informed consent and research protocol were institutionally approved. The preparation of MSC, performed as previously reported [3,4], was based on adhesion dependence of mesenchymal component of bone marrow. Briefly, BM sample was diluted 1:5 with Opti-MEM containing 10% foetal calf serum (FCS), penicillin 100 units/ml, streptomycin 100 $\mu\text{g}/\text{ml}$ and sodium ascorbate 50 $\mu\text{g}/\text{ml}$ (growth medium), placed in 100 mm polystyrene dishes and incubated at 37°C in a 5% CO_2 humidified atmosphere.

After 48 h the medium was collected and centrifuged at 800xg. The pellet, containing all non-adherent cellular elements, was discarded while the corresponding supernatant was added again to the dish. In three-four days, several foci of adherent spindle-like cells appeared and grew until subconfluence in the following two weeks. During this period, medium was refreshed every three days, each time leaving half of the old medium. Afterwards, cells were trypsinized and analyzed by flow cytometry using a wide panel of monoclonal antibodies. The cells expressed specific surface markers, such as CD13, CD29, CD44, CD105, CD166, and were negative for hematopoietic cell markers CD14, CD34 and CD45. Cultures between the second and fourth passage were used in our experiments.

Cell adhesion and proliferation tests

Cell adhesion to material surface and proliferation can be assessed by MTT vitality assay. The key component of this assay is 3-(4,5-dimethylthiazol-2-yl)-2,5-diphenyltetrazolium bromide (MTT). Mitochondrial dehydrogenases of living cells reduce the tetrazolium ring, yielding a blue formazan product, which can be measured spectrophotometrically. The amount of formazan produced is proportional to the number of viable cells present. MTT (5 mg/ml in DMEM without phenol red) was added to the wells in an amount equivalent to 10% of the culture medium. After an incubation of 4 h at 37°C , the liquid was aspirated and the insoluble formazan produced was dissolved in isopropanol. The optical densities were measured at 570 nm, subtracting background absorbance determined at 690 nm.

Scanning Electron Microscopy (SEM)

Cell layers were rinsed three times with PBS and fixed for 1 h with glutaraldehyde 2.5%. The fixed layers were washed again with PBS and then dehydrated by graded ethanol solutions from 30% to 100%. Samples were mounted on stubs, coated with Au/Pd alloy and examined by SEM (FEI Europe Company, the Netherlands).

Alkaline phosphatase assay

The effects on osteogenic differentiation were evaluated analyzing the activity of the early osteoblastic marker, namely alkaline phosphatase (AP). Once removed the medium, the wells were rinsed with 20 mM Tris/HCl-0.5 M NaCl, pH 7.4 (TBS) and the cells lysed with a specific buffer (20 mM Tris/HCl, pH 7.4, 0.5 mM NaCl, 0.25% Triton X-100). After 30 min in ice, the cell lysates were centrifuged at 13,000xg for 5 min, and the supernatants assayed for AP activity. Protein concentration was determined according to the method of Bradford. AP activity was determined by measuring the release of para-nitrophenol (PNP) from disodium para-nitrophenyl phosphate (PNPP). The reaction mixture contained 10 mM PNPP, 0.5 mM MgCl_2 , diethanolamine phosphate buffer pH 10.5, and 10-30 μg of cell lysate in a final volume of 0.5 ml. After 30 min at 37°C , the reaction was stopped by adding 0.5 ml of 0.5 M NaOH. PNP levels were measured spectrophotometrically at 405 nm. The AP activity was normalised to the protein content and expressed as units/mg protein, where one unit was defined as the amount of enzyme that hydrolyzes 1 nmol of PNPP/min under the specified conditions.

Results and Discussion

All the samples and the polystyrene bottoms used as controls were subjected to the same treatment outlined in the Materials and Methods sections, and then seeded with 10^4 cells/ cm^2 . After 4 days of incubation, cell proliferation was monitored by MTT test. As evident in FIG. 1, cell adhesion and vitality was similar for PCL and for PCL-DMAEA, while the worst performance was exhibited from PCL-MAGMA. Correspondingly, in order to directly analyze the cell morphology and colonization on the composites, scanning electron microscopy was carried out. The SEM images confirmed the previous results and evidenced that MSC attached and colonized PCL and PCL-DMAEA with ruffles and filapodia tightly anchoring them to the biomaterials, while cells on PCL-MAGMA were in lower number and showed a "spongy" morphology with few contacts to material (FIG. 2).

After 7 days from the plating, we analyzed the expression of the early biochemical marker of osteoblastic phenotype, namely alkaline phosphatase. The results confirmed for PCL and for PCL-DMAEA a similar extent of osteogenic capacity, while cells present on PCL-MAGMA expressed very low enzymatic activity levels (FIG. 3).

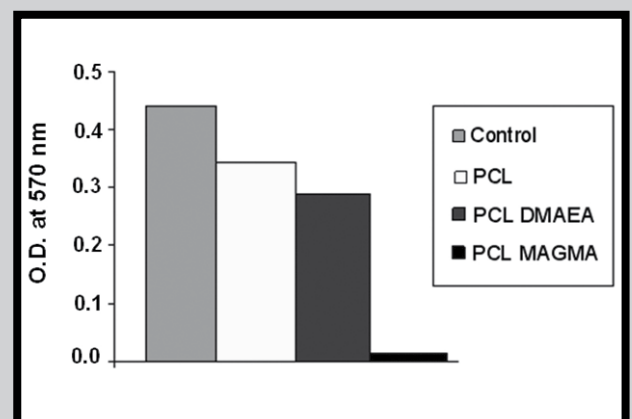


FIG. 1. MTT test on MSC cultured for 4 days onto the different materials. Control refers to cells grown on polystyrene bottom.

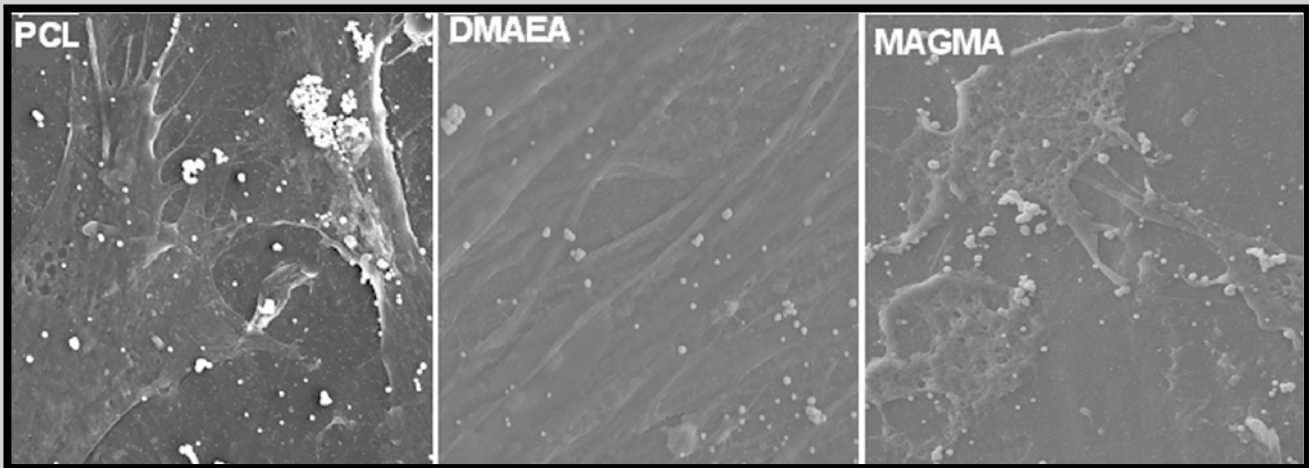


FIG. 2. SEM microphotographs of MSC cultured onto PCL and its two functionalized derivatives.

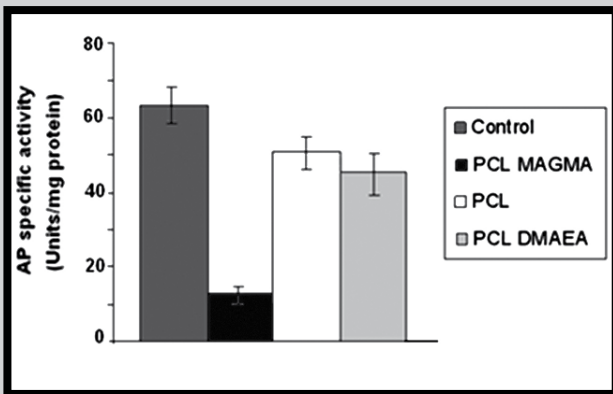


FIG. 3. Alkaline phosphatase specific activity of MSC cultured for 7 days on the various surfaces. Control refers to MSC grown onto the polystyrene bottom.

Conclusions

Altogether these results showed that PCL modified by insertion of anhydride groups, obtained by radical grafting of maleic anhydride and glycidylmethacrylate, i.e. PCL-MAGMA, exhibited scarce biocompatibility and osteogenic capacity, while the PCL modified by insertion of N-(dimethyl amino)ethylacrylate (PCL-DMAEA) appeared to be biocompatible and endowed with a good osteogenic capacity.

References

- [1] Gomez d'Ayala G., Di Pace E., Laurienzo P., Pantalena D., Somma E., Nobile M.R.: Poly(ϵ -caprolactone) modified by functional groups: Preparation and chemical-physical investigation. *Europ Polymer J* 45 (2009) 3217-29.
- [2] Laurienzo P., Malinconico M., Mattia G., Romano G.: Synthesis and characterization of functionalised crosslinkable poly(ϵ -caprolactone). *Macromol Chem Phys* 207 (2006) 1861-69.
- [3] Oliva A., Passaro I., Di Pasquale R., Di Feo A., Criscuolo M., Zappia V., et al.: Ex vivo expansion of bone marrow stromal cells by platelet-rich plasma: a promising strategy in maxillo-facial surgery. *Int J of Immunopathol and Pharmacol* 18 (2005) 47-53.
- [4] Annunziata M., Oliva A., Basile M.A., Giordano M., Mazzola N., Rizzo A., Lanza A., Guida L.: The effects of titanium nitride-coating on the topographic and biological features of TPS implant surfaces. *J Dentistry* 39 (2011) 720-728.

DEGRADATION ANALYSIS OF RADIOSENSITIZER CONTROL RELEASE SYSTEM BASED ON THE NMR SPECTROSCOPY

ANDRZEJ BUSZMAN^{1*}, JANUSZ KASPERCZYK^{1,2},
JOANNA JAWORSKA¹

¹ CENTRE OF POLYMER AND CARBON MATERIALS PAS,
M. CURIE-SKŁODOWSKIEJ 34 ST., 41-819 ZABRZE, POLAND

² DEPARTMENT OF BIOPHARMACY,
SCHOOL OF PHARMACY AND DIVISION OF LABORATORY MEDICINE,
MEDICAL UNIVERSITY OF SILESIA,
NARCYZÓW 1 ST., 41-200 SOSNOWIEC, POLAND

* E-MAIL: ABUSZMAN@CMPW-PAN.EDU.PL

Abstract

The degradation process of multilayer radiosensitizer releasing systems was conducted and examined via the nuclear magnetic resonance spectroscopy. Copolymers of glycolide and lactide with different chain microstructure were used as biocompatible drug carriers. Metronidazole was used as radiosensitizer. The changes of copolymers chain microstructure were monitored during 16 weeks of hydrolytic degradation of material in artificial Cerebro-spinal Fluid Solution. This study shows distinct differences in the rate of copolymer degradation and changes of the degree of randomness, directly connected with the type of comonomers and the comonomeric molar ratio. During 16 weeks of hydrolytic degradation, copolymers with L-lactidyl units remain resistant to hydrolysis while materials with D,L-lactidyl units are completely degraded. Examined materials can be used as carriers of agents for different types of short-, mid- and long-term therapies based on control release systems.

Keywords: biodegradable polyesters, NMR spectroscopy, hydrolytic degradation, polymeric chain microstructure

[Engineering of Biomaterials 113 (2012) 16-18]

Introduction

Among great variety of biomedical materials compatible with human tissues, aliphatic polyesters especially the poly(lactide-co-glycolide) copolymers are considered one of the most valuable and commonly used. Undergoing both hydrolytic and enzymatic degradation to glycolic acid and lactic acid they can be easily metabolized and eliminated by most human cells. It has been proved that PLGA chain microstructure determines the rate of polymer degradation and can be modified or even defined by proper conditions of material synthesis. Such factors as temperature, time, the type of polymerization (bulk, solution), type and amount of initiator used significantly influence the properties of synthesized material and its degradation time [1-3]. The high biocompatibility of PLGA combined with designable material properties make this copolymer suitable as carrier for creating drug control release systems. In our previous study the radiosensitizer metronidazole release system was tested in the *in vitro* conditions and the drug release profiles from different type of carriers were compared.

The purpose of this system is to be placed directly onto the brain tumor tissue to bypass the blood-brain barrier and obtain stable radiosensitizer release after proper amount of time without causing any toxic interactions within the brain tissue [4]. In this study, further hydrolytic degradation analysis of three different PLGA copolymers was carried out in order to detect and describe changes in copolymer chain for selecting the optimal material for brain glioma radiotherapy.

Materials and methods

Polymeric materials poly(glycolide-co-D,L-lactide) and poly(glycolide-co-L-lactide) were synthesized in Centre of Polymer and Carbon Materials PAScs, Zabrze by the ring-opening copolymerization held in bulk, using $Zr(acac)_4$ as nontoxic initiator. Molar ratio of comonomers/initiator was 1000:1. Obtained copolymers were dissolved in chloroform, precipitated in methyl alcohol and next dried at 25°C under reduced pressure to constant weight.

Artificial Cerebro-spinal Fluid Solution (aCFS) was prepared according to producer's (Alzet) instructions by stirring proper amounts of NaCl, KCl, $CaCl_2$, $MgCl_2 \cdot 6H_2O$, $Na_2HPO_4 \cdot xH_2O$ and $NaH_2PO_4 \cdot xH_2O$ with distilled water.

The initial copolymers and degradation products composition was confirmed by the ¹H-NMR analysis and the chain microstructure was examined by the ¹³C-NMR measurement (600 MHz on AVANCE II Ultra Shield Plus, Bruker) using DMSO as a solvent.

The copolymers molecular masses M_n and M_w were investigated by gel permeation chromatography (GPC, Physics SP 8800 chromatograph) with the use of chloroform as a solvent.

The copolymers glass-transition temperature T_g was determined by differential scanning calorimetry (TA DSC 2010 apparatus, TA Instruments, New Castle, DE).

Mono and triple layered radiosensitizer release systems containing metronidazole were obtained as previously described [4] and put into glass ampoules filled with amount of aCFS proportional to their weight (1 ml of aCFS per 15 mg of polymer). Material samples were gathered every two weeks and the whole amount of buffer was changed every single week to maintain the dynamic system similar to *in vivo* conditions. Incubation with constant ampoules shaking was held at 37°C (Memmert Precision Incubator INE 400) for 16 weeks.

Results and Discussion

Three different samples referring to three PLGA copolymeric materials were examined: A1 (PLA:GA, comonomeric ratio 84:16), B1 (PDLA:GA, comonomeric ratio 84:16), C1 (PDLA:GA, comonomeric ratio 47:53). The material properties are shown in TABLE 1. All materials were obtained in presence of $Zr(acac)_4$ as initiator and show semibloc chain microstructure (FIG. 1), with the degree of randomness (R) varied from 0,37 for A1 to 0,61 for B2 (TABLE 1).

TABLE 1. Characterization of obtained materials.

Sample	A1	B1	B2
material	PLA:GA	PDLA:GA	PDLA:GA
molar ratio	84:16	84:16	47:53
T_g [°C]	60.6	57.1	51
M_n [Da]	75 300	63 500	46 400
M_w [Da]	254 700	142 800	99 200
M_w/M_n	3.38	2.25	2.14
R	0.37	0.47	0.61

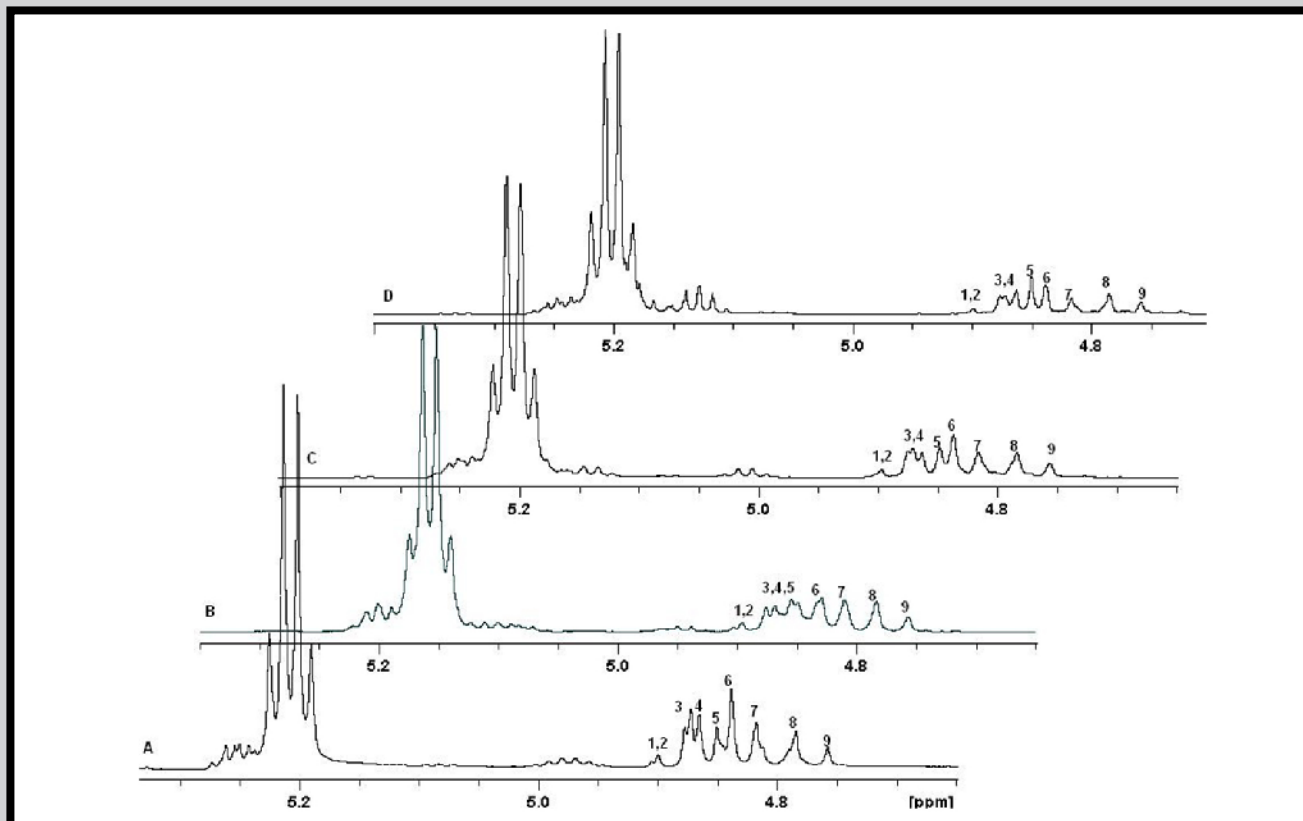


FIG. 1. NMR spectra of A1 PLA/GA,84/16 after 0 (A), 4 (B), 8 (C) and 16 (D) weeks of degradation. Methylen proton range of lactidyl units 5.1-5.3 ppm, methylen proton range of glycolidyl units 4.75-4.9 ppm. Sequences: 1- GLGGG or GGGLG, 2- LGGLG or GLGGL, 3- GGGGG, 4- LLGGL + LGLL, 5- GGGGL + LGGGG, 6- LLGGG + GGLL, 7- LLGLL + GLGLL + LLGLG + GLGLG, 8- GGGLG or GLGGG, 9- LGGGL + GLGGL or LGGLG.

TABLE 2. Lactidyl and glycolidyl units content changes during degradation.

Sample	Degradation time [weeks]	Lactidyl units LL [mole %]	Glycolidyl units GG [mole %]
A1	0	84	16
	4	86	14
	8	88	12
	16	89	11
B1	0	84	16
	4	87	13
	8	94	6
	12	85	15
B2	0	47	53
	2	54	46
	4	69	31
	8	45	55

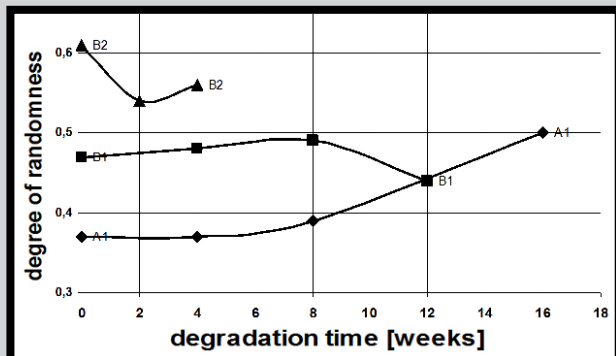


FIG. 2. Changes of degree of randomness during PLGA degradation.

The highest R value in the B2 sample (PDLA:GA, 47:53) results directly from the comonomeric ratio of this copolymer. With almost even amounts of comonomers, B2 possess the highest chance of random distribution of glycolidyl and lactidyl units in the copolymer chain during the synthesis. Similar results were described before [5] for the Zr(acac)₄ initiator. Sample A1 containing L-lactidyl units possess the lowest degree of randomness and also has the highest molar masses and polymeric dispersion (M_w/M_n) coefficient. During the 16 weeks of hydrolytic degradation, the slowest degradation rate for A1 sample was observed. Sample A1 also maintain the disc shape for the whole examined period. The changes in lactidyl and glycolidyl units content N_{LL} and N_{GG} (TABLE 2) indicate faster but stable degradation of glycolidyl units in comparison to L-lactidyl units in A1 copolymer. It is confirmed by slowly decrease of average glycolidyl blocks length (L_{GG}) (FIG. 3) and insignificant changes in average length of lactidyl blocks (L_{LL}) (FIG. 4). The L_{GG} value decreases steadily for the whole experimental period and confirms stable degradation of glycolidyl units in the A1 sample. On the contrary, the L_{LL} values increase during 8th week of degradation experiment and then decrease to the initial value in 16th week. Probably, in the first period of degradation only the short, alternating blocks of GLG type (formed by transesterification reaction during copolymerization) are degrade and in consequence both L_{LL} and N_{LL} values increase. After 8 weeks, the hydrolyzation of longer lactidyl blocks begins but still glycolidyl blocks degrade faster so the L_{LL} value decrease and N_{LL} increase to 89% [6-9].

Both copolymeric materials containing D,L-lactidyl units B1 and B2 degrade faster than A1 sample containing only L-lactidyl units which is proved by the split of initial disc-shape matrices into smaller various-shape pieces.

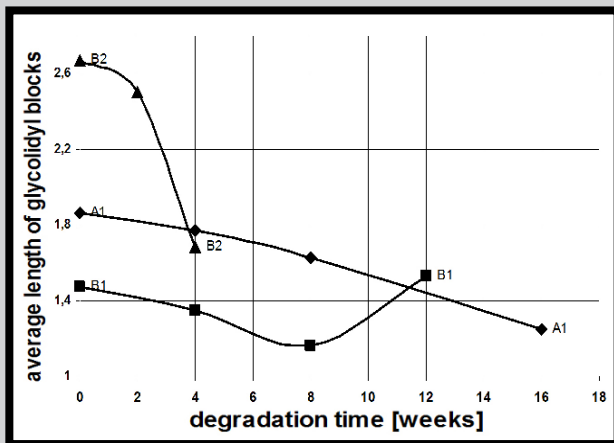


FIG. 3. Changes of average length of glycolidyl blocks during PLGA degradation.

The degradation of glycolidyl units for B1 and B2 is faster than in A1 (TABLE 2, FIG. 3) but only in the first period of experiment - during 8 weeks. After 8 weeks, the D,L-lactidyl units degrade much faster for B1 and B2 than the L-lactidyl units in A1 (TABLE 2, FIG. 4). The N_{GG} decreases rapidly from 16% to 6% for B1 and from 53% to 31% for B2 in the first period of degradation (TABLE 2) which is probably connected with easier water penetration to glycolidyl domains than lactidyl chains. However, after 4 (B2) or 8 (B1) weeks of degradation, the N_{LL} starts to decrease and the comonomeric molar ratio become similar to the initial value. It is probable that longer lactidyl chains start to split and thus the L_{LL} value decreases (FIG. 4, B1). The increase of N_{GG} value for B1 and B2 after 8 weeks can be explained by possible inhibition of further glycolic units degradation. This could be probably caused by presence of high crystalline domains within glycolidyl chains resistant to buffer influence, which is well noticeable for sample B1 (FIG. 3). The other explanation is the difference between the lactidyl and glycolidyl units degradation rates, also leading to the increase of N_{GG} though both copolymers degrade [6-11].

It's worth noting that further examination of samples B1 and B2 to the complete 16-weeks period couldn't be proceeded due to their fast degradation rate and insufficient amount of remaining material for the purpose of NMR analysis. However, it is expected that sample B2 would reveal the decrease of L_{LL} and grow of L_{GG} after 8 weeks of degradation, similar to sample B1 and confirmed by the N_{GG} and N_{LL} values (TABLE 2).

References

- [1] Jaworska J., Kasperczyk J., Dobrzyński P.: NMR spectroscopy as a tool in analysis of lactide/ ϵ -caprolactone copolymers degradation. *Engineering of Biomaterials* 65-66 (2007) 51-54.
- [2] Kasperczyk J., Li S., Jaworska J., Dobrzyński P., Vert M.: Degradation of copolymers obtained by ring-opening copolymerization of glycolide and ϵ -caprolactone: A high resolution NMR and ESI-MS study. *Polymer Degradation and Stability* 95, 5 (2008) 990-999.
- [3] Jelonek K., Dobrzyński P., Li S., Kasperczyk J., Jarząbek B.: Controlled poly(L-lactide-co-trimethylene carbonate) delivery system of cyclosporine A and rapamycin - the effect of copolymer chain microstructure on drug release rate. *International Journal of Pharmaceutics* 414, 1-2 (2011) 203-209.
- [4] Buszman A., Kasperczyk J., Jarząbek B., Stokłosa K., Smola A.: Biodegradable polymeric system releasing radiosensitizer - the in vitro studies. *Engineering of Biomaterials* 99-101 (2010) 67-71.
- [5] Bero M., Dobrzyński P., Kasperczyk J.: Application of zirconium (IV) acetylacetonate to the copolymerization of glycolide with ϵ -caprolactone and lactide. *Polymer Bulletin* 42 (1999) 131-139.

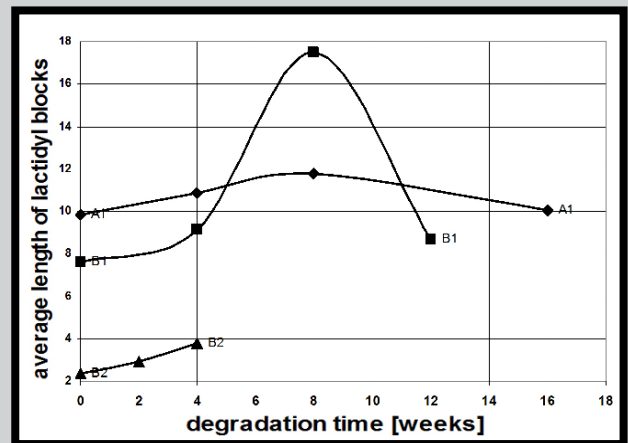


FIG. 4. Changes of average length of lactidyl blocks during PLGA degradation.

Conclusions

The nuclear magnetic resonance analysis reveals significant changes in the polymer chain microstructure for all examined materials. The poly(L-lactide-co-glycolide) (84:16) shows the longer degradation time, caused by the presence of long L-lactidyl chains resistant to hydrolytic degradation. During the 16 weeks of degradation poly(L-lactide-co-glycolide) with comonomeric ratio 84/16 (A1) remain unhydrolyzed in comparison to PDLA:GA, 84:16 (B1) and PDLA:GA, 47:53 (B2). It may be of good usage for stable release systems applied to harder tissues, where no mechanical damage can be done by the remaining polymer matrix. The poly(D,L-lactide-co-glycolide) copolymers B1 and B2 do not maintain the initial shape and after 16 weeks of degradation are almost completely disintegrated. They might be of great value as short- and mid-term release systems applied to soft tissues. The degree of randomness changed insignificantly for all examined copolymers which possess the semi-block chain microstructure.

Acknowledgements

This work was supported by the European Community from the European Social Fund within the RFSD2 project and by the MEMSTEM Project contract no UDA -POIG 01.03.01-00-123-08/03.

- [6] Li S., McCarthy S.: Further investigations on the hydrolytic degradation of poly(DL-lactide). *Biomaterials* 20, 1 (1999) 35-44.
- [7] Vert M., Li S., Garreau H.: More about the degradation of LA/GA-derived matrices in aqueous media. *Journal of Controlled Release* 16, 1-2 (1991) 15-26.
- [8] Jian Yang, Feng Liu, Liu Yang, Suming Li: Hydrolytic and enzymatic degradation of poly(trimethylene carbonate-co-D,L-lactide) random copolymers with shape memory behavior. *European Polymer Journal* 46, 4 (2010) 783-791.
- [9] Vert M., Mauduit J., Li S.: Biodegradation of PLA/GA polymers: increasing complexity. *Biomaterials* 15, 15 (1994) 1209-1213.
- [10] Vert M., Li S., Garreau H.: New insights on the degradation of bioresorbable polymeric devices based on lactic and glycolic acids. *Clinical Materials* 10, 1-2 (1992) 3-8.
- [11] Gębarowska K., Kasperczyk J., Dobrzyński P., Scandola M., Zini E., Li S.: NMR analysis of the chain microstructure of biodegradable terpolymers with shape memory properties. *European Polymer Journal* 47, 6 (2011) 1315-1327.

HARNESSING BIOPOLYESTERS IN THE DESIGN OF FUNCTIONAL MATERIALS FOR BIOMEDICAL APPLICATIONS

ESTELLE RENARD, JULIEN BABINOT, PIERRE LEMECHKO, JULIEN RAMIER, GWENAELLE VERGNOL, DAVY LOUIS VERSACE, DANIEL GRANDE, VALERIE LANGLOIS*

¹ INSTITUT DE CHIMIE ET DES MATÉRIAUX PARIS EST, UMR 7182 CNRS- UNIVERSITÉ PARIS EST CRÉTEIL, 94320 THIAIS, FRANCE

* E-MAIL: LANGLOIS@ICMPE.CNRS.FR

Abstract

The present contribution illustrates the versatility of poly(3-hydroxyalkanoate)s (PHAs) in the design of a wide variety of biodegradable and/or biocompatible macromolecular architectures with controlled degradability. Firstly, functionalized PHAs were prepared from unsaturated PHAs. Pendant double bonds have been turned into carboxyl, hydroxyl, alkyne or epoxy groups. These reactive functions were used for further grafting hydrolyzable polylactide (PLA) or poly(ϵ -caprolactone) (PCL) as well as hydrophilic poly(ethylene glycol) (PEG). Additionally, block copolymers with a PLA, PCL or PEG segment have been prepared by ring-opening polymerization or "click" chemistry from a PHA oligomeric macroinitiator. Functional PHAs represent biodegradable aliphatic polyesters with many possibilities to tune physico-chemical characteristics, such as hydrophilicity and degradation rate, thus making the resulting materials suitable as devices for drug delivery or as scaffolds for tissue engineering. Herein, we address the recent trends in the synthesis of these polymeric materials and their applications in controlled drug delivery and tissue engineering.

Keywords: poly(3-hydroxyalkanoate)s, block and graft copolymers, drug delivery, tissue engineering

[Engineering of Biomaterials 113 (2012) 19-22]

Introduction

Poly(3-hydroxyalkanoate)s (PHAs) represent a class of natural aliphatic polyesters accumulated by many bacteria as intracellular energy and carbon storage materials when they are subjected to stress conditions [1,2]. They constitute an enlarged family of bacterial polyesters that can be considered as promising biopolymers for biomedical applications, due to their biodegradability and biocompatibility. Using various substrates, a wide variety of PHAs can be synthesized, differing notably by the length of their side chains [3]. Two main types are distinguished, i.e. one type with short-chain length (scl-PHA) that possesses alkyl side chains up to two carbon atoms, and a second type with medium-chain length (mcl-PHAs) that displays between three and eight carbon atoms on its side chains (FIG. 1). The length of side chains strongly affects the physical properties of PHAs.

In this contribution, the versatility of PHAs in the design of a wide variety of biodegradable and/or biocompatible macromolecular architectures will be illustrated. First, unsaturated PHAs were chemically modified via the transformation of pendant double bonds into epoxy, carboxyl, hydroxyl or alkyne groups. Moreover, these reactive functions could further be used for grafting hydrolyzable polylactide (PLA) or poly(ϵ -caprolactone) (PCL) as well as hydrophilic poly(ethylene glycol) (PEG) through two distinct mechanisms, namely either a "grafting from" method or a "grafting onto" approach (direct esterification or "click" chemistry). PHA-b-PEG block copolymers were also synthesized by "click" chemistry, while totally degradable block copolyesters were generated by ring-opening polymerization of D,L-lactide or ϵ -caprolactone applying either conventional thermal heating or microwave dielectric activation. Finally, mucoadhesive degradable nanoparticles having a great potential for drug delivery applications were prepared from block copolymers. Such copolymers were also tested as biomaterials for tissue engineering, e.g. as degradable coatings in drug eluting stents.

Materials and Methods

PHB ($M_w=330\ 000\ \text{g}\cdot\text{mol}^{-1}$), PHBHV (14 mol.% HV, $M_w=240\ 000\ \text{g}\cdot\text{mol}^{-1}$), PHBHHx (9 mol.% HHx, $M_w=330\ 000\ \text{g}\cdot\text{mol}^{-1}$) were respectively purchased from Biomer, Goodfellow, and Procter & Gamble. PHOU samples were obtained from EMPA, Swiss Fed Labs Mat Testing & Res, Lab Biomat, CH-9014 St Gallen, Switzerland.

Synthesis of PHA oligomers

PHA oligomers with a terminal carboxyl group (PHB, PHBHHx, PHOHHx) were prepared by thermal degradation at 190°C for a determined time. Oligomers were purified by precipitation in ethanol. PHA oligomers with a terminal hydroxyl group were prepared by methanolysis as previously described [4].

Functionalization of PHAs and oligomers

Native PHOU samples were oxidized with KMnO_4 to introduce terminal carboxylic acid functions in side chains (PHOD-COOH), following a previously reported procedure [5].

The COOH groups in side chains or at the terminal position were also esterified with propargyl alcohol in the presence of EDC hydrochloride as a coupling agent [6,7].

Synthesis of graft copolymers

Different strategies were used to build PHA-g-PCL, PHA-g-PLA, and PHA-g-PEG graft copolymers. PHA-g-PCL were synthesized according to a "grafting from" method described in a previous paper by ROP of ϵ -caprolactone [8]. PHA-g-PLA were synthesized by direct esterification as previously reported [5,9]. PHA-g-PEG were prepared by "click" chemistry using the copper (I)-catalyzed azide-alkyne cycloaddition (CuAAC) [6].

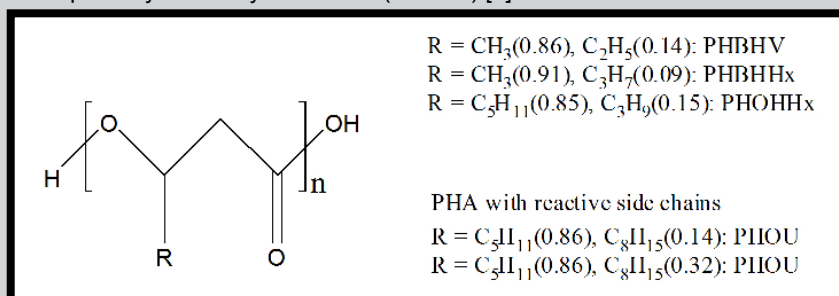


FIG. 1. Chemical structures of PHAs under investigation.

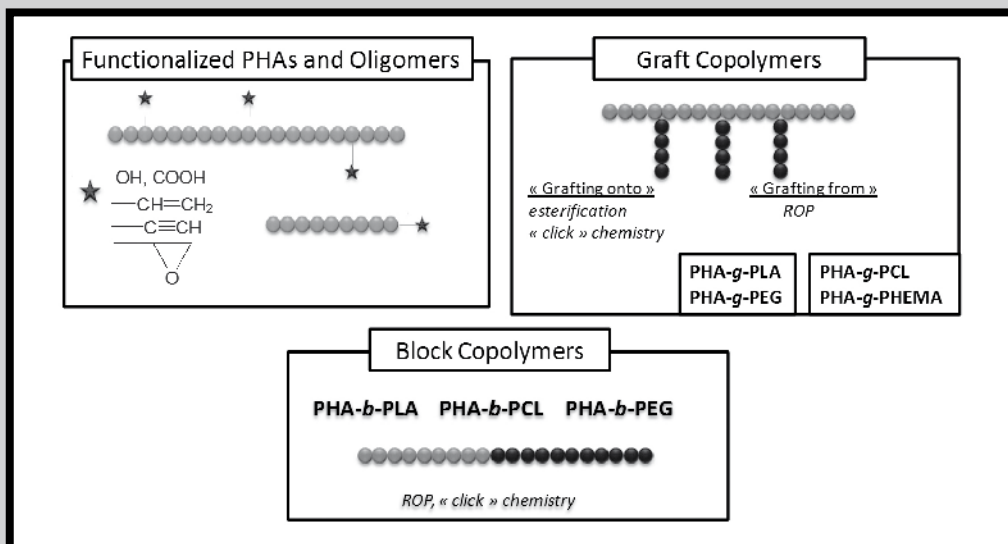


FIG. 2. Well-defined macromolecular architectures based on PHAs.

Synthesis of block copolymers

PHA-b-PEG diblock copolymers with controlled size and easy purification were prepared using the copper (I)-catalyzed azide-alkyne cycloaddition (CuAAC) [7]. PHA-b-PLA and PHA-b-PCL copolymers were prepared by ROP of D,L-lactide or ϵ -caprolactone, respectively [4].

The chemical structures and the physico-chemical features of the copolymers were investigated by NMR, SEC, DSC, and TGA analyses.

Cell adhesion

1 mL of human bladder carcinoma RT112 cells suspension containing 300000 cells and RPMI culture medium supplemented with 10% fetal calf serum, 0.05% streptomycin, and 0.05% penicillin was put on each well. Then the plates were placed at 37°C. The medium was changed every day. At different times, adhesive RT112 cells were counted by a colorimetric MTT. Briefly, a solution of 3-[4,5-dimethylthiazol-2-yl]-2,5-diphenyltetrazoliumbromide (MTT) 1 mg·mL⁻¹ was added in each well containing cells fixed on polymer after removing medium of culture with non-attached cells. Plates were placed at 37°C for 1 h. The intensity of the suspension was proportional to the quantity of living cells. By adding isopropanol, cells burst and released the colored solution whose absorption was measured by UV spectrophotometry. Cell adhesion was observed at 4 h and cell growth for 3 days. Experiments were repeated three times.

Nanoparticle preparation

Sub-micrometer particles were prepared by a solvent displacement/evaporation method. A copolymer (75 mg) was dissolved in 15 mL of acetone at 50°C under stirring. The solution was cooled down to room temperature. In the case of doxorubicin-loaded particles, 1.2 mL of a solution of doxorubicin (1 mg/6 mL ethanol) was added. The mixture was added dropwise in 45 mL of an aqueous solution of Pluronic F-68 (1% w/v) under stirring. The solution was stirred at room temperature in a flux of air during 4 h to completely remove the acetone.

Stent coating

A chloroform solution containing 0.5 wt.% of polymer and sirolimus (purity 99.9%, Biocon), in proportion 80/20 wt.% respectively, was sprayed on a stent. Drug Eluting Stents (DES) were dried at room temperature for 12 h. In the case of bilayered coatings, a solution of PHBV 0.5 wt% in chloroform was sprayed in a second step, and the solvent was evaporated. The total weight of coating was about 600 μ g for monolayered coatings and 900 μ g for bilayered coatings, with a content of 120 μ g \pm 10 μ g sirolimus per stent.

Results and Discussions

Block and graft copolymers

Compared to other degradable polyesters, poly(3-hydroxyoctanoate-co-3-hydroxyundecenoate) (PHOU) has the major advantage to be alkene-functionalized on its side chains, allowing for post-modifications. By taking advantage of the reactivity of pendant double bonds, novel functionalized PHAs were successfully prepared via the chemical transformation of (C=C) terminal unsaturations into carboxyl [5], alkyne [6], hydroxyl [8] or epoxy [10] groups (FIG. 2).

Moreover, these functional side groups can be used to further conjugate bioactive or targeting molecules, as well as reactive oligomers. Therefore, biocompatible oligomers based on hydrolyzable PLA or PCL as well as hydrophilic PEG were grafted to PHO through two distinct mechanisms, namely either a "grafting from" method [8] (PCL grafts) or a "grafting onto" approach via direct esterification [5,9] or "click" chemistry (PLA or PEG grafts). The latter mechanism turned out to be more efficient in the synthesis of PHO-g-PEG graft copolymers. Such amphiphilic architectures could yield stable nanoparticles in aqueous media. Furthermore, totally biodegradable PHA-based block copolymers were synthesized by ring-opening polymerization of D,L-lactide or ϵ -caprolactone initiated by hydroxy-terminated PHA oligomeric macroinitiators [4]. The latter macroinitiators were previously prepared by methanolysis of native PHAs. Alternatively, "click" chemistry was implemented to generate well-defined amphiphilic block copolymers based on PHA and PEG [7].

Biomedical applications

Tissue Engineering

Attachment and growth of human bladder carcinoma RT112 cells were investigated in vitro on biopolyesters films in a view to use them as scaffolds in tissue engineering [11]. The effect of the chemical structure of different bacterial polyesters on cell adhesion and proliferation was studied. Measurements of cell adhesion were carried out in the presence of collagen IV or fetal calf serum. The best results for cell attachment were obtained with PHOD-COOH, whatever be the experimental conditions (FIG. 3). The hydrophobic surface of PHO films also induced a good adhesion density of RT 112 cells. PHOD-g-PEG had a contrasted behavior, due to the presence of PEG grafts. Proliferation of human bladder carcinoma RT112 cells was observed on the same polymers. PHOD-COOH did not improve the cell proliferation and did not seem to be a favorable support. This preliminary study showed that PHO has a good potential to induce regeneration of a functional bladder wall.

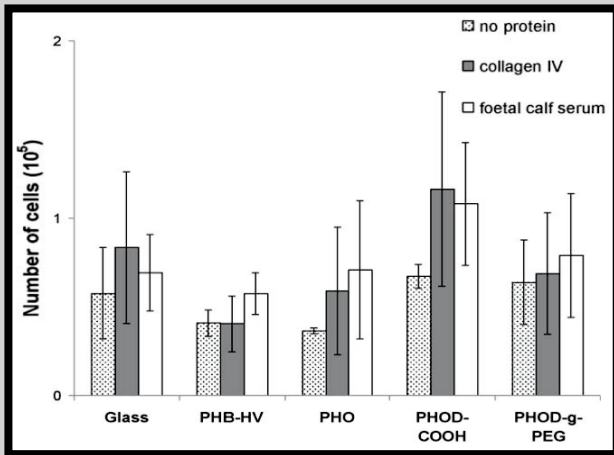


FIG. 3. Cell adhesion on PHA-based films after 4 h of incubation at 37°C.

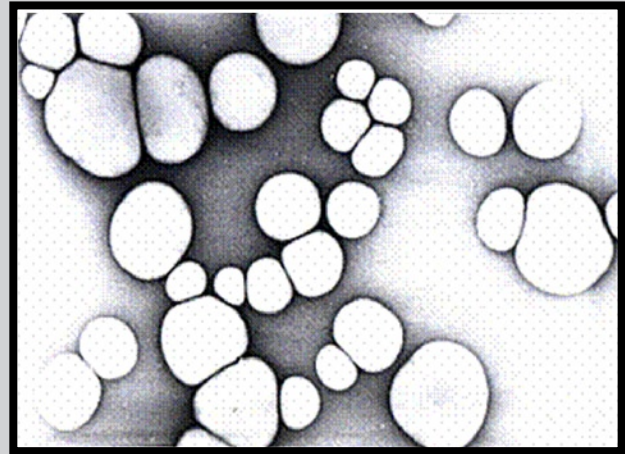


FIG. 4. Sub-micrometer particles of PHO-b-PCL (x 20 000).

Drug delivery systems

Particles based on PHO, PHOD-COOH, PHO-b-PCL and PHODCOOH-b-PCL were prepared using a solvent displacement/evaporation method (FIG. 4). The encapsulation efficiency of doxorubicin was larger than 50% due to the hydrophobicity of both doxorubicin and polyesters. The in vitro release behavior of doxorubicin-loaded particles at pH=6 (bladder pH) was investigated [12]. A typical two-phase release profile was observed (case of matricial type particles). These results were consistent with the method of particle preparation: doxorubicin was co-precipitated with the polymer. The burst effect was inferior to 10%. Interestingly, these nanoparticles were also mucocohesive (FIG. 5).

The association of a hydrophilic segment in conjunction with a hydrophobic block is a classical way to increase the stability of colloidal particles. In this investigation, PEG was used as a model molecule for the hydrophilic part in amphiphilic copolymers. PHBHV-PEG copolymers were unstable colloidal suspensions, whereas PHO-based copolymers resulted in very stable colloidal suspensions. They form stable micelles in aqueous media, with low critical micelle concentrations (FIG. 6). They can be envisioned for biomedical applications as drug delivery systems able to transport bioactive hydrophobic molecules.

Drug eluting stents are of great interest in the field of interventional cardiology by promising a long-term prevention of restenosis. An adequate drug release control, mechanical response to stent expansion, and degradability of the coating are of major importance. The present approach described the potential use of PHAs as biodegradable and compatible coatings. Rates of drug release from different monolayers of PHAs were very fast, and the maximum period of drug release observed was clearly too short to be of practical use (burst effect). The development of a new PHBHV-b-PLA copolymer as a coating enhanced the drug release profile by limiting the release of sirolimus. The extension of the drug release period is very promising by resorting to the bilayered system composed of PBHV-b-PLA containing the drug and PHBHV without drug (FIG. 7). Moreover, this bilayered coating had good mechanical properties in terms of flexibility and adherence to the metallic stent. Further studies are necessary to confirm their performances under in vivo conditions.

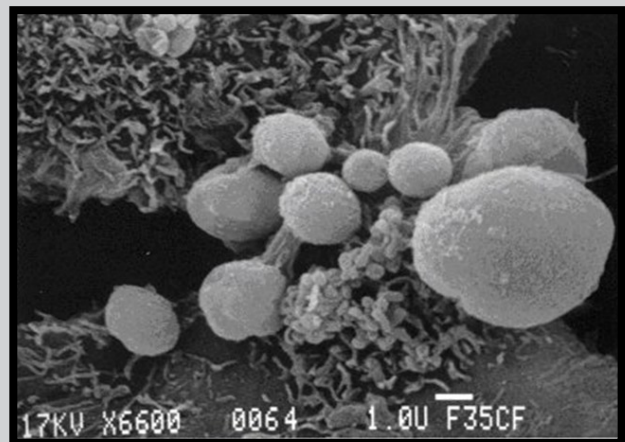


FIG. 5. SEM image showing mucoadhesivity of PHO-b-PCL particles containing 24% of PHO (x 6000).

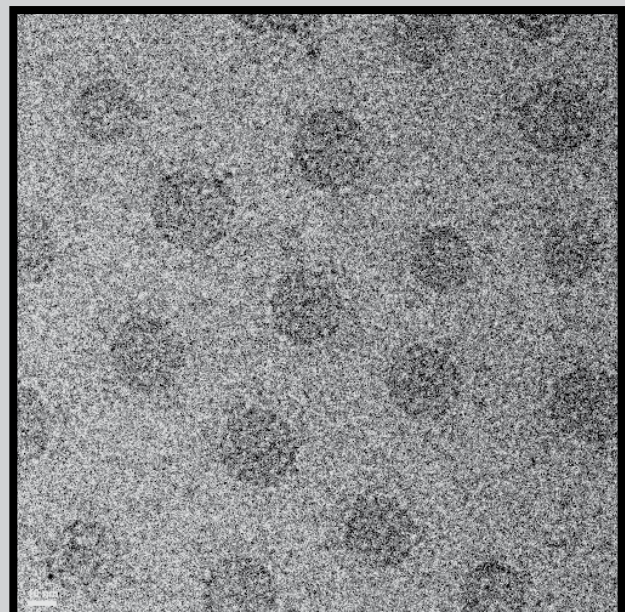


FIG. 6. Cryo-TEM of micelles formed in water by PEG-b-PHO copolymers (scale bar is 10 nm).

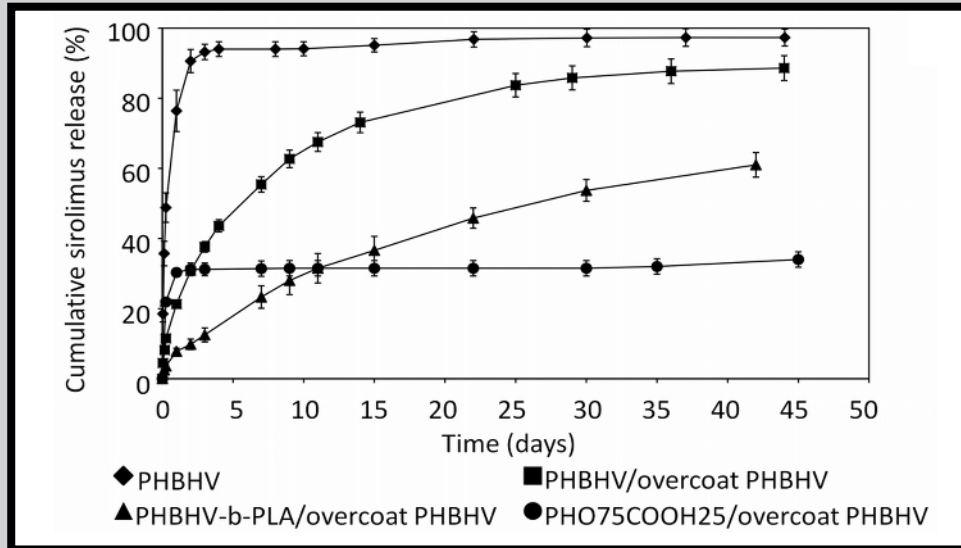


FIG. 7. Sirolimus release from different copolymer systems.

Conclusion

The potential of functional PHAs and relative copolymers in the drug release area and tissue engineering has been illustrated through the investigation of cell adhesion on functionalized PHA films, doxorubicin release from stable nanoparticles, performance of drug eluting stents, and micelle formation. These studies have shown the potentialities of introducing functional groups or segments either on side positions or on a terminal position of PHAs to fine-tune their physico-chemical properties, so as to reach specific applications.

The PHA-based frameworks can be adapted to other biomedical applications through tailor-making topology, composition, and functionality of macromolecular architectures to fit prerequisites corresponding to a specific device. The versatility of PHAs and their derivatives is a major motivation for developing new polyester-based frameworks and scaffolds.

Acknowledgments

The authors thank Dr Christophe Bureau (Alchimedics, France), and Ferial Haroun (Alchimedics, France) for helpful discussions and technical assistance. This work was supported by the French National Agency of Research ANR within the TecSan program.

References

- [1] Lenz, R. W.; Marchessault, R. H. *Biomacromolecules* 2005, 6, 1.
- [2] Chen, G. Q. *Chem. Soc. Rev.* 2009, 38, 2434.
- [3] Lee, S. Y. *Biotechnol. Bioeng.* 1996, 49, 1.
- [4] Timbart, L.; Renard, E.; Tessier, M.; Langlois, V. *Biomacromolecules* 2007, 8, 1255.
- [5] Kurth, N.; Renard, E.; Brachet, F.; Robic, D.; Guérin, P.; Bourbouze, R. *Polymer* 2002, 43, 1095.
- [6] Babinot, J.; Renard, E.; Langlois, V. *Macromol. Rapid Commun.* 2010, 31, 619.
- [7] Babinot, J.; Renard, E.; Langlois, V. *Macromol. Chem. Phys.* 2011, 212, 278.
- [8] Renard, E.; Poux, A.; Timbart, L.; Langlois, V.; Guérin, P. *Biomacromolecules* 2005, 6, 891.
- [9] Grande, D.; Renard, E.; Langlois, V.; Rohman, G.; Timbart, L.; Guérin, P. In *Degradable Polymers and Materials - Principles and Practice*; Khemani, K., Scholz, C., Eds.; ACS Symposium Series 939; American Chemical Society: Washington, DC, 2006; chap. 9, pp. 140-155.
- [10] Bear, M. M.; Leboucher-Durand, M. A.; Langlois, V.; Lenz, R. W.; Goodwin, S.; Guérin, P. *React. Funct. Polym.* 1997, 34, 65.
- [11] Renard, E.; Timbart, L.; Vergnol, G.; Langlois, V. *J. Appl. Polym. Sci.* 2010, 117.
- [12] Renard, E.; Vergnol, G.; Langlois, V. *IRBM* 2011, 32, 214.

BIOCOMPATIBILITY OF L-LACTIDE-CO-GLYCOLIDE-CO-TRIMETHYLENE-CARBONATE SHAPE MEMORY TERPOLYMER WITH HUMAN CHONDROCYTES

RAFAL KŁOSEK^{1*}, JAKUB KOMACKI¹, ARKADIUSZ ORCHEL¹,
KATARZYNA JELONEK², PIOTR DOBRZYŃSKI²,
JANUSZ KASPERCZYK^{1,2}, ZOFIA DZIERŻEWICZ¹

¹ DEPARTMENT OF BIOPHARMACY,
SCHOOL OF PHARMACY AND DIVISION OF LABORATORY MEDICINE,
MEDICAL UNIVERSITY OF SILESIA, KATOWICE

² CENTRE OF POLYMER AND CARBON MATERIALS PAS, ZABRZE

* E-MAIL: RAFALKLOSEK@GMAIL.COM

Abstract

Biomedical application of biodegradable shape memory terpolymers obtained from L-lactide, glycolide, trimethylene carbonate (TMC) have been intensively investigated in recent years. All applicable biomedical materials must be biocompatible, which means that they cannot cause toxic, cytotoxic, allergic, or carcinogenic reactions. The first study evaluating the biocompatibility of the material is determination of its cytotoxicity.

The purpose of this study was to assess the biocompatibility of poly(L-lactide-co-glycolide-co-trimethylene-carbonate) 75:13:12, synthesized using Zr(Acac)₄ as an initiator of polymerization. The terpolymer was degraded for 30, 60 and 90 days at 37°C in water. The effect of degradation products on the growth of human articular chondrocytes was determined using the sulforhodamine B assay. The examined terpolymer was characterized by means of NMR spectroscopy, GPC and DSC. The results showed that the studied terpolymer was biocompatible with tested cells.

Keywords: Shape-memory polymers (SMP), biodegradable polymers, cytotoxicity, degradation products, *in vitro*, biocompatibility of terpolymer

[*Engineering of Biomaterials 113 (2012) 23-25*]

Introduction

Shape memory effect is an ability of material to return from a temporary shape, which is obtained as a result of mechanical deformation, to the permanent (primary) shape, as a result of stimulation by various factors - physical (such as temperature, light (UV), IR radiation, magnetic or electrical field); or chemical (such as changes of pH, ionic strength etc.) [1,2].

The first materials used in medicine due to shape memory effect were metal alloys (SMA - shape memory alloys). The most commonly and most widely used is Nitinol - alloy of nickel and titanium. However, the SMA have a lot of disadvantages and because of this, researchers are still seeking for new innovative materials with shape memory effect. Nowadays, the most commonly used and studied materials are SMP - shape memory polymers. This is a group of polymers demonstrating the ability of shape memory effect.

The SMP when compared to SMA have many advantages e.g. lower manufacturing cost, the ability to recover the primary shape in expected return temperature (wide temperature range), and also SMP are much easier to process (easier production of various shapes and forms) [1,2].

Biodegradable materials derived from L-lactide, glycolide and trimethylene carbonate (TMC) are the subject of many studies in recent years. This is related with their biocompatibility and degradation to the nontoxic products of metabolism. They were already used in medicine as surgical sutures, scaffolds for tissue engineering or controlled drug delivery systems. Terpolymers derived from these monomers may have shape memory effect, which further increases their potential biomedical application as, for example, self-locking surgical staples, self-expanding stents etc. [3-5].

Regardless of the specific biomedical application, each new material must meet several basic features, including the most important – biocompatibility. This is the total compatibility of the material with the human body which is lack of toxic reactions, cytotoxic agents, allergic reaction or carcinogenic effects. First study, allowing for an initial evaluation of biocompatibility of the material, is a cytotoxicity test [6].

Cytotoxicity of the polymeric material may be affected by many factors – monomeric composition, molecular weight of the polymer, the weight of the final product, its structure and shape (the presence of sharp edges) and also the rate of degradation of the material [6,7]. Crucial importance may also have the residues from synthesis of polymer, released from the material as a result of its degradation - the initiator, solvent or trace amounts of other contaminants [8,9]. Monomeric composition determines the generated degradation products. The final products of degradation of polyesters as PLA, PGA, PCL or their copolymers are lactic acid, glycolic acid and 6-hydroxyhexanoic acid [10,11]. Release of these substances in large quantities and in short time can lead to a reduction in local pH (at the site of implantation of the material) and may induce inflammatory reaction [8]. This problem may be solved by using polymeric materials which degrade to inert products - good examples are the polymers derived from trimethylene carbonate which primary product of the degradation is 1,3-propanediol [12].

The terpolymer used in this paper was synthesized with zirconium acetylacetonate Zr(Acac)₄ as an initiator. Stannous octoate (II) (Sn(Oct)₂) is commonly used as an initiator of the polymerization reaction [8], but because of its toxicity, researches are looking for other, non-toxic initiators (such as calcium, iron or zirconium) [13]. Studies have shown that the use of Zr(Acac)₄ as the initiator have positive effect on the viability and activity of cells grown on a polymer (compared to polymers containing trace amounts of tin) [8].

The aim of this study was to evaluate the cytotoxicity of degradation products derived from poly(L-lactide-co-glycolide-co-trimethylene-carbonate) 75:13:12, on cultured human chondrocytes.

Materials and methods

The polymeric matrices were obtained from poly(L-lactide-co-glycolide-co-trimethylene carbonate) (P(L-LA-GA-TMC)) 75:13:12. The terpolymer was synthesized at the Centre of Polymer and Carbon Materials of Polish Academy of Sciences in Zabrze. Terpolymerization reaction was conducted in bulk at 120°C for 72 h, with the use of non-toxic Zr(Acac)₄ as an initiator.

Composition of terpolymer was examined with the use of 1-H NMR high resolution spectroscopy (AVANCE II Ultra Shield Plus, Bruker 600 MHz) with CDCl₃ as a solvent.

TABLE 1. Characteristic of P(L-LA-GA-TMC), (F_T , F_{LL} , F_{GG} - the percentage content of carbonate, lactidyl and glycolidyl units, respectively; M_n - number average molecular weight, D - molecular-weight dispersity M_w/M_n), T_g - glass transition temperature, T_m - melting temperature, ΔH_m - melting enthalpy).

	F_T	F_{LL}	F_{GG}	M_n [Da]	D	T_g [°C]	T_m [°C]	ΔH_m [J/g]
P(LA-GA-TMC)	12	75	13	39400	2.2	52	120	8

TABLE 2. Characteristic of P (L-LA-GA-TMC) matrices after 30, 60 and 90 days of degradation.

	F_T	F_{LL}	F_{GG}	M_n [kDa]	D	Weight loss [%]
0 days	12	75	13	39.4	2.2	-
30 days	14	74	12	11.9	3.4	4.5
60 days	14	74	12	2.6	6.4	6.1
90 days	14	74	12	2.1	5.2	7.4

Thermal properties were tested by differential scanning calorimetry (DSC) (TA DSC 2010; TA Instruments, New Castle, DE). Terpolymer was also characterized by number average molecular weight (M_n) and molecular weight dispersity (D) that were analyzed by means of gel permeation chromatography (Viscotek RImax; Viscotek 3580 columns), with chloroform as eluent and 1mL/min flow rate, based on polystyrene standards.

Matrices used in this study, were obtained by the compression method. The steel frame (area of 40.2 cm²) was placed under a hydraulic press and it was filled with appropriate amount of polymer (4.2 g). The compression occurred in elastic state of terpolymer (above T_g) between heated stainless steel blocks with pressure of 2.3 tons for 4 minutes. The film was cut in order to prepare 1cm diameter matrices. The matrices were sterilized with high-energy electron beam radiation in dose of 25 kGy.

In this study matrices of terpolymer in the form of discs were placed in sterile nonpyrogenic water (Hyclone, Thermo-Scientific) in test tubes with corks. The volume of degradation medium was dependent on the mass of the polymer disc and calculated by the following formula:

$$\text{Water volume} = 25 \times \text{matrix mass (g)}.$$

Then, the matrices were placed in an incubator at 37°C. The matrices degraded in water during 30, 60 and 90 days (ISO 10993-13 standard), then they were removed and aqueous solutions of degradation products were tested using the cytotoxicity test. Pure water was used as a negative control.

The first step of the testing of aqueous solutions was to prepare appropriate medium for the test. The culture medium was prepared using the basic medium: MEM concentrated x10 (Minimum Essential Medium Eagle's, Sigma). The concentrated medium was diluted with sterile, ultrapure deionized water, added in suitable proportions to obtain dilution x1. For the enrichment of the basic medium, following supplements were added:

- 10% fetal bovine serum (FBS) (PAA)
- penicillin 100 U/ml, streptomycin 100 g/ml (Sigma)
- AAMS supplement containing amino acids (Sigma)
- Glutamine to final concentration of 2 M (Sigma)
- NaHCO₃ a final concentration of 2 l (Sigma)
- ITS supplement (insulin, transferrin, selenium, Invitrogen)
- HEPES at a final concentration of 10 M (Sigma)

Cytotoxicity test was performed on normal human articular chondrocytes (Lonza). The cells were cultured in Chondrocyte Growth Medium (CGM BulletKit, Lonza) under standard conditions (at 37°C, in the atmosphere of 5% CO₂ / 95% air).

For the assessment of the cell proliferation, chondrocytes were seeded into 96-well plates (10³ cells/well in 0.2 ml of CGM). After 24 hours of incubation, CGM medium was removed from wells, and prepared aqueous solutions (in two dilutions: 1:4 and 1:20 with medium as described above) were added. The cells were incubated with solutions for 3 days.

Cell proliferation was quantified with the use of In Vitro Toxicology Assay Kit, Sulforhodamine B Based (Sigma-Aldrich) according to the manufacturer's protocol. Briefly, cells were fixed with TCA (trichloroacetic acid) and then stained with sulforhodamine B, which is a dye staining cellular proteins. The unbound dye was removed with 1% acetic acid and the incorporated dye was liberated from cells with Tris solution. Absorbance was measured at $\lambda = 570$ nm and $\lambda = 690$ nm (reference wavelength).

The last part of this study was statistical analysis of the results. Analysis was performed using Statistica 8, with quantity tests: normality tests, Leven's and Brown-Forsythe's variance tests, variance analysis (ANOVA) and RIR Turkey's test ($p < 0,05$).

Results and Discussion

The aim of present study was to assess the biocompatibility of degradation products of biodegradable polymer with the shape memory property. Terpolymeric matrices were obtained from poly(L-lactide-co-glycolide-co-trimethylene carbonate) (P(L-LA-GA-TMC)) 75:13:12, which was synthesized with Zr(Acac)₄ as an initiator of terpolymerization and processed by pressing. The characteristic of the material used in this work is shown in TABLE 1.

The analyzed P(L-LA-GA-TMC) 75:13:12 is a material with a high number average molecular weight (M_n) and low molecular-weight dispersity (D). The glass transition temperature of the polymer (T_g), determined by DSC was 52°C and $T_m = 120$ °C, however the melting enthalpy was very low. The changes of polymer composition, molecular weight and thermal properties after 30, 60 and 90 days of degradation were shown in TABLE 2. Significant decrease of M_n was noted between 30 and 60 days of degradation, however the weight loss was not significant. Faster degradation of lactidyl and glycolidyl units was determined after 30 days of degradation. Between 30 and 90 days of degradation the terpolymer composition did not changed, so all the units degraded evenly.

The results of cytotoxicity test of studied aqueous solutions of degradations products are shown in FIG. 1.

Aqueous solutions of the degradation products of P(L-LA-GA-TMC) at a dilution of 1:4 showed statistically significant inhibition of growth of chondrocytes only in samples obtained after 60 days degradation. The lack of cytotoxicity of the samples obtained after 90 days of degradation (despite the cytotoxicity of samples which degraded only 60 days) may show that the factor which was toxic to the cells, after an additional 30 days of degradation also degraded.

Aqueous solutions of the degradation products of P(L-LA-GA-TMC) at a dilution of 1:20 did not cause any statistically significant inhibition of growth of the studied cells – this may be caused by higher dilution of cytotoxic agent.

The cytotoxicity of these materials may be provoked by many factors. According to the literature [8], degradation products can provoke cytotoxicity if they have low molecular weight. There are also studies that show inflammatory reaction in correlation to the decrease of M_n of 10 – 0.5 kDa and undoubtedly inflammation has negative effect on tissue and cells [8]. Secondly, other factor that may be responsible for cytotoxicity is local pH decrease that may be provoked by acidic degradation products released from the material. According to Cordewener et al. [8] there is a strict correlation between pH decrease and toxicity effect. Finally, processing method may also be a factor affecting cytotoxicity. In this study, the terpolymeric matrices were obtained by compression method. The study of Chłopek et al. [14] shows that poly (L-lactide-co-DL-lactide) 70:30 changes its properties observed in biological environment depending on the processing method. Compression method may affect polymeric material and cause faster degradation, which may more significantly decrease pH of degradation medium. In this study, the effect of pH decrease was eliminated during preparations of the samples by adding of appropriate amounts of NaOH.

It should be noted that even lack of cytotoxicity is not sufficient to conclude that the material is completely biocompatible. However, such a result is required for further research in this aspect [6]. The results of this study suggest that the studied terpolymer (P(L-LA-GA-TMC) 75:13:12) is biocompatible, which should be further examined. It is not cytotoxic during first 30 days of degradation. After this time the degradation products obtained from P(L-LA-GA-TMC) show cytotoxic effect on human chondrocytes. Further studies of P(L-LA-GA-TMC) are needed to determine the cytotoxic factor; compare biocompatibility of polymer with the same composition but with higher molecular weight, or obtained by modified processing method.

Conclusion

Based on the results of this study, there was inhibition of growth of chondrocytes incubated with degradation products obtained from matrices of P(L-LA-GA-TMC) 75:13:12. However, terpolymer does not show cytotoxic effect to chondrocytes during the first 30 days of degradation.

Acknowledgements

This work was financially supported by project MEMST-ENT (Grant No: UDA-POIG.01.03.01-00-123/08-04).

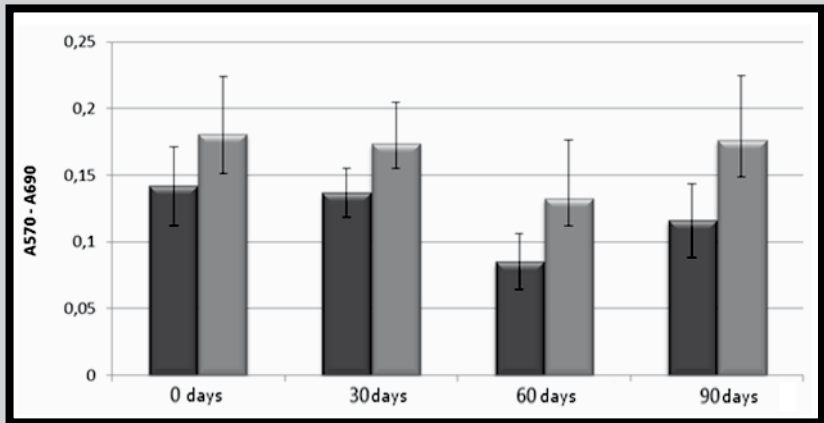


FIG. 1. Influence of water solutions on human chondrocyte growth. Bars show the average value of absorbance levels (\pm SD), $n=9$, $p<0.05$.

References

- [1] Behl M., Lendlein A.L. Shape-memory polymers. *Mater. Today* 10 (2000) 20-28.
- [2] Jaros A., Smola A., Kasperczyk J.: Biodegradowalne polimery z pamięcią kształtu do zastosowań medycznych. *Chemik* 64,2 (2010) 87-96.
- [3] Smola A. et al.: New semi-crystalline bioresorbable materials with shape-memory properties. *Engineering of Biomaterials* 89-91 (2009) 82-87.
- [4] Gębarowska K. et al.: Bioresorbable lactide/glycolide/trimethylene carbonate terpolymers with shape recovery properties. *Engineering of Biomaterials* 63-64 (2007) 48-50.
- [5] Ratna D., Karger-Kocsis J.: Recent advances in shape memory polymers and composites: a review. *J Mater Sci* 43 (2008) 264-265.
- [6] Błażewicz S., Stoch L.: *Biomateriały polimerowe*. [W:] Nałęcz M.: *Biocybernetyka i inżynieria biomedyczna 2000*, Warszawa: Akademicka Oficyna Wydawnicza Exit (2003).
- [7] Bostman O., Vijanen J., Salminen S., Pihlajamaki H.: Response of articular cartilage and subchondral bone to internal fixation devices made of poly-L-lactide: a histomorphometric and microradiographic study on rabbits. *Biomaterials* 21 (2009) 2553-2560.
- [8] Cordewener F. W., Maarten F., Joziassse C. A. P., Schmitz J. P., Bos R. R. M., Rozema F. R., Pennings A. J.: Cytotoxicity of poly(96L/4D-lactide): the influence of degradation and sterilization. *Biomaterials* 21 (2000) 2433-2442.
- [9] Pamuła E., Błażewicz M., Czajkowska B., Dobrzyński P., Bero M., Kasperczyk J.: Elaboration and Characterization of Biodegradable Scaffolds from Poly (L-lactide-co-glycolide) Synthesized with Low-Toxic Zirconium Acetylacetonate. *Annals of transplantation* 9 (2004) 64-67.
- [10] Bouissou C., Walle C.: Poly(lactic-co-glycolic acid) microspheres. In: Uchegbu I. F., Schatzlein A. G. *Polymers in Drug Delivery*. CRC Taylor&Francis (2006) 81-99.
- [11] Yu H., Wooley P. H., Yang S. Y.: Biocompatibility of Poly-ε-caprolactone-hydroxyapatite composite on mouse bone marrow-derived osteoblasts and endothelial cells. *J Orthop Surg Res* 4 (2009) 5.
- [12] Zhang Z., Grijpma D. W., Feijen J.: Creep-resistant Poros structures based on stereo-complex forming triblock copolymers of 1,3-trimethylene carbonate and lactides. *J Mater Sci-Mater M* 15 (2004) 381-385.
- [13] Dobrzyński P., Pastusiak M., Bero M.: Less toxic acetylacetonates as initiators of trimethylene carbonate and 2,2-Dimethyl-trimethylene carbonate ring opening polymerization. *J Polym Sci, Part A: Polym Chem* 43 (2005) 1913-1922.
- [14] Chłopek J., Morawska-Chochół A., Więtecha A.: The influence of processing on polylactide properties. *Engineering of Biomaterials* 89-91 (2009) 217-220.

DEGRADATION PROCESS OF TMC-BASED POLYMERS BY MASS SPECTROMETRY

JOANNA JAWORSKA*, JANUSZ KASPERCZYK, MAGDALENA MAKSYMIAK, GRAŻYNA ADAMUS, PIOTR DOBRZYŃSKI

CENTRE OF POLYMER AND CARBON MATERIALS, SKŁODOWSKIEJ- CURIE 34 ST., 41-819 ZABRZE, POLAND

* E-MAIL: MACIEJOWSKA@WP.PL

Abstract

This paper presents results of degradation process investigations of resorbable poly(lactide-trimethylene carbonate). Materials used in this work were synthesized by the ring opening polymerization. Polymerization was carried out in bulk using Zr(acac)₄ as initiator. The resulting copolymers were characterized by high resolution NMR spectroscopy. Then the copolymers were allowed to degrade in H₂O for 53 weeks. These conditions allowed to analyze the degradation products of poly(lactide-trimethylene carbonate) and to determine the structure of oligomers using multi-stage mass spectrometry technique (ESI-MSⁿ). ESI-MS analysis revealed the presence of two kinds of oligomers.

[Engineering of Biomaterials 113 (2012) 26-28]

Introduction

Poly(trimethylene carbonate) (PTMC) is an amorphous elastomer which exhibits good mechanical properties: high flexibility and high tensile strength [1]. Such elastic biodegradable material is required in the production of medical implants and porous scaffolds [2]. It was observed that in phosphate buffer saline at pH=7 and at a temperature of 37°C, PTMC degrades very slowly. However, *in vivo* degradation occurs rapidly by surface erosion [1].

High molecular weight statistical copolymers of TMC and DLLA were synthesized using Sn(oct)₂ as an initiator, characterized and compared with the corresponding homopolymers PTMC and PDLLA [3]. The obtained results showed that the thermal and mechanical properties of the polymers strongly depend on the composition. All materials were hydrophobic. The properties of the TMC and DLLA copolymers suggested their suitability as materials for resorbable biomedical devices. The highly elastic PTMC and copolymers with high TMC content seemed more suitable for application as coatings or drug delivery systems [3].

PTMC and TMC-based copolymers were also successfully synthesized by ring opening polymerization with the use of low toxic metals: iron, zinc, zirconium [1-2]. Degradation of LLA/TMC copolymers prepared with Zr(acac)₄ initiator was examined by Hua et al. [1]. By varying the chemical composition, chain microstructure and morphology various degradation behaviors and degradation rates were obtained.

Low-molecular weight poly(ε-caprolactone-co-1,3-trimethylene carbonate) and poly(1,3-trimethylene carbonate) were examined as potential vehicles for the delivery of water-soluble agents such as vitamin B12. The rate of release was the fastest for the amorphous oligomers and dependent on their viscosity [4].

Materials and Methods

Copolymers of lactide and trimethylene carbonate were obtained by ring opening polymerization using Zr(acac)₄ as initiators. Temperatures of reaction were 110°C and 180°C. The molar ratio of comonomers/initiator was 1000:1. Polymerization was carried out in bulk. The copolymers were compression moulded. Square specimens with approximately 0.5 mm thick were then cut from the material. The resulting form of copolymers was submitted to degradation in water at 37°C for 53 weeks. The resulting copolymers were characterized by ¹H NMR. NMR spectra were recorded with a Bruker Avance II spectrometer operating at 600 MHz, using CDCl₃ as a solvent. Chemical shifts (δ) were given in ppm using tetramethylsilane (TMS) as an internal reference. The spectra were obtained with 32 scans, 11 μs pulse width and 3.74 s acquisition time for ¹H NMR.

The structure of degradation products was determined with aid of multistage mass spectrometry technique (ESI-MSⁿ). Degradation medium was withdrawn at established periods of time, then samples were freeze-dried and dissolved in methanol/chloroform (1/1 v/v) solution and such solutions were introduced to the ESI source by continuous infusion by means of the instrument syringe pump at a rate of 3 mL/min. The ESI source was operated at 4.5 kV, with the capillary heater at 200°C, and sheath gas pressure 40 psi. For ESI-MSⁿ experiments mass-selected monoisotopic molecular parent ions were isolated in the trap and collisionally activated with 40% ejection RF-amplitude at standard He pressure. The experiments were performed in both positive- and negative-ion mode.

Results and Discussion

Copolymers samples PLATMC (50/50) with various chain microstructure were obtained changing the temperature of polymerization: 110°C (PLATMC110) and 180°C (PLATMC180).

The co-monomeric units content were estimated using high resolution NMR spectroscopy [1].

The structure of the degradation products of PLATMC was determined by multistage mass spectrometry technique (ESI-MSⁿ). It was possible to detect distinguishable signals since 41st week of degradation (FIG. 1).

Signals detected in ESI-MS spectra were associated with appropriate structure of oligomers. ESI-MS analysis revealed two kinds of oligomers (FIG. 2). Structures I and II possess carbonate unit: -O-(CH₂)₃-O-C(O)- and lactidyl unit: -O-CH(CH₃)-C(O)-. Structure I corresponds to oligomers with carboxyl-end of the chain as well as hydroxyl-end of the chain and is abbreviated as TL. Structure II corresponds to oligomers (in majority) with two carboxyl-ends of the chain and is abbreviated as T'L'. Second mode spectra of selected signals confirm these conclusions. One of them is presented in FIG. 3.

It is possible to identify a series of oligomers detected in ESI-MS spectra of PLATMC (FIG. 4).

In the case of PLATMC110, the observed series of oligomers are identified as following:

T'L'2÷T'3L'2, T'L'3÷T'3L'3 (41st week of degradation)
T'L'2÷T'5L'2, T'L'3÷T'5L'3, T2L÷T4L (53rd week of degradation)

In the case of PLATMC180, the observed series of oligomers are identified as following:

T'L'2÷T'3L'2, TL2÷T3L2, T'L'3÷T'3L'3, TL3÷T5L3, T2L÷T3L (41st week of degradation)

T'L'2÷T'6L'2, T2L÷T3L (53rd week of degradation)

It is clearly seen that oligomers detected in 41st week of degradation are short and consist of several units. Longer oligomers are detected in 53rd week of degradation.

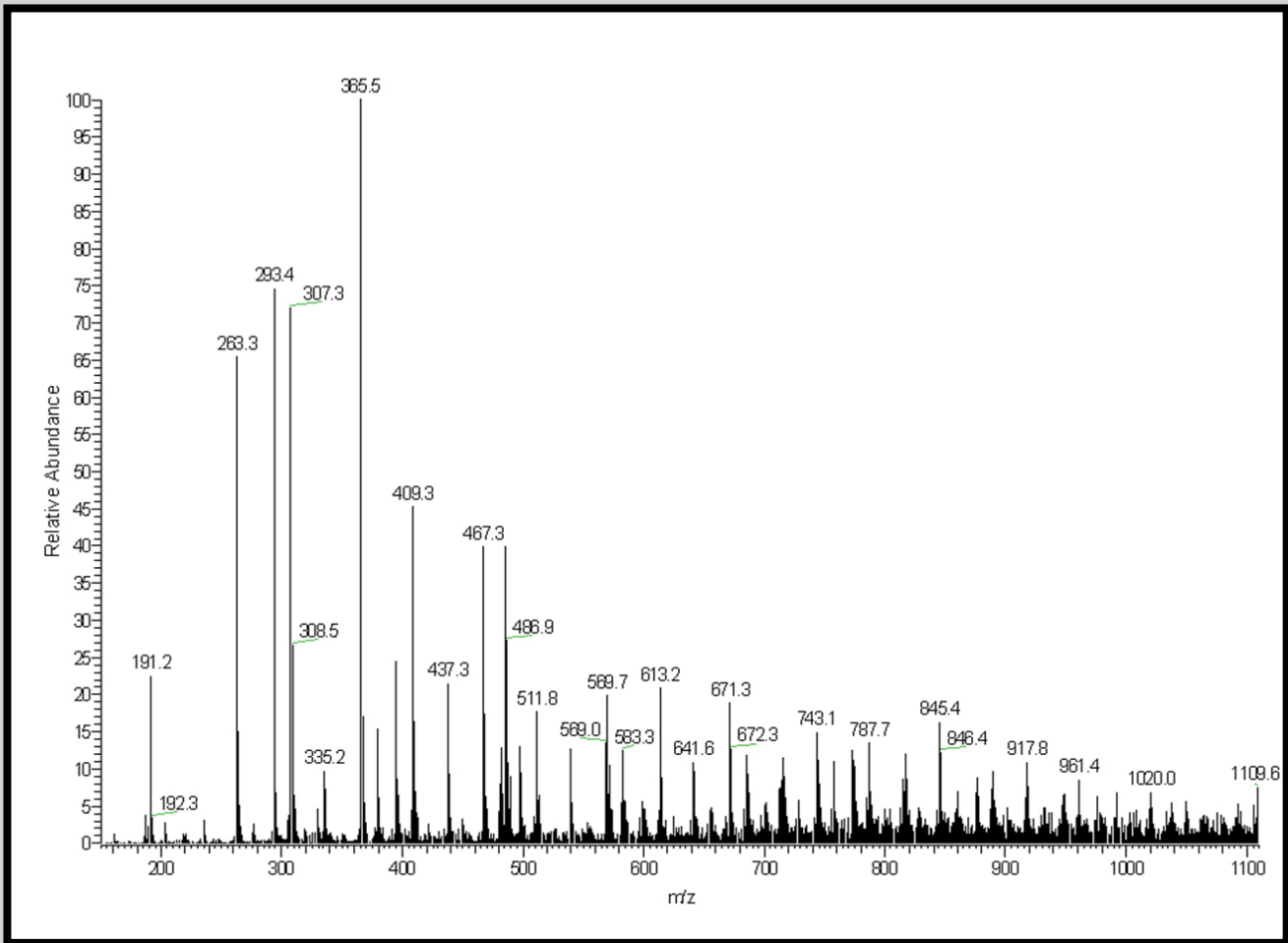


FIG. 1. ESI-MS spectrum of PLATMC180.

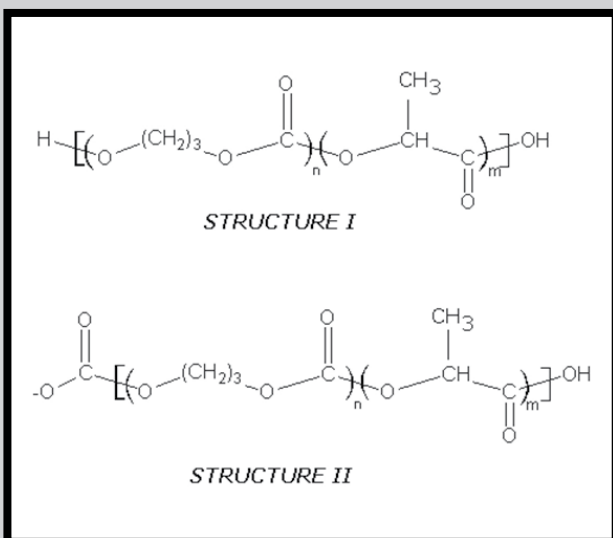


FIG. 2. Structures of oligomers detected in ESI-MS spectra.

Conclusions

Copolymers of lactide and trimethylene carbonate were allowed to degrade in H_2O for 53 weeks. These conditions allowed to analyze the degradation products and to determine the structure of oligomers using multistage mass spectrometry technique (ESI-MSⁿ). ESI-MS analysis revealed two kinds of oligomers:

- oligomers with carbonyl-end of the chain as well as hydroxyl-end of the chain and
- oligomers (in majority) with two carbonyl-ends of the chain.

It is possible to identify a series of oligomers detected in ESI-MS spectra of PLATMC. It is clearly seen that oligomers observed in 41st week of degradation are short and consist of several units. Longer oligomers are observed in 53rd week of degradation.

Acknowledgements

Researches were conducted with financial support from project no. UDA-POIG.01.03.01-00-123/08-00.

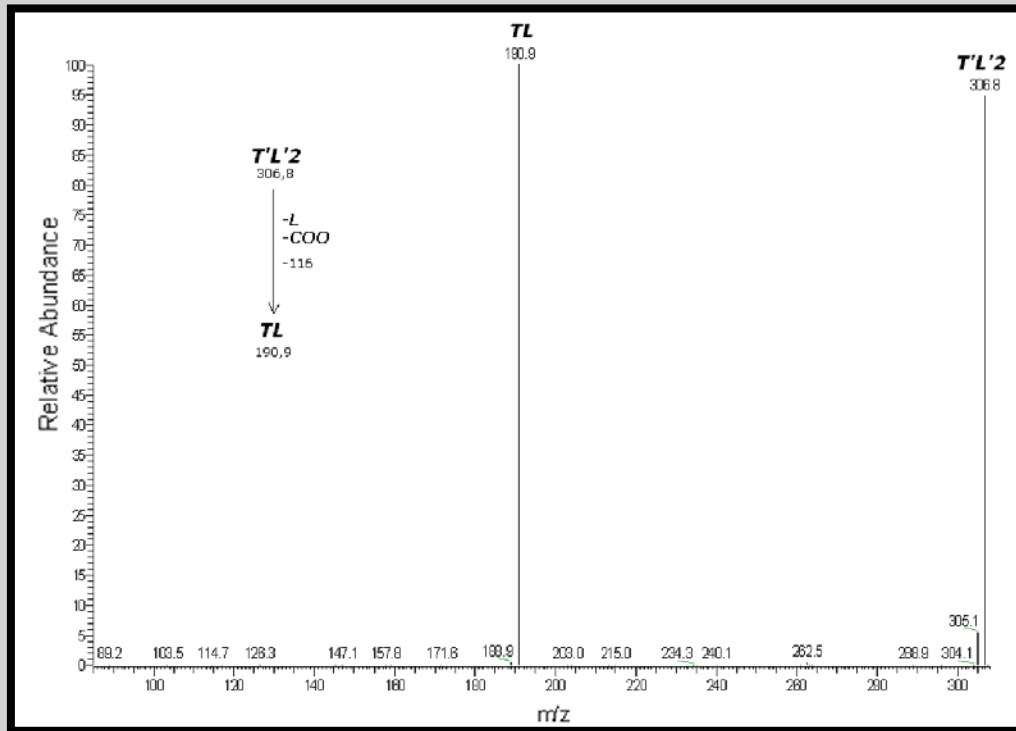


FIG. 3. Fragmentation of selected signal from ESI-MSⁿ spectrum of PLATMC180.

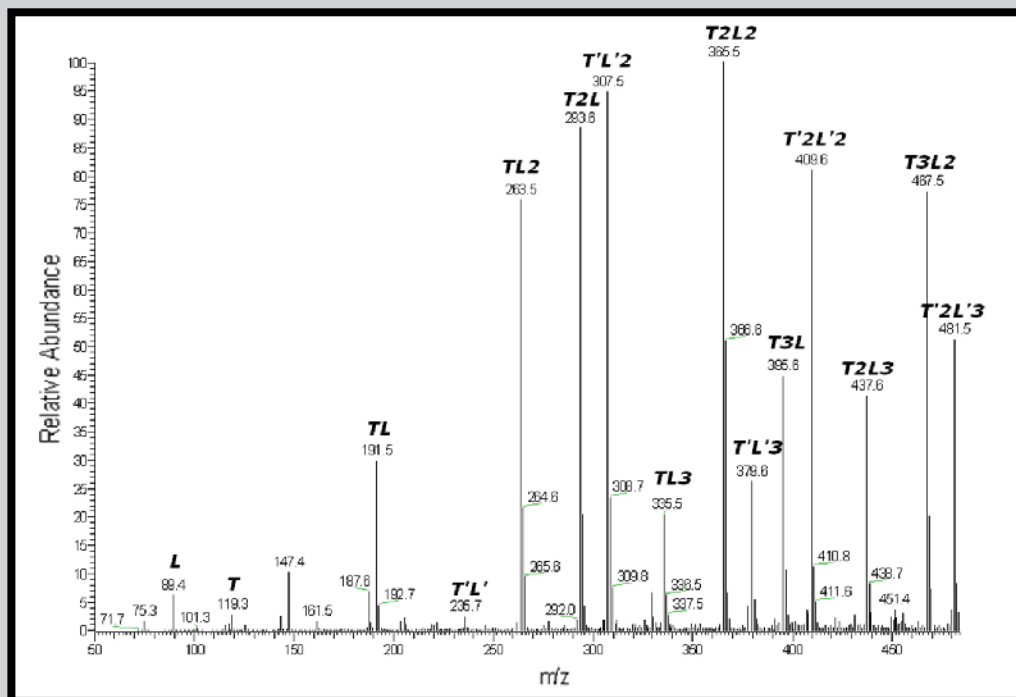


FIG. 4. ESI-MS spectrum of PLATMC180 (in spectral expansion in the mass range m/z 50–500). Assignment of the signals to appropriate oligomer structure.

References

- [1] Hua J., Gebarowska K., Dobrzynski P., Kasperczyk J., Wei J., Li S.: Influence of chain microstructure on the hydrolytic degradation of copolymers from 1,3-trimethylene carbonate and L-lactide, *J. Polym. Sci. Part A: Polym Chem.* 47 (2009) 3869-3879.
- [2] Dobrzynski P., Pastusiak M., Bero M.: Less toxic acetylacetonates as initiators of trimethylene carbonate and 2,2-dimethyltrimethylene carbonate ring opening polymerization, *J. Polym. Sci. Part A: Polym Chem.* 43 (2005) 1913-1922.
- [3] Pego P., Poot A.A., Grijpma D.W., Feijen J.: Physical properties of high weight 1,3-trimethylene carbonate and D,L-lactide copolymers, *J. Mater. Sci.: Mater. Med.* 14 (2003) 767-773.
- [4] Sharifpoor S., Amsden B.: In vitro release of a water-soluble agent from low viscosity biodegradable, injectable oligomers, *Eur. J. Pharm. And Biopharm.* 65 (2007) 336-345.

BIOMIMETIC Ca-P COATINGS OBTAINED BY CHEMICAL/ELECTROCHEMICAL METHODS FROM HANKS' SOLUTION ON A Ti SURFACE

M. PISAREK^{1*}, A. ROGUSKA^{1,2}, L. MARCON³, M. ANDRZEJCZUK²

¹ INSTITUTE OF PHYSICAL CHEMISTRY, POLISH ACADEMY OF SCIENCES, KASPRZAKA 44/52, 01-224 WARSAW, POLAND

² FACULTY OF MATERIALS SCIENCE AND ENGINEERING, WARSAW UNIVERSITY OF TECHNOLOGY, WOŁOSKA 141, 02-507 WARSAW, POLAND

³ INTERDISCIPLINARY RESEARCH INSTITUTE, USR CNRS 3078 PARC DE LA HAUTE BORNE, 50 AV. DE HALLEY 59658 VILLENEUVE D'ASCQ, FRANCE

* E-MAIL: MPISAREK@ICHF.EDU.PL

Abstract

The purpose of this study was to investigate the bioactivity of porous calcium phosphate coatings on titanium prepared using a two-step procedure (chemical etching or anodic oxidation of Ti followed by soaking in simulated body fluid or direct electrodeposition from Hanks' solution). In order to evaluate the potential use of the coatings for biomedical applications, the adsorption of serum albumin, the most abundant protein in the blood, and the attachment of living cells (osteoblasts, U2OS) were studied.

Keywords: biomaterials, biomimetic, surface analysis, protein adsorption, U2OS cells

[*Engineering of Biomaterials 113 (2012) 29-32*]

Introduction

The main requirements for metallic biomaterials, including titanium, are: (a) biocompatibility, (b) resistance to biological corrosion and (c) antisepticity. Those requirements may be met by developing perspective titanium biomaterials with surface layers of strictly-defined microstructure, chemical and phase composition. Recently, various surface modifications have been applied to form a bioactive layer on a Ti surface, which is known to accelerate osseointegration [1]. Chemical processes for modifying surfaces of Ti and its alloys are widely employed to increase the biocompatibility of those materials [2]. Methods, such as Ti etching in alkaline solutions (e.g. NaOH [2,3]), acidic solutions (H₂SO₄ [3,4]) or hydrogen peroxide (H₂O₂ [5]) at high temperatures, combined with subsequent prolonged soaking of samples in artificial physiological solutions (SBF- Simulated Body Fluid, Hanks' solution) of pH~7, allow to obtain porous oxide layers with built-in calcium and phosphorous ions [6-8]. Electrochemical processes are also commonly applied for modifying surfaces of Ti in order to increase its biocompatibility [9,10]. The chemical composition of the resulting coatings is close to that of hydroxyapatite, which is known to support bone osseointegration and ingrowth when used in orthopaedic or dental applications [1,7]. The anodic polarization at constant voltage of Ti and its alloys in acidic or neutral solutions containing fluorides is a typical electrochemical method for obtaining oxidized layers of uniform chemical composition, different thickness and refined nanoporosity [11-13].

The addition of a suitable fluoride concentration to an electrolyte ensures that a porous morphology is obtained, in the form of titanium dioxide nanotubes [11-13]. Such structures can provide very promising substrates which increase biological tolerance, since it is possible to precisely control the thickness of the layers (by the end voltage of the anodic polarization) and their surface morphology (porosity). Further chemical treatment aimed at introducing additional factors increasing biocompatibility, such as ions of calcium and phosphorus, can be carried out by immersing the oxide layers in artificial physiological solutions [14,15]. To evaluate a potential use of the Ca-P coatings, thus obtained, for biomedical implants protein adsorption and living cells attachment were examined. Serum albumin, the most abundant protein in blood, and U2OS cells were used in this study [8,16,17].

Materials and methods

a) Material substrate: Ti foil 0.25 mm-thick (99.5% purity, Alfa Aesar, USA).

b) Chemical pretreatment: the samples were soaked in a 3 M NaOH aqueous solution at 70°C for 24 h, or in an H₃PO₄ + H₂O₂ solution (with a volume ratio of 1:1) at room temperature for 24 h.

c) Electrochemical pretreatment: titanium oxide nanotube layers were fabricated by anodic oxidation of Ti in an optimized mixture of NH₄F (0.86 wt.%) + DI water (47.14 wt.%) + glycerol (52 wt.%) electrolyte at room temperature, applied voltage $V_{max} = 20$ V, 2 h. After anodization, the samples were annealed in air at 600°C for 2 h.

d) Deposition of calcium phosphate coatings: soaking in Hanks' solution (7 days, at 37°C) or electrodeposition from Hanks' electrolyte ($E = -1.5$ V vs. OCP, for 2h 15 min). The Hanks' solution was prepared by dissolving reagent-grade (g/L): NaCl 8.00, KCl 0.40, Na₂HPO₄·2H₂O 0.06, KH₂PO₄ 0.06, MgSO₄·7H₂O 0.20, NaHCO₃ 0.35, CaCl₂ 0.14 into distilled water and buffering at pH = 7.4.

e) Surface characterization: SEM (Hitachi S-5500), XPS (Microlab 350, Thermo Electron), FTIR (Nicolet iN10-MX, Nicolet 6700, Thermo Electron Scientific).

f) Biological tests: bovine serum albumin (BSA) (Sigma, purity of 99.8%) was dissolved in phosphate buffered saline - PBS, pH=7.4 and used as a model protein. Human osteosarcoma U2OS cells were used to evaluate the biocompatibility of the Ca-P coatings under study. Dulbecco's modified eagle's medium (DMEM, Invitrogen) supplemented with 10% fetal bovine serum (Invitrogen) and 1% of a penicillin/streptomycin mixture was used as a cell culture medium. Cells were seeded on the sample surfaces at 1.0×10^4 cells/cm² and cultured at 37°C in a humidified atmosphere containing 5% CO₂ for 120 h. Cells were transiently transfected with memb-mCherry 24 h before observation allowing the expression of fluorescent mCherry protein localized in the cell membranes. FuGENE HD (Roche Diagnostics, Switzerland) was used as a transfection reagent according to the manufacturer's recommendations. Cell nuclei were then stained 1 h before observation with Hoechst 33342 (Life Technologies, USA) according to the manufacturers' instructions. Cell morphology was examined using an optical microscope (Eclipse 80i, Nikon Instruments, Tempe, AZ).

g) All samples were sterilized by autoclaving at 121°C for 20 min prior to the cell culture experiments [18].

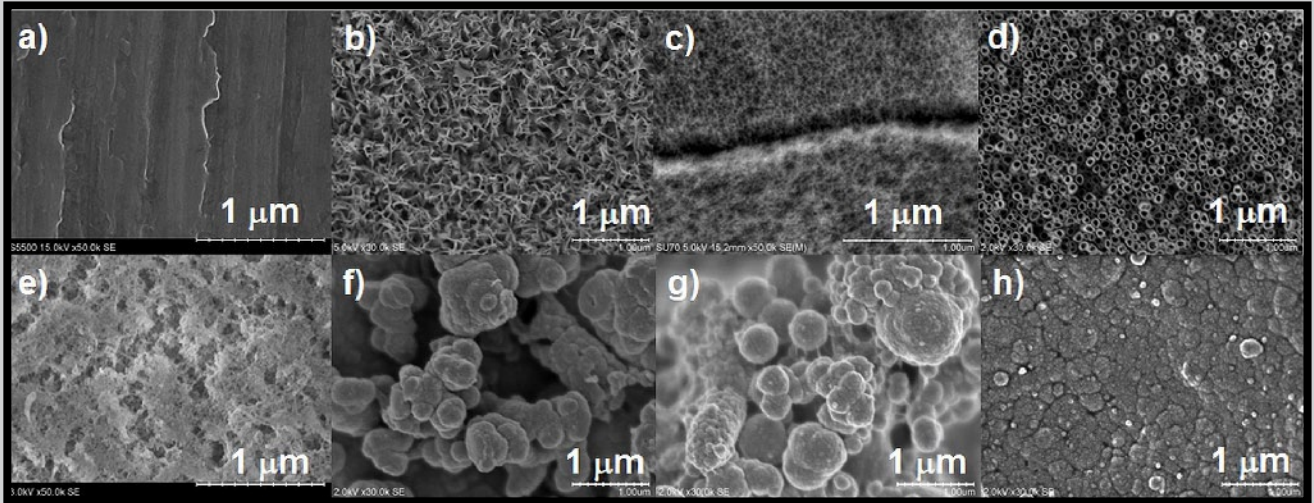


FIG. 1. SEM images of un-treated Ti (a); chemically treated in NaOH solution, 24 h at 70°C (b); H₃PO₄ + H₂O₂ solution: 24 h, room temperature (c); electrochemically treated in 0.86 wt.% NH₄F+glycerol+water DI electrolyte: 20 V, 2h (d); electrodeposited in Hanks' solution: - 1.5 V, 8000 s (e) and after subsequent immersion in Hanks' solution: 7 days, temp. 37°C, pH = 7.4 (f, g, h) – top view.

TABLE 1. Ca2p_{3/2}, P2p_{3/2} and O1s binding energies as determined from corrected XPS spectra after chemical/electrochemical treatment in Hanks' solution, and estimated Ca/P atomic ratio.

Ti surface modification	Ca2p _{3/2} / eV	P2p _{3/2} / eV	O1s / eV	Ca/P at.% ratio, average volume
NaOH pretreatment and soaking in Hanks' solution for 7 days	347.5 – 347.9 / Ca ²⁺	132.6 – 133.4 / PO ₄ ³⁻	531.1 – 531.6 / O ₂ ⁻	1.08
H ₃ PO ₄ + H ₂ O ₂ pretreatment and soaking in Hanks' solution for 7 days				1.09
after electrodeposition in Hanks' solution (- 1.5 V vs. OCP)				1.10
anodic oxidation pretreatment (20 V) of Ti and soaking in Hanks' solution for 7 days				1.37

Results and Discussions

SEM images of Ti before and after chemical/electrochemical pretreatment are shown in FIGs. 1a, b, c, d. The reference sample is smooth (pure Ti, FIG. 1a), with no particular morphological features. In contrast, immersion in 3 M NaOH at 70°C for 24 h results in the formation of a 'coral-like' topography (FIG. 1b). The surface layer exhibits a developed, rough morphology characterized by a network of sharp-edged pores. After pre-treatment in H₂O₂ + H₃PO₄ at room temperature, the morphology is quite different, and seems to be less developed (with shallower 'valleys') than that obtained after NaOH pre-treatment. Ti treated in H₂O₂ + H₃PO₄ exhibits sponge-like porosity, as FIG. 1c suggests. A distinct texture with round nano-sized pores is clearly seen. The nanopores are uniformly distributed across the surface. The optimized anodization conditions resulted in the formation of TiO₂ nanotubes (hollow cylinders) arranged perpendicularly to the substrate and separated from each other, as shown in FIG. 1d. SEM examinations revealed that the nanotubes were open at the top. It is generally accepted that rough and porous surfaces can stimulate nucleation and the growth of calcium phosphates. SEM images of a typical morphology of calcium phosphate coatings obtained on pretreated Ti by chemical/electrochemical methods are shown in FIGs. 1e, f, g, h. After immersion for 7 days in Hanks' solution, the Ca-P surface layer formed is composed of many spheroidal particles tightly packed together (FIGs. 1f, g, h). The Ca-P coating formed on TiO₂ nanotubes is denser, and seems to be better crystallized than on Ti chemically pretreated in alkali and acidic solutions.

As the SEM investigations show, an electrodeposited calcium phosphate coating exhibits a completely different morphology characterized by a network of longitudinal pores of different shapes (FIG. 1e). All the obtained morphologies are similar to that reported in the literature [5,6,9,10,15,19], and seem to be promising for biomedical applications.

XPS measurements were then performed to evaluate the chemical state of the calcium and phosphorous in the coatings deposited on chemically/electrochemically treated titanium.

TABLE 1 shows the binding energies of the O 1s, Ca 2p_{3/2}, and P 2p_{3/2} signals, and the suggested chemical composition of the coatings. Position of the main peak of P 2p_{3/2} may change within a range of 132.6-133.4 eV for all coatings. The spectral data for Ca suggest as well the presence of calcium phosphate compounds (Ca 2p_{3/2}: 347.5 - 347.9 eV). The main component of the O 1s peak at BE = 531.1 - 531.6 eV is attributed to PO₄³⁻ groups. X-ray photoelectron spectroscopy analysis revealed that the surface is enriched in calcium and phosphorous, where the Ca/P molar ratio is 1.08 (NaOH solution), 1.09 (H₂O₂ + H₃PO₄), 1.10 (electrodeposited layer) and 1.37 (TiO₂ nanotubes). This is less than the stoichiometric hydroxyapatite ratio of 1.67. However, our EDS results show that the atomic concentration ratio of Ca/P for the all samples may vary from place to place, oscillating around the average value indicated above. However, higher Ca/P ratios (up to 1.62, 1.64 and 1.75, respectively) were also measured locally.

TABLE 2. Results of local EDS analysis (Ca/P atomic ratio) of calcium phosphate coatings deposited on pure Ti or pretreated Ti from Hanks' solution by chemical/electrochemical methods.

EDS results	Ca/P at.% local ratio	Ca/P at.% ratio, average volume
Ti/Ca-P -1.5 V vs. OCP	1.17 – 1.64	1.38
Ti(NaOH) + Ca-P chemical treatment in NaOH solution + immersion in Hanks' medium	1.14 – 1.62	1.29
Ti(H ₃ PO ₄ +H ₂ O ₂) + Ca-P chemical treatment in H ₃ PO ₄ +H ₂ O ₂ solution + immersion in Hanks' medium	1.15 – 1.75	1.33
Ti(TiO ₂ NT) + Ca-P electrochemical treatment in NH ₄ F+glycerol+water electrolyte + immersion in Hanks' solution	1.13 – 1.75	1.34

TABLE 2 presents the average value of the Ca/P molar ratio – 1.38 for electrodeposited Ca-P coating on Ti, 1.29 for Ti(NaOH), 1.33 for Ti(H₂O₂ + H₃PO₄) and 1.34 for Ti(TiO₂ NT). It is worth to mention that, the XPS measurements provide surface information from the few uppermost nanometers of the samples. This may suggest that a nucleation of CaP phases with lower Ca/P ratio is limited to the outermost surface only. This observation does not concern calcium phosphate layers obtained on TiO₂ NT. The differences in the thickness and crystallinity of the titanium oxide layers fabricated by chemical etching and anodic polarization may play a role here [20].

The differences in the molar Ca/P ratio may result from different formation stages within the bulk comparing to those in the outermost layer of the coating. Local supersaturation and pH fluctuation during precipitation of the hydroxyapatite generally cause the formation of metastable transient phases, where Ca/P ratio may change from 1.2 to 2.2, which then transform into HAp in the process of hydrolysis [21,22]. The estimated molar Ca/P ratio by EDS measurements suggest formation of octacalcium phosphate (OCP, Ca/P = 1.33), and probably various intermediate Ca-P phases [23]. The OCP compound is thought to be a precursor for the crystallization of bone-like apatite/hydroxyapatite [21].

To evaluate the potential use of our materials for biomedical applications, we examined protein adsorption on the surfaces studied. Serum albumin (SA) was used in this study, as it is the most abundant protein in blood. FTIR spectra of SA adsorbed on titanium before and after chemical/electrochemical modification are presented in FIG. 2.

Plasma protein was found to interact with the surfaces studied. The bands at ~1650 cm⁻¹ and ~1540 cm⁻¹ are assigned to amides I and II, respectively [24]. However, changes in the shape and frequency of the amide II band for the electrodeposited Ca-P layer are noticeable. This may be a result of some changes in the protein tertiary structure (3D) due to the interactions with the investigated surfaces.

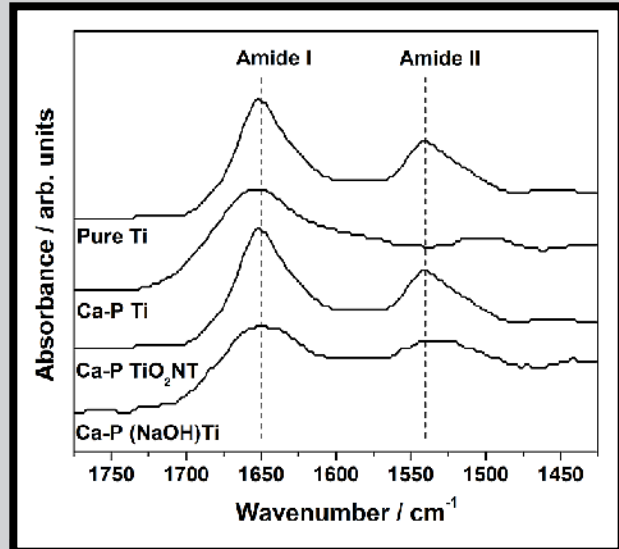


FIG. 2. FTIR spectra of amide I and amide II bands of SA adsorbed on pure Ti and on chemically/electrochemically-treated Ti.

The electrodeposited Ca-P coating seems to have a different effect on adsorbed SA conformation than does the Ca-P layer obtained by chemical methods, but the implication of this finding is not clear at present. The chemistry and morphology of the substrates may play a role here.

FIG. 3 shows the cell morphology on an un-treated Ti surface and on Ti after chemical/electrochemical pretreatment (with a calcium phosphate coating). Fluorescence microscopy observations revealed that the cells are well-extended, and exhibit an elongated morphology, similar to those on pure Ti (reference sample). Nuclei are clearly defined (dark gray color), although cell membranes form a dendritic like-structure (light gray color).

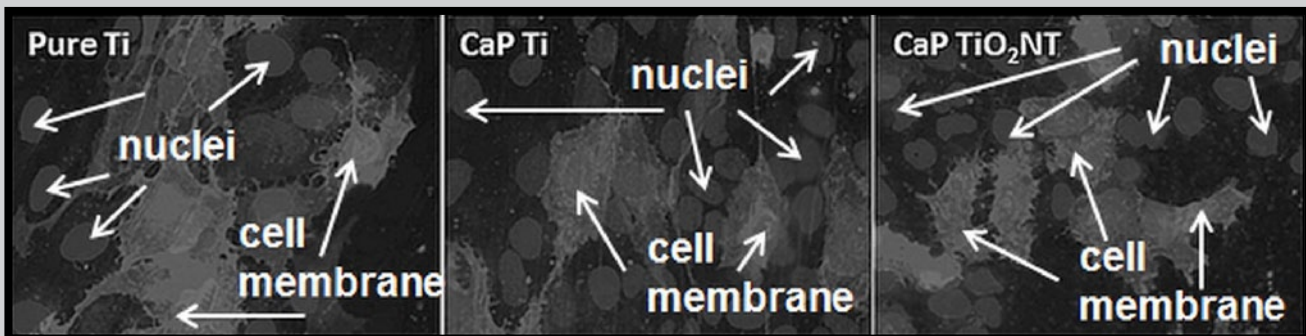


FIG. 3. Fluorescence microscopy images of U2OS cells cultivated for 120 h on pure Ti (a), an electrodeposited Ca-P coating on Ti (b), and a Ca-P layer covered with TiO₂ nanotubes (c). Cells express fluorescent mCherry protein localized in the cell membranes (light gray) and cell nuclei (dark gray) are stained with Hoechst 33342.

After 120h of incubation the cells on presented coatings exhibited cytoplasmic links, as shown in FIG. 3. Ca-P coatings induce cell membrane extension, as shown in FIG. 3, meaning that the cells adhered well to the Ca-P coated surfaces [17,25]. Preliminary results of the response of human osteosarcoma U2OS cells to the surfaces investigated are in qualitative agreement with the protein adsorption experiments.

Conclusions

The present investigations show that biomimetic calcium phosphate coatings of porous apatite-like structure can be grown following a specific morphology by chemical/electrochemical methods from Hanks' solution on a titanium surface. FTIR investigations showed that serum albumin (SA) adsorbed readily on calcium phosphate coatings. Such a Ca-P layer enhances osteoblast-like cell attachment as well. Thus, one may anticipate that chemically/electrochemically Ca-P coatings on Ti may promote early bone apposition and implant fixation by enhancing the adhesion between new bone and the surface of an implant.

References

- [1] Wierzchoń T., Czarnowska E., Krupa D.: Inżynieria powierzchni w wytwarzaniu biomateriałów tytanowych. Oficyna Wydawnicza Politechniki Warszawskiej. Warszawa 2004.
- [2] Wei M., Kim H-K, Kokubo T., Evans J.H.: Optimizing the Bioactivity of Alkaline-Treated Titanium Alloy. *Materials Science and Engineering C* 20 (2002) 125-134.
- [3] Pisarek M., Lewandowska M., Roguska A., Kurzydłowski K.J., Janik-Czachor M.: SEM, Scanning Auger and XPS characterization of chemically pretreated Ti surfaces intended for biomedical applications. *Materials Chemistry Physics* 104 (2007) 93-97.
- [4] Chen Y., Lee Chi-Y, Yeng M-Y, Chin H.T.: Preparing titanium oxide with various morphologies. *Materials Chemistry and Physics* 81 (2003) 39-43.
- [5] Park Ji-H, Lee Y-K, Kim K-M, Kim K-N.: Bioactive calcium phosphate coating prepared on H₂O₂-treated titanium substrate by electrodeposition. *Surface Coatings and Technology* 195 (2005) 252-257.
- [6] Takadama H., Kim H-M, Kokubo T., Nakamura T.: XPS study of the process of apatite formation on bioactive Ti6Al4V alloy in simulated body fluid. *Science and Technology of Advanced Materials* 2 (2001) 389-396.
- [7] Vallet-Regi M., Gonzalez-Calbet J.M.: Calcium phosphates as substitution of bone tissues. *Progress in Solid State Chemistry* 32 (2004) 1-31.
- [8] Pisarek M., Roguska A., Andrzejczuk M., Marcon L., Szunerits S., Lewandowska M., Janik-Czachor M.: Effect of two-step functionalization of Ti by chemical processes on protein adsorption. *Applied Surface Science* 257 (2011) 8196-8204.
- [9] Park Ji-H, Lee D-Y, Oh K-T, Lee Y-K, Kim K-M, Kim K-N.: Bioactivity of calcium phosphate coatings prepared by electrodeposition in a modified simulated body fluid. *Materials Letters* 60 (2006) 2573-2577.
- [10] Wang H., Eliaz N., Hobbs L.W.: The nanostructure of an electrochemically hydroxyapatite coating. *Materials Letters* 65 (2011) 2455-2457.
- [11] Zhao J., Wang X., Chen R., Li L.: Fabrication of titanium oxide nanotube arrays by anodic oxidation. *Solid State Communications* 134 (2005) 705-710.
- [12] Macak J.M., Tsuchiya H., Ghicov A., Yasuda K., Hahn R., Bauer S., Schmuki P.: TiO₂ nanotubes: Self-organized electrochemical formation, properties and applications. *Current Opinion in Solid State and Materials Science* 11 (2007) 3-18.
- [13] Krasicka-Cydzik E., Głazowska I., Kaczmarek A., Białas-Heltowski K.: Wpływ stężenia jonów fluorokowych na wzrost anodowej samoorganizującej się warstwy nanorurek TiO₂. *Inżynieria Biomateriałów* 77-80 (2008) 46-48.
- [14] Roguska A., Pisarek M., Andrzejczuk M., Dolata M., Lewandowska M., Janik-Czachor M.: Characterization of a calcium phosphate – TiO₂ nanotube composite layer for biomedical applications. *Materials Science and Engineering C* 31 (2011) 906-914.
- [15] Dey T., Roy P., Fabry B., Schmuki P.: Anodic mesoporous TiO₂ layer on Ti for enhanced formation of biomimetic hydroxyapatite. *Acta Biomaterialia* 7 (2011) 1873-1879.
- [16] Cai K., Bossert J., Jandt K.D.: Does the nanometer scale topography of titanium influence on protein adsorption and cell proliferation? *Colloids Surfaces B:Biointerfaces* 49 (2006) 136-214.
- [17] ter Brugge P.J., Dieudonne S., Jansen J.A.: Initial interaction of U2OS cells with non-coated and calcium phosphate coated titanium substrates. *Journal of Biomedical Materials Research A* 61 (2002) 399-407.
- [18] Dorozhkin S.V., Schmitt M., Bouler J.M., Daculsi G.: Chemical transformation of some biologically relevant calcium phosphates in aqueous media during steam sterilization. *Journal of Materials Science: Materials in Medicine* 11 (2000) 779-786.
- [19] Kokubo T., Kim H-M, Miyaji F., Takadama H., Miyazaki T.: Ceramic-metal and ceramic-polymer composites prepared by a biomimetic process. *Composites Part A* 30 (1999) 405-409.
- [20] Uchida M., Kim H-M, Kokubo T., Fujibayashi S., Nakamura T.: Structural dependence of apatite formation on titania gels in a simulated body fluid. *Journal of Biomedical Materials Research Part A* 64A (2003)164-170.
- [21] Dorozhkin S.V.: Calcium orthophosphates. *Journal of Materials Science* 42 (2007) 1061-1095.
- [22] Praca zbiorowa pod red. M. Nałęcza.: Biocybernetyka i inżynieria biomedyczna 2000, Tom 4 – Biomateriały (red. S. Błazewicz, L. Stoch). Akademyka Oficyna Wydawnicza Exit. Warszawa 2003.
- [23] Lu H.B., Campbell C.T., Graham D.J., Ratner B.D.: Surface characterization of hydroxyapatite and related calcium phosphates by XPS and TOF-SIMS. *Analytical Chemistry* 72 (2000) 2886-2894.
- [24] Twardowski J.: Spektroskopia Ramana i podczerwieni w biologii. Państwowe Wydawnictwo Naukowe. Warszawa 1988.
- [25] Zhu X., Chen J., Scheideler L., Reichl R., Geis-Gerstorfer J.: Effects of topography and composition of titanium surface oxides on osteoblast responses. *Biomaterials* 25 (2004) 4087-4103.

Acknowledgments

This work was financially supported by the National Science Center (decision No. DEC-2011/01/B/ST5/06257), and by the Institute of Physical Chemistry PAS and Interdisciplinary Research Institute.

A REVISED SURGICAL CONCEPT OF ANTERIOR CRUCIATE LIGAMENT REPLACEMENT IN A RABBIT MODEL. PRELIMINARY INVESTIGATIONS

KRZYSZTOF FICEK^{1*}, JAROSŁAW WIECZOREK²,
EWA STODOLAK-ZYCH³, YURIY KOSENYUK²

¹GALEN - ORTHOPAEDICS,

6 JERZEGO ST., 43-150 BIERUN, POLAND

²NATIONAL RESEARCH INSTITUTE OF ANIMAL PRODUCTION,
DEPARTMENT OF BIOTECHNOLOGY REPRODUCTION ANIMALS,
1 KRAKOWSKA ST., 32-083 BALICE, POLAND

³AGH UNIVERSITY OF SCIENCE AND TECHNOLOGY,
FACULTY OF MATERIALS SCIENCE AND CERAMICS,
DEPARTMENT OF BIOMATERIALS,
30 MICKIEWICZ AV, 30-059 KRAKOW, POLAND

* E-MAIL: GALEN@GALEN.PL

Abstract

In this project the anterior cruciate ligament (ACL) replacement in a rabbit model was performed for the preclinical phase of investigations of a new form of biomaterial i.e. polymer beads (granules). This material, based on resorbable aliphatic polyester (polylactide - PLA) was used as a filler of the bone tunnels to enhance tendon-to-bone healing. The high specific surface area and well known biocompatibility of this material designated it as an osteoconductive agent in reconstructive ligament surgery. Additionally, a new surgical concept was proposed which retains the natural elasticity of the harvested tendon. This method ensures fixation of the grafted tendon within the bone tunnels in their entire length.

Keywords: ACL reconstruction, tendon implant, resorbable material

[*Engineering of Biomaterials 113 (2012) 33-34*]

Introduction

ACL is the most frequently injured ligament in the knee. The treatment options for ligament ruptures include conservative management but the most broadly accepted procedure is reconstruction with intra-articular grafts [1-2]. The outcome of reconstructive ligament surgery is dependent on the quality of healing of the transplanted grafts in the bone tunnels. Different techniques ensure only a partial graft fixation in some areas of the bone tunnel [2-4]. A major part of the transplant anchored inside the bone is suspected to integrate with the bone by biological processes occurring naturally within the tunnels. Improper graft fixation may cause inadequate joint stability. In this study we tested a new form of material dedicated to filling the tunnels covering the transplanted grafts. The role of the polymer granules was to create a three-dimensional scaffold for osteoblasts to adhere to, enabling them to proliferate faster than they otherwise would in the blood of the bone tunnel (FIG. 1).

The aim of this experiment was to verify the effect of the bioresorbable material on the healing process between the outer surface of the tendon and the inner part of the bone wall to obtain entire intratunnel fixation.

Materials and methods

Polymer granules were produced using commercial copolymer; poly L/DL lactide (L/DL; 80:20; PURAC) which was approved by FDA. Porous granules were obtained using leaching technique described elsewhere [5]. Specific surface area of the granules was about 20 m²/g.

An in vivo experiment concerned 12 rabbits (Ethic Committee approval 668/09) which were divided into 4 groups of 3 animals each: Group 1 (control), no PLA, implantation time 6 weeks; Group 2, PLA, implantation time 6 weeks; Group 3 (control), no PLA, implantation time 12 weeks; Group 4, PLA, implantation time 12 weeks. Under general anesthesia the long digital extensor tendon of the right hind limb at the lateral femoral condyle was exposed and through its insertion (attachment) site, threads were applied without cutting the tendon off (FIG. 2a). The tunnels were arranged in proximal tibia metaphysis medially and in distal femur metaphysis laterally. The natural ACL insertions served as the footprints to drill the tibial and femoral bone tunnels. Bone tunnel diameters were 2.6-3.5 mm and were about 1 mm wider than their grafts. According to other authors, in the surgical set-up the long digital extensor tendon is exposed and immediately detached. Our innovative algorithm offers the alteration of the surgery to maintain the biological and physical properties of the tendon. The tendon was detached as late as possible to avoid its contraction, which might change its physical parameters and then implanted in the bone tunnel applying appropriate tension.

The grafted tendon was pulled through the tunnels and covered with the polymer granules. PLA material was evenly distributed around the graft, starting from its tibial distal entrance next to femoral proximal one. (FIG. 2c). Because of the electrostatic properties of the polymer granules, the majority of the porous beads were mixed with autogenous peripheral bone blood. This composition in a paste form filled the bone tunnels. The graft ends were sutured to the tibial and femoral periosteum with the non-absorbable threads (Prolene 2.0). The patella was reduced and the joint was closed and sutured in layers. 24 hours after surgery all rabbits returned to their normal activity. The animals were euthanized 6 or 12 weeks after surgery.

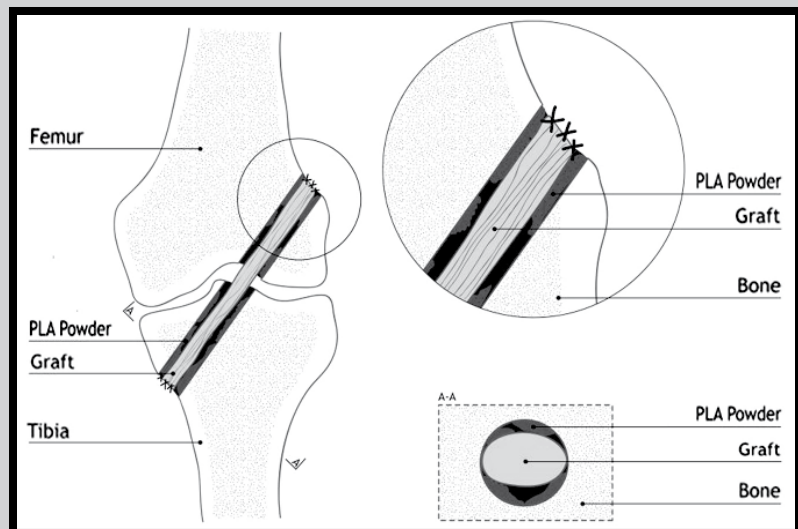


FIG. 1. Model of graft implantation using PLDLA granules.

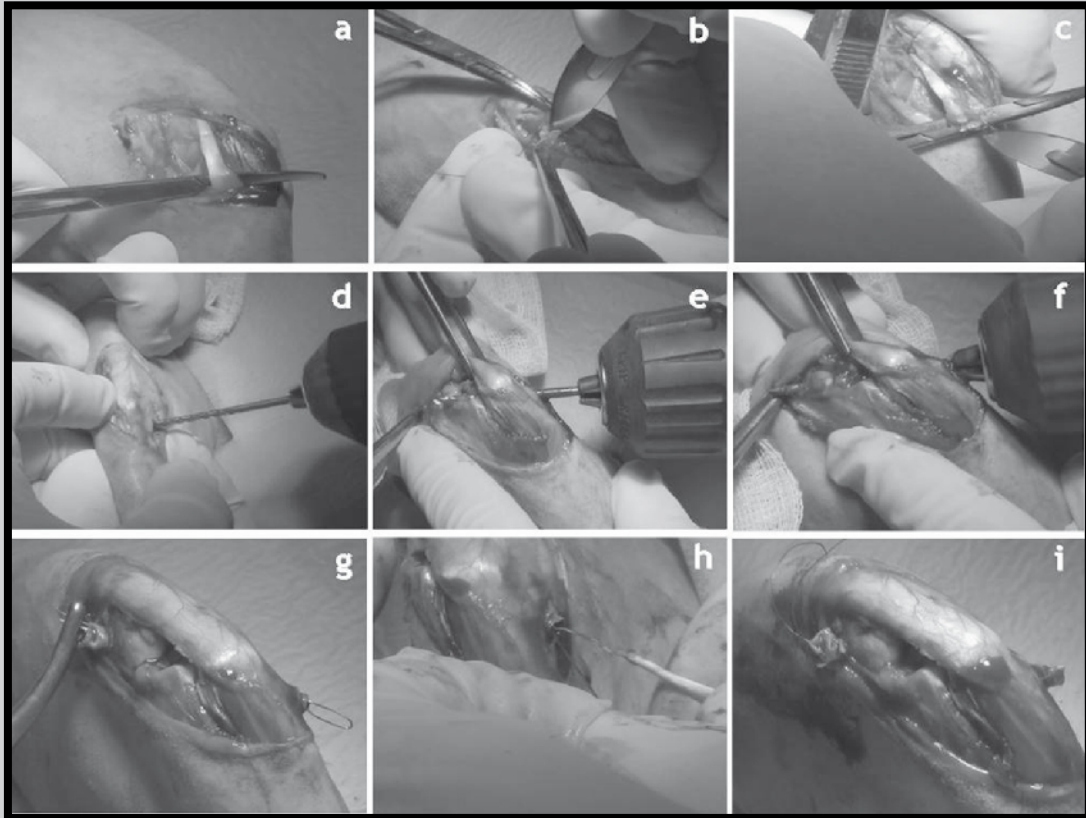


FIG. 2. Surgical procedure; the long digital extensor tendon was detached (a-c), the natural ACL insertions served as the footprints to drill the tibial and femoral bone tunnels (d-f), the grafted tendon was pulled through the tunnels and covered with the PLDLA granules (g-i).

Results

The polymer granules applied in the experiment show a tendency to interact electrostatically, which makes the operation difficult. The polymer powder tightly covers the syringe needle and surface of the tools which hinder its introduction inside the bone loss. Moreover, introduction of the powder has only a local character and the powder is not homogeneously distributed inside the bone tunnel. It may significantly influence the course of osteointegration process, which could be faster in areas reach in the polymer granules, and slower in areas where the granules are absent e.g. in a middle part of the tunnel. The granules with specific surface area of $20 \text{ m}^2/\text{g}$ and size $1\text{-}10 \text{ }\mu\text{m}$ are a sufficient carrier of active substances of blood e.g. platelet rich plasma. During the operation blood drawn from the patient's wound is mixed with the polymer granules. According to the literature [6] the main criterion of proportion between a natural (i.e. binder) and a synthetic component is consistence of the material which should be paste-like. In the case of the described treatment the rate between the polymer powder and patient's circulating blood was 3:1. Such paste in quantity about 3.5-4 ml was easily introduced into a syringe and then injected to the bone tunnel. It seems that, the applied method should provide a homogenous distribution of the paste within the defect area. An adaptable, pliable paste consisting of mesoporous PLA beads and blood marrow cells was used to fill vacant areas between the tendon and bone in the bone tunnels, which facilitated and enhanced tendon - to - bone healing. This protocol displays the alter, total grafted tendon fixation through the entire length of bone tunnels. Final confirmation of homogenous distribution of the paste and its influence on the ossification process rate will be possible after histopathological analysis.

Conclusions

Total graft fixation in contrast to the commonly used partial one guarantees optimal joint stability after ligament reconstruction. Further study is required to attain better handling procedures in order to ensure uniform distribution of PLA paste within the bone tunnels. The healing effect can be intensified by mixing PLA beads with autogenous marrow blood cells or platelet - rich plasma and/or growth factors.

Acknowledgements

Bioresorbable polylactide implants used in the study were kindly provided by Prof. Sylwester Gogolewski, D.Sc., Ph.D.

References

- [1] Miller S.L., Gladstone J.N.: Graft selection in anterior cruciate ligament reconstruction. *Orthopedic Clinics of North America* 33, 4 (2002) 675-683.
- [2] Strickland S.M., MacGillivray J.D., Warren R.F.: Anterior cruciate ligament reconstruction with allograft tendons. *Orthopedic Clinics of North America* 34 (2003) 41-47.
- [3] Paul Neuman, et al.: Prevalence of Tibiofemoral Osteoarthritis 15 Years After Nonoperative Treatment of Anterior Cruciate Ligament Injury. *American Journal of Sports Medicine* 36 (2008) 1717-1725.
- [4] Bruce D. Beynon, et al.: Anterior Cruciate Ligament Replacement: Comparison of Bone-Patellar Tendon-Bone Grafts with Two-Strand Hamstring Grafts. *Journal of Bone and Joint Surgery* 84 (2002) 1503-1513.
- [5] Gogolewski S., Gugala Z.: Differentiation, growth and activity of rat bone marrow stromal cells on resorbable poly(L/DL - lactide) membrane. *Biomaterials* 25 (2004) 2299-2307.
- [6] Chen F-M., Zhang J., Zhang M., An Y., Chen F., Wu Z-F.: A review on endogenous regenerative technology in periodontal regenerative medicine. *Biomaterials* 31 (2010) 7892-7927.

ELEKTROPRZĘDZONE MEMBRANY KOMPOZYTOWE STYMULUJĄ MINERALIZACJĘ W HODOWLACH KOMÓREK KOSTNYCH

IZABELLA RAJZER^{1*}, ELŻBIETA MENASZEK²

¹ ATH AKADEMIA TECHNICZNO-HUMANISTYCZNA W BIELSKU-BIAŁEJ, WYDZIAŁ NAUK O MATERIAŁACH I ŚRODOWISKU, INSTYTUT INŻYNIERII TEKSTYLÓW I MATERIAŁÓW POLIMEROWYCH, UL. WILLOWA 2, 43-309 BIELSKO-BIAŁA

² UJ UNIWERSYTET JAGIELLOŃSKI, COLLEGIUM MEDICUM, ZAKŁAD CYTOBIOLOGII, UL. MEDYCZNA 9, 30-068 KRAKÓW

* E-MAIL: IRAJZER@ATH.BIELSKO.PL

Streszczenie

Biodegradowalne nanowłókniste membrany poddano badaniom in vitro, pozwalającym na ocenę stopnia różnicowania się i mineralizacji komórek kostnych w obecności potencjalnych podłoży tkankowych. Przedstawione badania oceniają wpływ mikrostruktury i składu chemicznego wytworzonych podłoży na przyczepność, proliferację i morfologię osteoblastów (NHOst). Badania procesu mineralizacji i aktywności ALP pozwoliły na ocenę procesu różnicowania się komórek.

Słowa kluczowe: podłoża dla inżynierii tkankowej, elektroprzędzone membrany, mineralizacja, różnicowanie komórek

[Inżynieria Biomateriałów 113 (2012) 35-39]

Wprowadzenie

Od materiałów stosowanych na podłoża dla inżynierii tkankowej kości wymaga się, aby były bioaktywne, biodegradowalne, porowate, i aby stymulowały komórki kostne. Ponieważ komórki łatwo reagują na bodźce otaczającego je środowiska, a tym samym na właściwości wytworzonego podłoża, równie istotna dla inżynierii tkankowej jest analiza oddziaływań komórka-materiał [1].

Elektroprzędzenie jest techniką często wykorzystywaną do wytwarzania nanowłóknistych podłoży naśladujących naturalną matrycę zewnątrzkomórkową (ECM), jednakże średnia średnica porów w podłożach wytwarzanych tą metodą, dla potrzeb inżynierii tkankowej kości, jest niewystarczająca [2]. Nasze wcześniejsze badania wykazały, że połączenie metody elektroprzędzenia z techniką wypłukiwania porotwórczych dodatków pozwala wytwarzać podłoża o pożądanym rozkładzie porów i odpowiedniej mikrostrukturze [3]. Polikaprolakton (PCL) jest polimerem często wykorzystywanym do produkcji podłoży dla inżynierii tkankowej ze względu na dłuższy czas jego resorpcji [4]. PCL po implantacji charakteryzuje się lepszymi właściwościami mechanicznymi niż inne bioresorbowalne polimery a czas jego degradacji jest dopasowany do czasu regeneracji tkanki kostnej [5]. Jednakże słaba hydrofilowość podłoży z PCL wpływa na gorszą adhezję, proliferację i różnicowanie się komórek. Ponadto podłoża z PCL nie wykazują właściwości bioaktywnych, dlatego często modyfikowane są bioaktywnymi dodatkami m.in. hydroksyapatytem. Elektroprzędzenie kompozytowych podłoży PCL/HAp może wpłynąć na polepszenie przyczepności i proliferacji oraz na szybsze różnicowanie się komórek.

COMPOSITE ELECTROSPUN MEMBRANES STIMULATE MINERALIZATION IN BONE CELL CULTURE

IZABELLA RAJZER^{1*}, ELŻBIETA MENASZEK²

¹ ATH UNIVERSITY OF BIELSKO-BIALA, FACULTY OF MATERIALS AND ENVIRONMENTAL SCIENCES, INSTITUTE OF TEXTILE ENGINEERING AND POLYMER SCIENCE, 2 WILLOWA ST., 43-309 BIELSKO-BIALA, POLAND

² UJ JAGIELLONIAN UNIVERSITY, COLLEGIUM MEDICUM, DEPARTMENT OF CYTOBIOLOGY, 9 MEDYCZNA ST., 30-068 KRAKOW, POLAND

* E-MAIL: IRAJZER@ATH.BIELSKO.PL

Abstract

A biodegradable nanofibrous nonwoven membranes were analyzed in vitro as potential scaffolds for differentiation and mineralization of bone cells. In this study we investigate the effects of electrospun membranes microstructure and chemical composition on attachment, proliferation, and morphology of human NHOst osteoblasts. Mineralization process and ALP activity were studied to estimate the cells differentiation.

Keywords: scaffolds for tissue engineering, electrospun membranes, mineralization, cell differentiation

[Engineering of Biomaterials 113 (2012) 35-39]

Introduction

Scaffolds for bone tissue engineering are required to be bioactive, biodegradable, porous and to stimulate bone cells. Optimizing cell-material interactions is critical in tissue engineering because cells are known to sense and respond to the physical properties of their environment and those of tissue scaffolds [1]. Electrospinning technique has been widely used to fabricate nanofibrous scaffold that mimic native extracellular matrix (ECM), however the average pore size in scaffold obtained using electrospinning is insufficient [2]. It was found in our previous study that the combined use of two techniques namely electrospinning and porogen-leaching, could be beneficial to fabricate desired pore size and final structure of scaffolds by varying the salt particle size [3]. The advantage in using poly(ϵ -caprolactone) (PCL) scaffolds in bone tissue engineering deals with its desirable biostability [4]. PCL exhibits more prolonged mechanical strength than other bioresorbable polymeric materials and degrades at a rate compatible with the bone regeneration [5]. However poor hydrophilicity of PCL caused a reduction in the ability of cell adhesion, proliferation and differentiation. PCL does not show any intrinsic bioactivity, therefore hydroxyapatite is often incorporated into material substrates. Electrospinning of PCL along with nanoparticles of hydroxyapatite can improve the cell attachment kinetics.

The aim of this work was to investigate the effects of electrospun membranes microstructure and chemical composition on attachment, proliferation, and morphology of bone cells. Mineralization process and ALP activity were studied to estimate the cells differentiation.

Praca miała na celu zbadanie wpływu mikrostruktury i składu chemicznego elektroprowadzonych podłoży na przyczepność, proliferację i morfologię komórek kostnych. Badania procesu mineralizacji i aktywności ALP pozwoliły na ocenę procesu różnicowania komórek.

Materialy i metody

Membrany z polikaprolaktonu (PCL) oraz polikaprolaktonu modyfikowanego hydroksyapatytem (PCL/HAp) wytworzono metodą elektroprowadzenia. 2,5 g PCL rozpuszczono w 40 ml mieszaniny chloroform/methanol 1:1 w temperaturze 50°C. Kompozytowe membrany PCL/HAp wytwarzano dodając do roztworu 20% wag. hydroksyapatytu, roztwór mieszało przy użyciu homogenizatora ultradźwiękowego. Następnie roztwór umieszczano w strzykawce (10 ml) zakończonej igłą ze stali nierdzewnej o średnicy 0,7 mm, prędkość dozowania roztworu wynosiła 1,5 ml/h. Doprowadzone do igły napięcie wynosiło 30 kV. Kolektor (owinięty papierem do pieczenia) znajdował się w odległości 15 cm od kapilary. Częsteczki soli dozowano na kolektor w trakcie elektroprowadzenia. Następnie wytworzoną membranę płukano w wodzie destylowanej w celu usunięcia soli i wygenerowania porów o większej średnicy. PCL wykorzystany w badaniach zakupiono w Sigma-Aldrich (Mn= 70 000-90 000 g/mol). Chloroform i metanol zakupiony został w firmie POCH (Polska). Hydroksyapatyt wytworzono w AGH-UST (Kraków, Polska). Średnia wielkość cząsteczek HAp wynosiła 23 nm. Jako środek porotwórczy wykorzystano chlorek sodu (POCH, Polska; wielkość cząstek: 2,5-4,5 μm). W rezultacie otrzymano cztery rodzaje nanowłóknistych materiałów:

1. PCL (polikaprolakton 100%);
2. PCL/HAp (polikaprolakton modyfikowany hydroksyapatytem);
3. PCL/P (polikaprolakton o zwiększonej porowatości, próbka wytworzona metodą elektroprowadzenia połączoną z tradycyjną techniką wypłukiwania dodatków);
4. PCL/HAp/P (polikaprolakton modyfikowany hydroksyapatytem o zwiększonej porowatości, próbka wytworzona metodą elektroprowadzenia połączoną z tradycyjną techniką wypłukiwania dodatków);

Fizyko-chemiczne właściwości wytworzonych materiałów (takie jak: mikrostruktura, porowatość oraz właściwości mechaniczne) przedstawione zostały w poprzedniej pracy [3].

Badania *in vitro*

Interakcje biomateriał/komórka porównano w hodowli pierwotnej ludzkich osteoblastów NHOst (Lonza, Szwajcaria). Komórki hodowano w plastikowych butelkach (Nunclon, Dania) o pojemności 75 ml w pożywce hodowlanej OGM BulletKit (Lonza, USA), składającej się z medium hodowlanego OGM, 10% surowicy cielęcej FBS oraz 5% roztworu antybiotyków: gentamycyny i amfoterycyny-B, w atmosferze 5% CO₂ i temperaturze 37°C. Do badań użyto komórki z pasażu od 5-6. Zawiesinę komórek uzyskano przez dodanie 5% trypsyny z EDTA (Lonza, USA). Po przepłukaniu i odwirowaniu komórki doprowadzano do stężenia 2x10⁴ komórek/ml w medium różnicującym z dodatkiem czynników różnicujących OGM Differentiation SingleQuot Kit (Lonza, USA), po czym 1 ml zawiesiny komórek umieszczano w studzienkach 24-dółkowej płytki hodowlanej (Nunclon, Dania), zawierających sterylne krążki badanych materiałów. Kontrolę pozytywną stanowił polistyren dna pustych dołków płytki hodowlanej (TCPS). Inkubację komórek NHOst w obecności krążków włókniny o modyfikowanym składzie prowadzono przez 3 i 7 dni oraz 7, 14 i 21 dni (test mineralizacji) w inkubatorze HeraCell (Heraeus, Thermo Scientific, Niemcy), w atmosferze 5% CO₂ i temperaturze 37°C. Po upływie wyznaczonego czasu komórki rosnące na powierzchni próbek poddano testowi przylegania i żywotności.

Materials and Methods

Polycaprolactone (PCL) and polycaprolactone/hydroxyapatite (PCL/HAp) membranes used in the work were formed using electrospinning. The manufacturing began with dissolving 2.5 g of PCL in 40 ml of 1:1 chloroform/methanol solvent mixture at 50°C. In order to obtain PCL/HAp membranes, PCL solution was mixed with 20 wt% of HAp using sonicator. The solutions were fed into 10 ml plastic syringe fitted with a stainless-steel blunt needle of 0.7 mm in diameter and an injection rate of 1.5 mL/h using an infusion pump. A high voltage of 30 kV was applied. The fibres were collected on a flat collector wrapped with a piece of baking paper sheet which was kept at a distance of 15 cm from the needle tip. In order to improve the pore size of electrospun nanofibrous scaffold, salt particles were incorporated within the poly(ε-caprolactone) nanofibrous matrix and then were leached out to generate some macropores. PCL used in the study was purchased from Sigma-Aldrich (Mn= 70 000-90 000 g/mol). Chloroform and methanol (POCH, Poland) were used as solvents. Hydroxyapatite was produced at the AGH-UST (Krakow, Poland). An average size of the HAp particles was 23 nm. Fine sodium chloride (POCH, Poland; particle size: 2.5-4.5 μm) was used as porogen. As a result four types of materials were obtained:

1. PCL (polycaprolactone 100%);
2. PCL/HAp (hydroxyapatite-modified polycaprolactone);
3. PCL/P (polycaprolactone with increased porosity; the sample was produced by electrospinning combined with the traditional technique of leaching additives);
4. PCL/HAp/P (hydroxyapatite-modified polycaprolactone; the sample was produced by electrospinning combined with the traditional technique of leaching additives);

Physico-chemical properties of obtained materials (such as microstructure, porosity and mechanical properties) were previously described [3].

Cell culture

Biomaterial/cell interactions were compared in primary cultures of human NHOst osteoblasts (Lonza, Switzerland). Cells were cultured in plastic bottles (Nunclon, Denmark) in the culture medium OGM BulletKit (Lonza, USA), consisting of OGM culture medium, 10% calf serum FBS and 5% solution of antibiotics: gentamicin and amphotericin-B, in an atmosphere of 5% CO₂ and temperature 37°C. The tests were conducted on cells from passages 5-6. The cell suspension was obtained by addition of 5% trypsin with EDTA (Lonza, USA). After flushing and centrifugation, the cells were concentrated to 2 x 10⁴ cells/ml in OGM medium with addition of differentiating factors: OGM Differentiation SingleQuot Kit (Lonza, USA). Next, 1 ml of the cell suspension was placed in the wells of a 24-well culture plate (Nunclon, Denmark), containing sterile discs of tested materials. The polystyrene bottom of empty culture plate wells (TCPS) constituted positive control. Incubation of NHOst cells in the presence of nonwovens discs lasted for 3 and 7 days and 7, 14 and 21 days (mineralization test) in a HeraCell incubator (Heraeus, Thermo Scientific, Germany), in an atmosphere of 5% CO₂ at 37°C.

After the specified time, cells growing on the surface of the samples were tested for adhesion and viability. Cell viability was determined using ViaLight Assay. Cell enzymic activity and mineralization were assessed by alkaline phosphatase (ALP) activity assay and by OsteoImage mineralization test (Lonza, USA), respectively. Cell morphology was evaluated in the optical fluorescence microscope (Olympus, Japan).

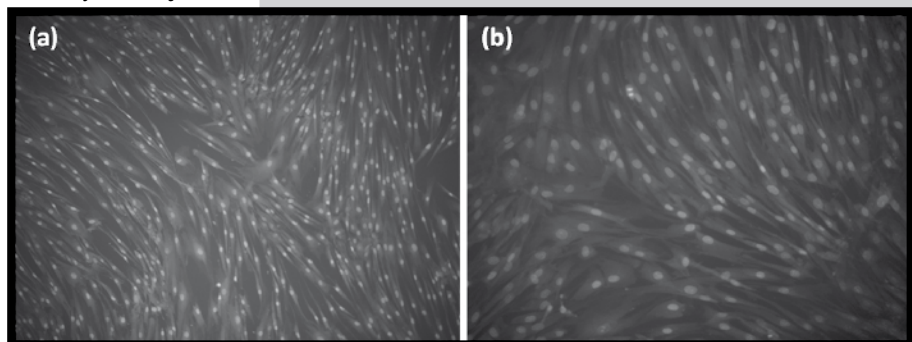
Żywotność komórek oznaczono testem ViaLight® (Lonza, USA). Enzymatyczną aktywność komórek oraz postęp mineralizacji oznaczono odpowiednio określając aktywność fosfatazy alkalicznej (ALP) oraz mierząc stężenie hydroksyapatytów testem OsteoImage (Lonza). Morfologię komórek oceniano w optycznym mikroskopie fluorescencyjnym (Olympus, Japonia).

Wyniki i dyskusja

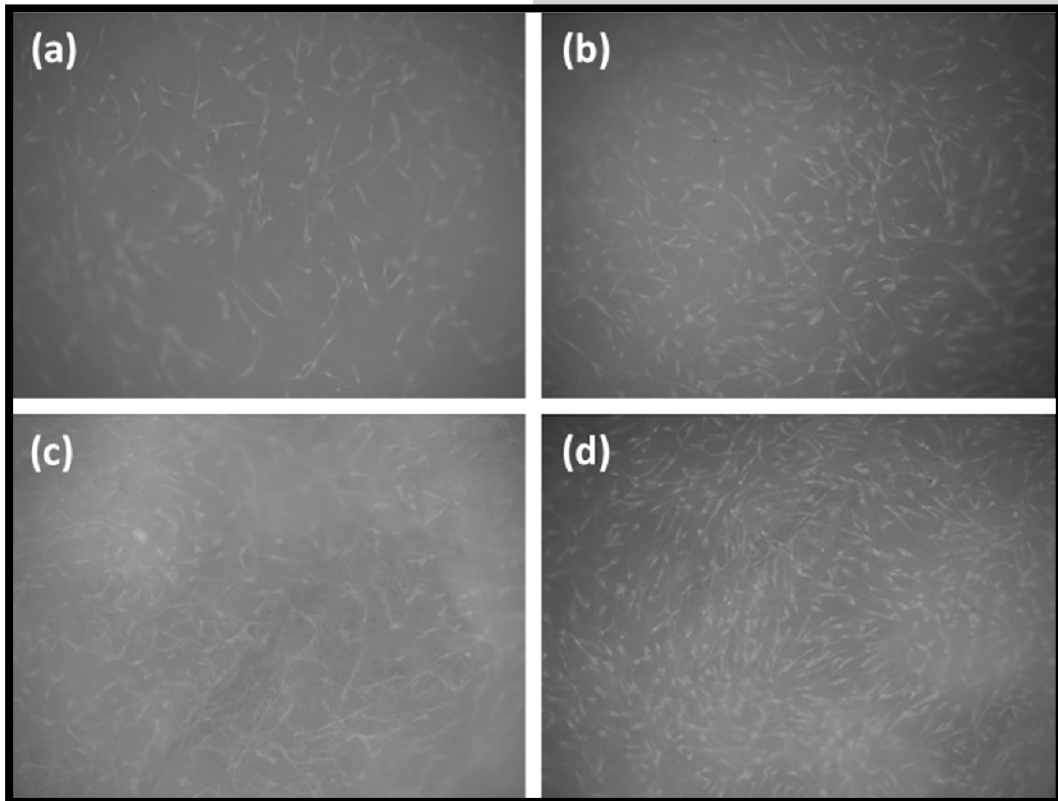
Przyleganie komórek do powierzchni jest istotne dla licznych zjawisk, takich jak odpowiedź immunologiczna, gojenie i integracja tkanek z biomateriałami. Przyłgnięcie, adhezja i rozpostarcie komórek należą do pierwszej fazy interakcji, jakie zachodzą na styku komórka/biomateriał. Prawidłowy przebieg tych procesów wpływa na proliferację i różnicowanie się komórek na powierzchni biomateriałów. Obserwacja komórek pod mikroskopem (RYS. 1-2) wykazuje znaczną różnicę w morfologii komórek w porównaniu do kontroli. Niezależnie od rodzaju włókniny komórki przybierają kształt bardziej wydłużony, wrzecionowaty, mają dłuższe i cieńsze wypustki, tworzące sieć połączeń. Taki kształt komórek wymuszony jest przede wszystkim własnościami powierzchni włóknistego podłoża. Stosunkowo niska jakość zdjęć spowodowana jest wchłanianiem fluorescencyjnego barwnika przez włókniny i brakiem kontrastu między podłożem a komórkami. Na podkreślenie zasługuje fakt, że ze względu na porowatość powierzchni sieć połączonych wypustkami komórek ma strukturę trójwymiarową. Morfologia komórek rosnących na włókninach wskazuje na ich różnicowanie się. Za różnicowaniem komórek przemawiają również wartości testu OsteoImage, za pomocą którego oceniono postęp procesu mineralizacji w hodowli. Dla wszystkich materiałów modyfikowanych fosforanami wapnia obserwuje się istotny statystycznie przyrost wartości w porównaniu do kontroli, mimo mniejszej liczby komórek (RYS. 3). Zastanawiający jest spadek stężenia hydroksyapatytu w serii 14 dniowej w stosunku do 7-dniowej. Spowodowany jest on prawdopodobnie rozpuszczaniem wyjściowych hydroksyapatytów, będących składnikiem niektórych włóknin. O stopniu różnicowania komórek osteoblastycznych świadczy również, aktywność alkalicznej fosfatazy - enzymu będącego markerem wczesnego różnicowania się osteoblastów (RYS. 4). Struktura włóknin istotnie wpływa na żywotność komórek, zarówno w 3, jak i w 7 dniu hodowli (RYS. 5). Żywotność komórek na biomateriałach jest znacząco niższa w porównaniu do kontroli. Należy jednak podkreślić, że powierzchnia TCPS jest powierzchnią wyjątkowo sprzyjającą przyleganiu i intensywnej proliferacji komórek, natomiast nie wpływa ona na ich różnicowanie. Niższa proliferacja komórek na badanych włókninach niż na materiale kontrolnym, związana jest prawdopodobnie z szybszym różnicowaniem się komórek w obecności nanowłóknistych podłoży. Powszechnie wiadomo, że proliferacja komórek ulega zmniejszeniu kiedy rozpoczyna się proces ich różnicowania [6]. Wyniki badań in vitro wykazały dobrą przyczepność komórek do elektroprzędzonych materiałów, przy czym najlepszą przeżywalność komórek zaobserwowano w przypadku nanowłóknistych podłoży modyfikowanych hydroksyapatytem. Biologiczna ocena materiałów in vitro wykazała, że materiały modyfikowane hydroksyapatytem zapewniają wyższą aktywność ALP i lepszą mineralizację.

Results and Discussions

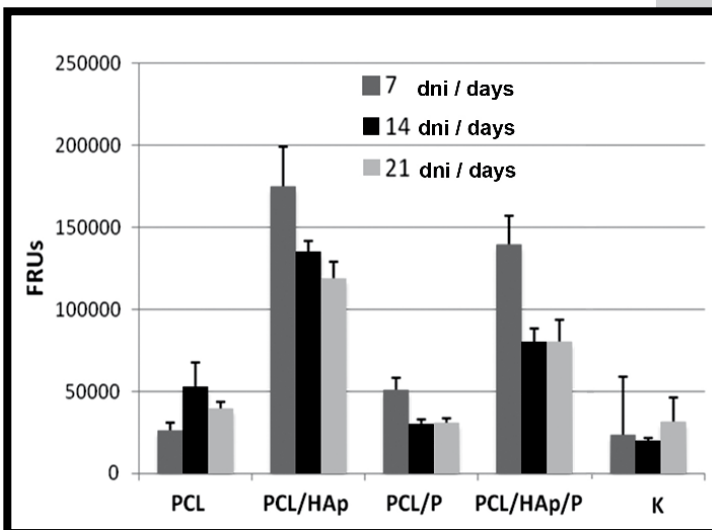
Cell adhesion to the surface is important for many phenomena, such as immune response, healing and tissue integration with biomaterials. Adherence, adhesion and spreading of cells belong to the first phase of the interactions that occur at the cell/biomaterial interface. These processes affect the proliferation and differentiation of cells on the surface of biomaterials. The microscopic observation of cells (FIG. 1-2), shows a significant difference in cell morphology compared to the control. Regardless of the type of nonwoven fabric, the cells assume a more elongated, spindle-like shape, have long and slender extensions. Such cell shape is primarily forced by surface properties of the fibrous scaffold. The relatively low quality of images obtained by fluorescent microscopy is caused by the absorption of the fluorescent dye by the nonwoven fabric and the lack of contrast between the scaffold and the cells. It is worth emphasizing that, due to the porosity of the surface, the network of cells connected by cytoplasmic extensions has a three-dimensional structure. The shape of the cells growing on nonwoven fabric indicates probably the differentiation of the cells. Cell differentiation is also shown in the OsteoImage test values, through which the progress of mineralization is assessed. For all materials modified with calcium phosphates, statistically significant increase in values is observed as compared to the control, despite a smaller number of cells (FIG. 3). Striking is the decrease in the concentration of hydroxyapatite in the 14-day series compared to the 7-day series. It is probably due to dissolution of the initial hydroxyapatite, which is a component of some fabrics. The degree of cell differentiation is also shown by the activity of alkaline phosphatase - marker enzyme of osteoblast early differentiation (FIG. 4). Nonwoven fabric structure significantly affects cell viability, both on the 3rd and on the 7th day of the culture (FIG. 5). Results of viability tests of cells growing on biomaterials are significantly lower compared to the control. It should be noted, however, that the TCPS surface is a surface extremely favorable to adhesion and intense proliferation of cells, but it does not affect their differentiation. Electrospun samples evoked faster cell differentiation, therefore the cell proliferation on the control material was much higher than on investigated samples. It is known that cell proliferation decreases when cells reach confluence and initiate their differentiation process [6]. The results of in vitro studies showed that cells attached well to electrospun samples, and the highest cells viability was observed in the case of HAp modified nonwoven fabrics. In vitro biological evaluation showed that the presence of HAp particles offered higher activity of ALP and better mineralization.



RYS. 1. Morfologia komórek NHOst hodowanych przez 7 dni na powierzchni kontrolnej TCPS (a) pow. obiektywu 10x, (b) pow. obiektywu 20x.
FIG. 1. Morphology of NHOst cell cultured for 7 days on the surface of on the TCPS control surface (a) org. magnification 10x, (b) org. magnification 20x.

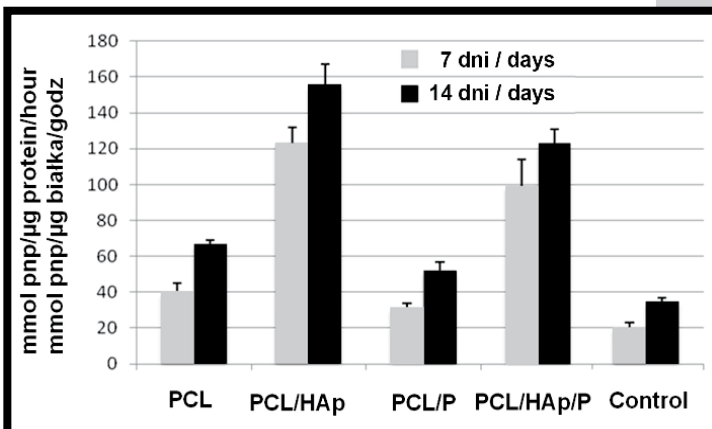


RYS. 2. Morfologia komórek NHOst hodowanych przez 7 dni na powierzchni elektropędzonych materiałów (pow. obiektywu 10x): (a) PCL, (b) PCL/HAp, (c) PCL/P, (d) PCL/HAp/P.
 FIG. 2. Morphology of NHOst cell cultured for 7 days on the surface of electrospun materials (magnified 10x): (a) PCL, (b) PCL/HAp, (c) PCL/P, (d) PCL/HAp/P.



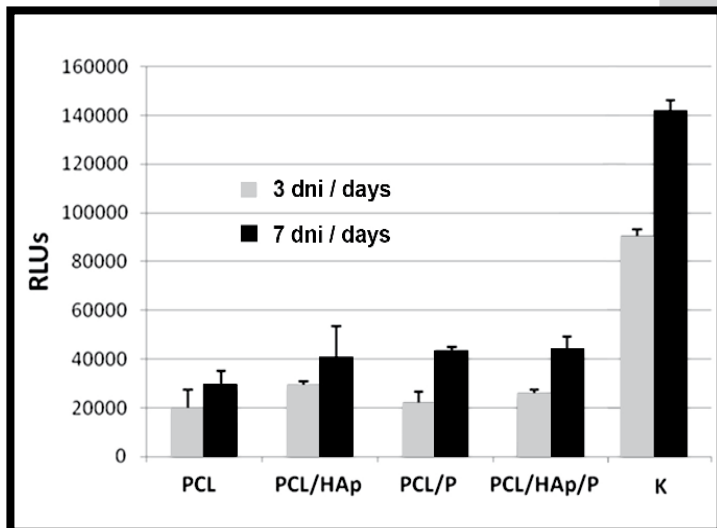
RYS. 3. Postęp mineralizacji mierzony stężeniem hydroksyapatytów w 7, 14 i 21 dniu hodowli komórek NHOst na powierzchni kontrolnej TCPS (K) oraz na powierzchni krążków włókniny. FRUs – względne jednostki fluorescencji. Różnice istotne statystycznie w stosunku do kontroli (wg testu T-Tukeya dla $p < 0.05$) wykazują materiały PCL/HAp oraz PCL/HAp/P.

FIG. 3. Mineralization progress measured by the concentration of hydroxyapatites on the 7th, 14th and 21st day of NHOst cell culture on the TCPS control surface (K) and on the surface of the nonwoven discs. RFUs – relative fluorescence units. Statistically significant differences compared to the control (according to the Tukey's t-test for $p < 0.05$) are exhibited by materials PCL/HAp and PCL/HAp/P.



RYS. 4. Aktywność fosfatazy alkalicznej w 7 i 14 dniu hodowli komórek NHOst na powierzchni kontrolnej TCPS (K) oraz na powierzchni krążków włókniny.

FIG. 4. Alkaline phosphatase activity on the 7th and 14th day of NHOst cell culture on the TCPS control surface (K) and on the surface of the nonwoven discs.



RYS. 5. Żywotność komórek NHOst oznaczona testem Vialight w 3 i 7 dniu hodowli na powierzchni kontrolnej TCPS (K) oraz na powierzchniach krążków włókniny. Różnice istotne statystycznie między kontrolą a wszystkimi badanymi materiałami wg testu T-Tukeya dla $p < 0.05$. Rysunek przedstawia żywotność komórek w wartościach względnych luminescencji RLUs (Relative Luminescence Units).

FIG. 5. NHOst cell viability indicated using the Vialight test on the 3rd and 7th day of the culture on the TCPS control surface (K) and the surfaces of nonwoven fabric discs. Statistically significant differences between the control group and all the materials examined according to Tukey's t-test for $p < 0.05$. The figure shows cell viability in relative luminescence units (RLUs).

Wnioski

Naprawa ubytków kostnych wymaga biokompatybilnego podłoża umożliwiającego przyleganie, proliferację i różnicowanie się komórek tkanki kostnej. W badaniach biologicznych modyfikowanych włókien z polikaprolaktonu udowodniono, że stanowią one podłoże o własnościach korzystnych dla rekonstrukcji tkanki kostnej. Dzięki przestrzennej strukturze włókien, umożliwiającej dyfuzję składników odżywczych i gazów w głąb podłoża, hodowla osteoblastów tworzy trójwymiarową sieć połączonych wypustkami komórek. W porównaniu z dwuwymiarowym podłożem kontrolnym tempo proliferacji komórek jest słabsze, co jednak jest spowodowane głównie korzystnym efektem różnicowania się komórek. O różnicowaniu się komórek świadczy ich morfologia, aktywność enzymu - fosfatazy alkalicznej i wytwarzanie hydroksyapatytów, będących istotnym składnikiem substancji międzykomórkowej kości.

Podziękowania

Praca naukowa finansowana ze środków Narodowego Centrum Nauki (projekt numer: N N507550938, 2010-2013) oraz ze środków Ministerstwa Nauki i Szkolnictwa Wyższego (Iuventus Plus IP2011044671).

Conclusions

Repair of bone loss requires a biocompatible surface allowing the adhesion, proliferation and differentiation of bone cells. In biological studies of modified PCL nonwoven fabrics it was proven that they are a substrate with advantageous properties for the reconstruction of bone tissue. Due to the spatial structure of fabrics, allowing diffusion of nutrients and gases into the substrate, osteoblast cultures create a three-dimensional network of cells. In comparison with the two-dimensional control substrate, the cell proliferation rate is lower, but this is mainly due to favourable effect of cell differentiation. The differentiation of cells is demonstrated in their morphology, activity of the enzyme - alkaline phosphatase, and the production of hydroxyapatites, which are an essential component of intercellular bone material matrix.

Acknowledgments

This work was supported by National Science Center (project number: N N507550938, 2010-2013) and by Polish Ministry of Science and Higher Education (project Iuventus Plus IP2011044671).

Piśmiennictwo

- [1] Chatterjee K., Lin-Gibson S., Wallace W.E., Parekh S.H., Lee Y.J., Cicerone M.T., Young M.F., Simon C.G.: The effect of 3D hydrogel scaffold modulus on osteoblast differentiation and mineralization revealed by combinatorial screening. *Biomaterials* 31 (2010) 5051-5062.
- [2] Rnjak-Kovacina J., Wise S.G., Li Z., Maitz P.H.M., Young C.J., Wang Y., Weiss A.S.: Tailoring the porosity and pore size of electrospun synthetic human elastin scaffolds for dermal tissue engineering. *Biomaterials* 32(28) (2011) 6729-6736.
- [3] Rajzer I.: Evaluation of PCL and PCL/HAp scaffolds processed by electrospinning and porogen leaching techniques. *Engineering of Biomaterials* 103 (2011) 4-7.

References

- [4] Sravanthi R.: Preparation and characterization of poly (ϵ -caprolactone) PCL scaffolds for tissue engineering applications. National Institute of Technology Rourkela (ORISSA). Thesis (2009).
- [5] Fabbri P., Bondioli F., Messori M., Bartoli C., Dinucci D., Chiellini F.: Porous scaffolds of polycaprolactone reinforced with in situ generated hydroxyapatite for bone tissue engineering. *Journal of Materials Science: Materials in Medicine* 21 (2010) 343-351.
- [6] Owen T.A., Aronow M., Shalhoub V., Barone L.M., Wilming L., Tassinari M.S.: Progressive development of the rat osteoblast phenotype in vitro: reciprocal relationships in expression of genes associated with osteoblast proliferation and differentiation during formation of the bone extracellular matrix. *Journal of Cell Physiology* 143 (1990) 420-30.



STUDIA PODYPLOMOWE

Biomateriały – Materiały dla Medycyny 2012/2013

Organizator: Akademia Górniczo-Hutnicza im. Stanisława Staszica w Krakowie Wydział Inżynierii Materiałowej i Ceramiki Katedra Biomateriałów	Adres: 30-059 Kraków, Al. Mickiewicza 30 Pawilon A3, p. 108 lub 107 tel. 12 617 44 48, 12 617 34 41; fax. 12 617 33 71 email: epamula@agh.edu.pl; stodolak@agh.edu.pl; krok@agh.edu.pl http://www.agh.edu.pl/pl/studia/studia-podyplomowe/biomateriały-materiały-dla-medycyny.html
Kierownik: Dr hab. inż. Elżbieta Pamuła, prof. AGH	
Charakterystyka: Tematyka prezentowana w trakcie zajęć obejmuje przegląd wszystkich grup materiałów dla zastosowań medycznych: metalicznych, ceramicznych, polimerowych, węglowych i kompozytowych. Studenci zapoznają się z metodami projektowania i wytwarzania biomateriałów, a następnie możliwościami analizy ich właściwości mechanicznych, właściwościami fizykochemicznymi (laboratoria z metod badań: elektronowa mikroskopia skaningowa, mikroskopia sił atomowych, spektroskopia w podczerwieni, badania energii powierzchniowej i zwilżalności) i właściwościami biologicznymi (badania: <i>in vitro</i> i <i>in vivo</i>). Omawiane są regulacje prawne i aspekty etyczne związane z badaniami na zwierzętach i badaniami klinicznymi (norma EU ISO 10993). Studenci zapoznają się z najnowszymi osiągnięciami medycyny regeneracyjnej i inżynierii tkankowej.	
Sylwetka absolwenta: Studia adresowane są do absolwentów uczelni technicznych (inżynieria materiałowa, technologia chemiczna), przyrodniczych (chemia, biologia, biotechnologia), a także medycznych, stomatologicznych, farmaceutycznych i weterynaryjnych, pragnących zdobyć, poszerzyć i ugruntować wiedzę z zakresu inżynierii biomateriałów i nowoczesnych materiałów dla medycyny. Słuchacze zdobywają i/lub pogłębiają wiedzę z zakresu inżynierii biomateriałów. Po zakończeniu studiów wykazują się znajomością budowy, właściwości i sposobu otrzymywania materiałów przeznaczonych dla medycyny. Potrafią analizować wyniki badań i przekładać je na zachowanie się biomateriału w warunkach żywego organizmu. Ponadto słuchacze wprowadzani są w zagadnienia dotyczące wymagań normowych, etycznych i prawnych niezbędnych do wprowadzenia nowego materiału na rynek. Ukończenie studiów pozwala na nabycie umiejętności przygotowywania wniosków do Komisji Etycznych i doboru metod badawczych w zakresie analizy biozgodności materiałów.	
Zasady naboru: Termin zgłoszeń: od 20.09.2012 do 20.10.2012 (liczba miejsc ograniczona - decyduje kolejność zgłoszeń) Wymagane dokumenty: dyplom ukończenia szkoły wyższej Miejsce zgłoszeń: Kraków, Al. Mickiewicza 30, Pawilon A3, p. 108, 107 lub 501 Osoby przyjmujące zgłoszenia: Dr hab. inż. Elżbieta Pamuła, prof. AGH (tel. 12 617 44 48, e-mail: epamula@agh.edu.pl) Dr inż. Ewa Stodolak (tel. 12 617 34 41, e-mail: stodolak@agh.edu.pl) Mgr inż. Małgorzata Krok (tel. 12 617 44 48, e-mail: krok@agh.edu.pl)	
Czas trwania: 2 semestry (od XI 2012 r. do VI 2013 r.)	Opłaty: 2 600 zł
Informacje dodatkowe: Zajęcia: 8 zjazdów (soboty-niedziele) 1 raz w miesiącu. Przewidywana liczba godzin: 160.	